Analysis on regulation of neural activity and behavior by glutamate neurotransmission in the thermotaxis neural circuit of *C. elegans*

（線虫*C. elegans*の温度走性を司る神経回路におけるグルタミン酸を介した神経伝達による神経活性と行動の制御機構の解析）

大西 憲幸

Contents

Summary

Elucidation of the mechanism by which massive information is processed in complex neural circuits of the brain is a fundamental problem in neuroscience. Here, we show that glutamate signals from two distinct sensory neurons bidirectionally affect the same postsynaptic interneuron, thus producing the opposite behaviors of the nematode *Caenorhabditis elegans*. EAT-4/VGLUT dependent glutamate signals from AFD thermosensory neuron inhibit the postsynaptic AIY interneurons through activation of GLC-3/GluCl inhibitory glutamate receptor and behaviorally drive migration toward colder temperature. By contrast, EAT-4 dependent glutamate signals from AWC thermosensory neurons stimulate the AIY neurons to induce migration toward warmer temperature. Alteration of the strength of glutamate signals from AFD and AWC leads to significant changes of AIY activity, resulting in drastic modulation of behavioral outputs. We thus provide an important insight on information processing, where two glutamate transmissions encoding opposite information flows regulate neural activities to produce a large spectra of behavioral outputs.

Introduction

Animals can sense a vast numbers of environmental stimuli and give rise to approximate behavioral outputs through processing immense neural information in complex neural circuits of the brain. Elucidation of the mechanism by which massive information is processed is a fundamental problem in neuroscience. In the course of processing, neurons communicate neural information through synaptic transmissions. To gain insight into information processing, it is important to delineate each information flow communicated through synaptic transmissions, whereby modulating behavioral outputs. Although studies in vertebrates have provided a wealth of data on mechanisms of synaptic transmissions, dissection of information flow conveyed between neurons has been hindered by difficulty of the identification of neural codes, because of the complexity of the vertebrate nervous system (Di Maio, 2008).

The nematode *C. elegans* is well suited for the analysis of information processing in neural circuits because of its simple nervous system consisting of only 302 neurons with entirely known synaptic connections and gap junctions (White et al, 1986). In addition, because of the accessible genetics of *C. elegans* (Brenner, 1974), we can isolate and analyze mutants of genes required for information processing. Recent technical advances also improve the analysis of information processing in *C. elegans*. A growing number of promoters which drive gene expression in specific neurons allow us to label specific neurons and neuronal

components with fluorescence protein tags in live worms (Chalfie et al, 1994; Nonet, 1999), and define the neurons in which particular gene functions (Kuhara et al, 2002). Further, physiological analysis of neurons in live worms has become possible by cameleon, a genetically encoded calcium indicator used to monitor calcium influx (Kerr et al, 2000; Miyawaki et al, 1997).

As a model organism with many advantages for analyzing information processing, *C. elegans* exhibits various behavioral outputs in response to many different environmental stimuli (de Bono & Maricq, 2005). Thermotaxis is one of the most plastic behaviors in *C. elegans*, in which the animals remember the ambient temperature in association with the past feeding state and migrates to and move isothermally around the previous experienced temperature when placed on a temperature gradient (Hedgecock & Russell, 1975; Mohri et al, 2005; Mori & Ohshima, 1995). To analyze details of thermotaxis, two types of thermotaxis assay systems have established; the individual TTX assay that is suitable for scoring isothermal tracking (IT) behavior (Figure 1; Gomez et al, 2001; Mori & Ohshima, 1995) and the population TTX assay that is suitable for quantitatively assessing the migration ability to the cultivation temperature (Figure 2; Ito et al, 2006). The neural circuit model for thermotaxis has been proposed. Temperature is sensed and remembered by AFD and AWC sensory neurons, thermal information from AFD and AWC is transmitted to AIY interneuron, and the subsequent information from AIY is further transmitted to AIZ and RIA interneurons for further neural information processing (Figure 3. ; Biron et al, 2008; Clark et al, 2006; Kuhara et al, 2008; Mori & Ohshima, 1995).

Previous attempts to dissect thermotaxis successfully identified several molecular components related to temperature sensing signal transduction in AFD and AWC thermosensory neurons. In AFD neurons, three guanylyl cyclases, GCY-8, GCY-18 and GCY-23 appear to redundantly produce cGMP as a second messenger, and cGMP-dependent cation channel composed of TAX-2 and TAX-4 increase internal Ca^{2+} concentration upon reception of temperature change (Figure 4; Inada et al, 2006; Kimura et al, 2004; Komatsu et al, 1996). Additional molecules such as TAX-6 (Calcineurin) and TTX-4 (PKC-1; nPKC-epsilon/eta), both of which likely adjust the temperature input in AFD, have been also reported (Kuhara et al, 2002; Okochi et al, 2005). In AWC thermosensory neurons, ODR-1 (guanylyl cyclase) produces cGMP through activation of ODR-3 (G-alpha), and TAX-4 (cGMP-dependent cation channel) increases internal Ca^{2+} concentration upon reception of temperature stimuli (Figure 4; Kuhara et al, 2008). It have been also reported that EAT-16 RGS (regulator of G protein signaling) suppressed the G protein coupled signaling in AWC (Figure 4; Kuhara et al, 2008). However, how critical neurons for the thermotaxis neural circuit communicate with each other to modulate the neural activity still remains to be understood.

Although the nervous system of *C. elegans* is less complex than those of vertebrates, *C. elegans* contains many of neurotransmitters found in vertebrates, including acetylcholine, serotonin, dopamine, gamma-aminobutyric acid (GABA), and glutamate (de Bono & Maricq, 2005). Many genes involved in

synaptic transmission through these transmitters have been identified. EAT-4 is one of the key components of glutamate-mediated neurotransmission; a *C. elegans* homolog of mammalian vesicular glutamate transporter (VGLUT) that concentrates glutamate into synaptic vesicles (Figure 9; Bellocchio et al, 2000; Lee et al, 1999; Takamori et al, 2000). Past study of EAT-4 revealed that EAT-4 is involved in chemotaxis, habituation of the tap-withdrawal response, local search, and migration toward colder temperature (Chalasani et al, 2007; Clark et al, 2007; Hills et al, 2004; Rankin & Wicks, 2000). In this study, molecular, genetic and calcium imaging analysis revealed that coordinated functions of EAT-4 dependent glutamate signals from AFD and AWC thermosensory neurons and RIA interneurons are essential for thermotaxis. EAT-4 dependent glutamate signals from AFD inhibit AIY through activation of GLC-3/GluCl inhibitory glutamate receptor (Horoszok et al, 2001), whereas EAT-4 dependent glutamate signals from AWC stimulate AIY. Alteration of the strength of EAT-4 dependent AFD and AWC glutamate signals onto AIY leads to significant changes of AIY activity, which, through EAT-4 dependent glutamate signals from RIA, results in drastic modulation of thermotaxis. Our results provide an important insight on information processing, where two glutamatergic synaptic transmissions encoding opposite information flows regulate neural activities to generate various behavioral outputs.

Results

Thermotaxis defects of *nj2* and *nj6* mutants are caused by defective function of *eat-4* gene

In our attempt to analyze thermotaxis defective mutants through forward genetic approach, we isolated *nj2* and *nj6* mutants that exhibit abnormal migration in a radial temperature gradient (Figure 5 and 6). Both *nj2* and *nj6* mutations mapped to the region including *eat-4* gene and the thermotaxis defects of *nj2* and *nj6* mutants are restored by introducing the genomic fragment including *eat-4* gene (Figure 7). Our sequencing of *nj2* and *nj6* genomes revealed that *nj2* is associated with two missense mutations of the conserved amino acid (G16E) and the putative transmembrane domain (G355R), and that *nj6* is a missense mutation of the conserved amino acid (G494R) (Figure 8; Ni et al, 1994). These results suggest that thermotaxis defects of *nj2* and *nj6* mutants are caused by defective function of *eat-4* gene.

VGLUT homolog EAT-4 is essential for thermotaxis behavior

To ensure the importance of EAT-4 for thermotaxis, we performed two types of thermotaxis (TTX) assays of *eat-4(ky5)* mutants carrying loss-of-function mutation in *eat-4* gene. The individual TTX assay is suitable for scoring isothermal tracking (IT) behavior (Figure 1; Gomez et al, 2001). Although many wild-type animals (55% ± 8%) exhibited IT behavior in a radial thermal gradient

form 17°C to 25°C after cultivation at 20°C in well-fed conditions, no *eat-4(ky5)* mutants (0%) exhibited IT behavior (Figure 5B and 6). In addition to IT behavior defect, *eat-4(ky5)* mutants showed severe impairment in the population TTX assay that is suitable for quantitatively assessing the migration ability to the cultivation temperature (Figure 2; Ito et al, 2006). After cultivation at 23°C, 20°C, and 17°C in well-fed conditions, most of wild-type animals migrated up or down the linear temperature gradient (0.45°C/cm) until they reached the region nearly corresponding to the previous cultivation temperature (Figure 10A). However, *eat-4(ky5)* animals had little tendencies to migrate toward cultivation temperature and mostly dispersed in a wide area (Figure 10A). TTX indices, quantified as shown in Figure 1C, of 23°C-cultivated and 17°C-cultivated *eat-4(ky5)* mutants (0.47 ± 0.14 at 23°C, -1.46 ± 0.08 at 17°C) differed significantly from those of wild-type animals (2.27 ± 0.19 at 23°C, -2.96 ± 0.22 at 17°C; Figure 10B). Although *eat-4(ky5)* mutants did not show locomotion defect, they dispersed less than wild-type animals in the absence of a temperature gradient (Figure 11; Ségalat et al, 1995), indicating the possibility that abnormal TTX indices of *eat-4(ky5)* mutants could result from other defects, such as local search defect. Nevertheless, *eat-4(ky5)* mutants dispersed more broadly from cultivation temperature than wild type animals on a thermal gradient (Figure 10A). This tendency was also observed in the population TTX assay of 20°C-cultivated *eat-4(ky5)* mutants after placed at the higher and lower temperature positions in the gradient (Figure 12). These results suggest that *eat-4(ky5)* mutants indeed exhibit thermotaxis defect, implicating the behavioral regulation by EAT-4/VGLUT dependent glutamatergic neurotransmission

(Figure 9).

EAT-4/VGLUT is expressed in subsets of neurons including constituents of the thermotaxis neural circuit

Previous report showed that *eat-4::lacZ* and *eat-4::gfp* fusion genes, which contain the 2.4kb fragment upstream of *eat-4* as a promoter, did not appear to express in neurons critical for the thermotaxis neural circuit (Lee et al, 1999). These results are consistent with our result that *eat-4* genomic fragment driven by this 2.4kb promoter did not restore the normal thermotaxis in *eat-4* mutants (Figure 13). Hence, the 2.4kb promoter region does not drive sufficient expression of *eat-4* gene for thermotaxis behavior. Given that another gene resides 5.5 kb upstream of *eat-4* gene, we constructed *full length eat-4::gfp* fusion gene that contains the whole *eat-4* genomic fragment and the 5.5kb upstream fragment (Figure 14A). We found that this *full length eat-4::gfp* fusion gene rescued the abnormal thermotaxis of *eat-4* mutants (Figure 13).

To identify cells expressing EAT-4, we observed the expression pattern of *full length eat-4::gfp* in wild-type animals (Figure 14B), and also in *unc-104(e1265)* mutants defective in UNC-104/KIF1A kinesin-like motor protein in order to prevent the EAT-4::GFP-caused strong fluorescence of the nerve ring (Figure 14C; Hall & Hedgecock, 1991; Otsuka et al, 1991). Based on cell-body positions and morphologies (Sulston & Horvitz, 1977; Sulston et al, 1983), we observed consistent expression of EAT-4::GFP in many head neurons including AFD

thermosensory neurons, AWC thermosensory neurons, AIZ interneurons and RIA interneurons, which are constituents of the thermotaxis neural circuit (Figure 14B, C, and D; Kuhara et al, 2008; Mori & Ohshima, 1995).

EAT-4/VGLUT dependent glutamatergic neurotransmissions from AFD and RIA neurons are essential for isothermal tracking

Expression of *eat-4* cDNA from its own promoter (5.5kb) and in all neurons strongly rescued the IT behavior defect of *eat-4(ky5)* mutants (50% ± 2% and 31% ± 2%, respectively) in the individual TTX assay (Figue 15), suggesting that neuronal expression of EAT-4 is essential for thermotaxis. To identify neurons that require EAT-4 mediated glutamatergic neurotransmission for thermotaxis, we conducted cell-specific rescue experiments by introducing *eat-4* cDNA under the control of various cell-specific promoters into *eat-4(ky5)* mutants. In the individual TTX assay, expression of EAT-4 in AFD, AWC or AIZ neurons did not induce any changes in IT behavior defect of *eat-4(ky5)* mutants (0%), whereas expression of EAT-4 in RIA interneurons weakly rescued IT behavior defect (10% ± 2%) (Figure 15). Remarkably, simultaneous expression of EAT-4 in AFD and RIA rescued IT behavior defect (39% ± 1%), as expression of EAT-4 under the control of *eat-4* promoter did ($p > 0.05$) (Figure 15). The rescue efficiency of the transgenic animals expressing EAT-4 in AFD and RIA was not increased by additional expression of EAT-4 in other neurons (Figure 15). These results suggest that EAT-4 dependent glutamate transmissions from AFD thermosensory neurons and RIA interneurons are crucial steps that process and

convey thermal information in the thermotaxis neural circuit.

EAT-4/VGLUT dependent glutamatergic neurotransmissions from AFD, AWC, and RIA neurons regulate migration toward cultivation temperature

Since expression of *eat-4* cDNA from its own promoter and in all neurons also strongly restored normal migrations to cultivation temperature ($p > 0.05$ compared with wild-type animals at every cultivation temperature) in the population TTX assay (Figure 16), we performed the population TTX assay for cell-specific rescue experiments (Figure 16). Similar to the results of individual TTX assay, expression of EAT-4 in AIZ interneurons did not induce any changes in thermotaxis behavior of *eat-4(ky5)* mutants (Figure 16). In contrast, expression of EAT-4 in AFD thermosensory neurons, in AWC thermosensory neurons, or in RIA interneurons induced different migration pattern from that of *eat-4(ky5)* mutants (Figure 16). Further, each expression had different effects on migration; the transgenic animals expressing EAT-4 in AFD migrated toward colder temperature than *eat-4(ky5)* mutants, the transgenic animals expressing EAT-4 in AWC migrated toward warmer temperature after cultivated at 20°C and 23°C, and the transgenic animals expressing EAT-4 in RIA neurons migrated toward warmer temperature only after cultivated at 23°C (Figure 16). These results imply that EAT-4 dependent glutamate transmissions from AFD, AWC, and RIA to their postsynaptic neurons are involved in regulation of thermotaxis and each transmission induces different behavioral outputs.

Because of the importance of EAT-4 in RIA interneurons that lie downstream of AFD and AWC thermosensory neurons (Figure 3 and 15), it was difficult to detect the effect of EAT-4 solely in AFD or AWC for thermotaxis behavior without expression of EAT-4 in RIA. To reconcile this problem, we introduced several doses of *AFDp::eat-4 cDNA* and *AWCp::eat-4 cDNA* with constant 5ng/ul dose of *RIAp::eat-4 cDNA* into *eat-4(ky5)* mutants, and performed the population TTX assay (Figure 17). Through the analysis, we found that simultaneous expression of EAT-4 in AFD, AWC, and RIA with 0.2ng-5ng-5ng/ul of *AFDp::eat-4 cDNA*, *AWCp::eat-4 cDNA,* and *RIAp::eat-4 cDNA,* respectively, almost rescued the defective migration to cultivation temperature of *eat-4(ky5)* mutants (Figure 17). Although the rescue was not complete in these transgenic animals, they showed similar behavior to that of *eat-4(ky5)* mutants expressing EAT-4 in all neurons (Figure 17). As shown in Figure 16, these results further suggest that EAT-4 dependent glutamate transmission from AFD, AWC, and RIA to their postsynaptic neurons regulates thermotaxis behavior.

Glutamatergic neurotransmissions from AFD and AWC neurons induce opposite migration

In the population TTX assay for cell-specific rescue experiments with simultaneous expression of EAT-4 in AFD, AWC, and RIA, alteration in introducing doses of *AFDp::eat-4 cDNA* and *AWCp::eat-4 cDNA* induced various migration (Figure 17). Simultaneous expression of EAT-4 in AFD and RIA with both 5ng/ul doses enhanced migration toward colder temperature than

wild-type animals after cultivation at 20°C and 23°C (cryophilic movement) (Figure 17). Although tracks of these transgenic animals in the individual TTX assay did not indicate cryophilic phenotype (Figure 18), cryophilic phenotype would not be detectable on the assay plate, where the steepness of thermal gradient differs in different areas (Figure 1A). Simultaneous expression of EAT-4 in AFD, AWC and RIA with introduction of 5ng-5ng-5ng/ul, 2ng-5ng-5ng/ul, and 0.5ng-5ng-5ng/ul of *AFDp::eat-4 cDNA*, *AWCp::eat-4 cDNA*, and *RIAp::eat-4 cDNA*, respectively, into *eat-4(ky5)* mutants still drove tendency to migrate toward cold temperature, while the cryophilic movement of these transgenic animals weakened as compared with the animals expressing EAT-4 in AFD and RIA at 20°C and 23°C (Figure 17). In contrast, simultaneous expression of EAT-4 in AWC and RIA neurons with 5ng/ul enhanced migration toward warmer temperature than wild-type animals after cultivation at 17°C and 20°C (thermophilic movement) (Figure 17). These results suggest that glutamate transmission from AFD induces cryophilic movement and that glutamate transmission from AWC induces thermophilic movement. Considering that EAT-4 in AWC was not necessary for IT behavior (Figure 15) and simultaneous expression of EAT-4 in AFD, AWC, and RIA induced migration toward cold temperature until the introduction dose of *AFDp::eat-4 cDNA* to the *eat-4* mutants was reduced up to less than one tenth of *AWCp::eat-4 cDNA* (Figure 17), AFD-mediated glutamate transmission is likely to be more influential than AWC-mediated glutamate transmission for thermotaxis behavior.

RIA neurons have multiple neurotransmitter outputs

As already described in Figure 15, EAT-4 dependent glutamate transmission from RIA is crucial for thermotaxis. Nevertheless, *eat-4* transgenic mutants expressing EAT-4 only in AFD but not in RIA (*eat-4 (AFD+)*) could migrate to colder temperature as opposed to *eat-4(ky5)* mutants that dispersed in broader area in the population TTX assay (Figure 16). In addition, the phenotype of *eat-4 (AFD+)* did not change with additional expression of EAT-4 in RIA (Figure 17). These results raise two possibilities: signals from AFD flow either through RIA independent pathway or through RIA dependent pathway coupled with both EAT-4 dependent and independent synaptic transmissions. To distinguish these possibilities, we examined the effect of genetically imparied RIA on *eat-4 (AFD+)* (Figure 19). Correct localization of synapses in RIA requires TTX-7/IMPase, and *ttx-7(nj50)* mutants showed abnormal thermotactic phenotype, similar to that of wild-type animals in which RIA was ablated (Tanizawa et al, 2006). Thermotactic defect of *ttx-7(nj50)* mutants completely masked the defect of *eat-4 (AFD+)* (Figure 19), suggesting the essential role of RIA dependent pathway involving both EAT-4 dependent and independent transmissions.

EAT-4/VGLUT dependent glutamatergic neurotransmissions is influential for the thermal response of AIY

As an attempt to analyze molecular physiology of the EAT-4 dependent

glutamate transmission for thermotaxis, we conducted calcium imaging of AIY interneurons that are postsynaptic to both AFD and AWC neurons in *eat-4(ky5)* mutants after being cultivated at 20°C (Figure 3 and 21). We monitored the temperature-dependent neural activity changes of intact AIY interneurons by measuring temperature stimulus-evoked calcium concentration changes using cameleon, a genetically encoded calcium indicator (Figure 20; Miyawaki et al, 1997; Nagai et al, 2004). We verified that expression of cameleon (yc3.60) in AIY itself did not affect thermotaxis, since wild type animals transgenic with cameleon construct (*AIYp::yc3.60*) showed normal thermotaxis (Figure 18B). Consistent with our previous results representing the responsiveness of AIY neurons to temperature change, the calcium concentration in AIY neurons of wild-type animals increased with warming (Figure 21A; Kuhara et al, 2008). The fluorescence resonance energy transfer (FRET) ratios did not return to baseline, which might be caused by faster degradation of YFP fluorescence than CFP fluorescence in yc3.60 (Figure 21A and Figure 22). Upon warming, fluorescence resonance energy transfer (FRET) ratios in AIY neurons of *eat-4(ky5)* mutants changed more than those of wild-type animals (11% ± 1% for *eat-4(ky5)* mutants and 8% ± 0.6% for wild-type animals at 90S after starting temperature change) (Figure 21A and C), which likely represents the hyper-responsiveness of AIY neurons in *eat-4(ky5)* mutants. These results suggest that EAT-4 dependent glutamate transmission is quite influential for the response of AIY neurons to temperature change.

Glutamatergic neurotransmissions from AFD and AWC neurons oppositely modulate activity of postsynaptic neuron AIY in response to warming

Previous reports showed that activation of AIY interneurons mediates movement toward warmer temperature (Hobert et al, 1997; Kuhara et al, 2008; Mori & Ohshima, 1995) indicate the correlation between the activity of AIY neurons and behavioral output. Hence, we hypothesized that glutamate transmission from AFD and AWC neurons have opposite effects on the activity of AIY neurons, similar to the opposite effect of AFD and AWC on behavioral outputs. To test this hypothesis, we monitored the activity of AIY on warming in transgenic *eat-4(ky5)* animals expressing EAT-4 in either AFD or AWC after being cultivated at 20°C by calcium imaging (Figure 21). Since EAT-4 dependent glutamate transmission from RIA is absolutely important for connecting neural activity and behavioral output (Figure 15), we also expressed EAT-4 in RIA of transgenic animals as shown in Figure 4. The FRET ratio changes in AIY of *eat-4(ky5)* mutants expressing EAT-4 in RIA (*eat-4 (RIA+)*) were larger than those of wild-type animals and similar to those of naïve *eat-4(ky5)* mutants (*eat-4*) (10% ± 0.6% at 90S) (Figure 21A and C), suggesting that expression of EAT-4 in RIA has almost no effect on the AIY activity. Additional expression of EAT-4 in AFD neurons of *eat-4(ky5)* mutants (*eat-4 (AFD+,RIA+)*) induced smaller change of FRET ratios in AIY neurons (3.9% ± 1.5% at 90S) as compared with e*at-4(ky5)* mutants and wild-type animals (Figure 21A and C). Notably, smaller change in FRET ratio observed in *eat-4 (AFD+,RIA+)* were similarly observed in *eat-4(ky5)* mutants expressing EAT-4 only in AFD (*eat-4 (AFD+)*), which argues against any feedback pathway to AIY through RIA (Figure 23). Expression of EAT-4 in AWC

and RIA (*eat-4 (AWC+,RIA+)*) caused not only the larger change like *eat-4(ky5)* mutants (*eat-4*) (10.6% ± 1% at 90S), but also faster change of FRET ratios in AIY (5.1% ± 0.7% at 45s) (Figure 21). Consistent to our hypothesis, our results on calcium imaging of AIY in 20°C-cultivated animals suggest that glutamate transmissions from AFD or from AWC thermosensory neurons inhibit or stimulate AIY interneurons, respectively.

We also monitored activity of AIY on warming in 17°C- and 23°C-cultivated wild-type animals and the *eat-4(ky5)* transgenic animals by calcium imaging (Figure 24). After being cultivated at 17°C , whereas the FRET ratio changes in AIY of *eat-4 (AFD+,RIA+)* were similar to those of wild-type animals, the ratio changes of *eat-4 (AWC+,RIA+)* were larger than those of wild-type animals (Figure 24A and B). In contrast, whereas the ratio changes of *eat-4 (AWC+,RIA+)* were similar to those of wild-type animals, the ratio changes of *eat-4 (AFD+,RIA+)* were smaller than those of wild-type animals after being cultivated at 23°C (Figure 24C and D). Thus, our results on response of AIY upon warming closely correlated with behavioral data shown in Figure 17 in every cultivation temperature, further suggesting the opposite modulation of AIY activity by glutamate transmissions from AFD and AWC.

Glutamatergic neurotransmissions from AFD neurons inhibit activity of AIY neurons in response to cooling

To verify the effect of glutamate signals on the response of AIY, we also

conducted calcium imaging of AIY on cooling in 20°C-cultivated wild-type animals and the *eat-4(ky5)* transgenic animals (Figure 25). Upon cooling, FRET ratios in AIY of *eat-4(ky5)* mutants did not decrease as much as those of wild-type animals (-14% ± 0.7% for *eat-4(ky5)* mutants and -19% ± 1.0% for wild-type animals at 120S) (Figure 25). Consistent with the results on warming shown in Figure 21, this result likely represents hyperactive state of AIY in *eat-4(ky5)* mutants (Figure 25). The FRET ratios in AIY of *eat-4 (RIA+)* and *eat-4 (AWC+,RIA+)* showed the similar change to those of *eat-4(ky5)* mutants (-14% ± 0.8% for *eat-4 (RIA+)* and for *eat-4 (AWC+,RIA+)* at 120S) (Figure 25), implicating no effects of glutamate signals from AWC and RIA on the response of AIY to cooling. By contrast, the FRET ratios in AIY of *eat-4 (AFD+,RIA+)* decreased to the similar level to those of wild-type animals (-18% ± 0.9% for *eat-4 (AFD+,RIA+)* at 120S) (Figure 25), suggesting that inhibition through glutamate transmission from AFD regulates the response of AIY to cooling. Altogether, our results on calcium imaging of AIY demonstrate that glutamate transmission from AFD inhibits AIY activity in response to both warming and cooling, and glutamate transmission from AWC stimulates AIY activity in response to only warming, thereby implying that AFD-mediated glutamate transmission more effectively contributes to thermotaxis behavior than AWC-mediated glutamate transmission.

Opposite glutamate signals from AFD and AWC neurons induce drastic changes in behavioral output

To elucidate whether various behavioral outputs shown in Figure 17 are caused by modulation of AIY activity through EAT-4 dependent glutamate transmission from AFD and AWC neurons, we investigated dose-dependency of AIY activity in transgenic *eat-4(ky5)* mutants expressing relative different doses of EAT-4 in AFD, AWC and RIA neurons with calcium imaging (Figure 26). Intriguingly, FRET ratios showed similar small changes when introducing 5ng, 2ng or 0.5ng of *AFDp::eat-4 cDNA* to the *eat-4* mutants, whereas FRET ratios dramatically increased when introducing 0.2ng or 0ng of *AFDp::eat-4 cDNA* (Figure 26), which is consistent with the results of cell-specific rescue experiments shown in Figure 17. Thus, our results demonstrated that modulation of the AIY activity by opposite glutamate signals from AFD neurons and from AWC neurons induces drastic change of behavioral output.

Identification of glutamate receptors involved in thermotaxis

Our analysis of EAT-4/VGLUT in thermotaxis suggested that glutamate receptors receive EAT-4 dependent glutamate signals in AIY interneurons and motorneurons postsynaptic to RIA interneurons. In *C. elegans*, four classes of glutamate receptors are predicted (Table 1); AMPA (alpha-amino-3-hydroxy-5-methyl-4-isoxazolepropionic acid)-type glutamate-gated cation channels (GluR) encoded by eight *glr* genes, NMDA (N-methyl-D-aspartic acid)-type glutamate-gated cation channels (NR) encoded by two *nmr* genes, glutamate-gated

chloride channels (GluCl) encoded by four *glc* genes and two *avr* genes, and metabotropic G-protein-coupled glutamate receptors (mGluR) encoded by three *mgl* genes (Brockie & Maricq, 2003; Dillon et al, 2006; Yates et al, 2003). Of those, MGL-1/mGluR and GLC-3/GluCl were reported to be expressed in AIY interneurons (Horoszok et al, 2001; Wenick & Hobert, 2004), and GLR-1/GluR and AVR-14/GluCl were reported to be expressed in many motorneurons (Dent et al, 2000; Hart et al, 1995). In addition, the previous research of AIY interneurons showed the similarity between AIY interneurons and vertebrate bipolar cells in which mGluR is indicated to receive glutamate from presynaptic photo receptor neurons (Hobert et al, 1997; Nakajima et al, 1993; Nakanishi, 1994; Satterlee et al, 2001). Because these reports imply the possible involvement of GLC-3/GluCl, GLR-1/GluR, AVR-14/GluCl, and three mGluRs (MGL-1, MGL-2, and MGL-3) in thermotaxis, we performed the population TTX assay of mutants containing mutations in each gene encoding these glutamate receptors (Figure 27 and 28). *glr-1(n2461)* mutants migrated to their cultivation temperature normally in the population TTX assay (Figure 27). In contrast, *glc-3(ok321)* mutants migrated to warmar temperature than the cultivation temperature after cultivation at 17°C and 20°C (thermophilic movement), and *avr-14(ad1302)* mutants migrated to colder temperature than the cultivation temperature after cultivation at 20°C and 23°C (cryophilic movement) (Figure 27). Additionally, although single mutants of mGluRs (*mgl-1(tm1811)*, *mgl-2(tm355)*, and *mgl-3(tm1766)*) migrated to their cultivation temperature normally, *mgl-3(tm1766); mgl-1(tm1811)* double mutants and *mgl-2(tm355); mgl-3(tm1766); mgl-1(tm1811)* triple mutants migrated to colder temperature

than the cultivation temperature after cultivation at 23°C and after cultivation at 20°C and 23°C, respectively (Figure 28). These results imply that GLC-3/GluCl, AVR-14/GluCl, MGL-1/mGluR, and MGL-3/mGluR are involved in thermotaxis.

Cell-specific rescue experiments of thermotaxis-defective *avr-14(ad1302)* mutants

To identify neurons that require AVR-14/GluCl for thermotaxis, we tried to conduct cell-specific rescue experiments by introducing *avr-14* cDNA under the control of various cell-specific promoters into *avr-14(ad1302)* mutants. Because two types of *avr-14* cDNAs were predicted (Dent et al, 2000), we constructed both of *avr-14* cDNAs and introduced them simultaneously. First, to elucidate that *avr-14* cDNAs are functional and AVR-14 functions in neural circuit, we performed the population TTX assay of transgenic *avr-14(ad1302)* animals expressing *avr-14* cDNAs from its own promoter or in all neurons (Figure 29). Contrary to my expectation, neither of these expressions induced any changes in thermotaxis defect of *avr-14(ad1302)* mutants after being cultivated at 23°C (Figure 29).

MGL-3/mGluR functions in sensory neurons for thermotaxis

Expression of *mgl-3* cDNA in all neurons fully rescued the thermotaxis defect of *mgl-2(tm355); mgl-3(tm1766); mgl-1(tm1811)* triple mutants cultivated at 23°C in the population TTX assay (Figure 30), suggesting that neuronal expression of

MGL-3/mGluR is important for thermotaxis. To identify neurons that require MGL-3/mGluR for thermotaxis, we introduced *mgl-3* cDNA under the control of various cell-specific promoters into *mgl-2(tm355); mgl-3(tm1766); mgl-1(tm1811)* triple mutants and performed the population TTX assay of them after being cultivated at 23°C (Figure 30). Interestingly, expression of *mgl-3* cDNA in sensory neurons rescued thermotaxis defect of the triple mutants, suggesting the requirement of MGL-3/mGluR in several sensory neurons for thermotaxis (Figure 30). These results imply the regulation of thermotaxis through glutamatergic neurotransmission not being detected by our analysis of *eat-4*.

GluCl homolog GLC-3 inhibits the activity of AIY interneurons in thermotaxis

We also conducted cell-specific rescue experiments of *glc-3(ok321)* mutants by introducing *glc-3* cDNA under the control of various cell-specific promoters and found that the thermotaxis defect of *glc-3(ok321)* mutants was fully rescued by expressing *glc-3* cDNA in AIY interneurons but not in any other neurons (Figure 31). These results suggest that GLC-3/GluCl is required in AIY interneurons for thermotaxis.

Given that the activation of AIY interneuron mediates movement toward warmer temperature (Hobert et al, 1997; Kuhara et al, 2008; Mori & Ohshima, 1995) and glutamate-gated chloride channels (GluCls) mediate inhibitory neurotransmission (Dent et al, 1997), we hypothesized that GLC-3/GluCl

regulates thermotaxis through inhibition of the AIY activity. Consistent with this hypothesis, FRET ratios in AIY neurons of *glc-3(ok321)* mutants changed more than that of wild-type animals (10% ± 0.5% for *glc-3(ok321)* mutants and 6.6% ± 0.6% for wild-type animals at 90S) (Figure 32), implicating the hyper-responsiveness of AIY neurons in *glc-3(ok321)* mutants. The increased change of FRET ratios was rescued by expressing *glc-3* cDNA in AIY interneurons (6.2% ± 0.4% at 90s) (Figure 32), suggesting that GLC-3 cell autonomously inhibits the activity of AIY.

GLC-3/GluCl receives glutamatergic signals from AFD thermosensory neurons

We addressed whether GLC-3 glutamate receptors in AIY interneuron perceive EAT-4 dependent glutamate signals from AFD or AWC thermosensory neurons. Thermosensory signal transduction in AFD neurons is thought to be mediated by the change in intracellular concentration of cGMP through GCY-23, GCY-8, and GCY-18 guanylyl cyclases (Figure 4A; Inada et al, 2006), and *gcy-23(nj37) gcy-8(oy44) gcy-18(nj38)* triple mutants showed abnormal thermotactic phenotype, similar to that of wild-type animals in which AFD neurons were ablated (Figure 33; Inada et al, 2006; Kuhara et al, 2008). *gcy-23 gcy-8 gcy-18; glc-3* quadruple mutants showed quite similar thermotactic abnormality to that of *gcy-23 gcy-8 gcy-18* triple mutants in the population TTX assay, suggesting that the abolishment of thermosensory signaling in AFD by *gcy-23 gcy-8 gcy-18* mutation entirely suppressed *glc-3(ok321)* mutation (Figure 33). Likewise,

thermotactic defect of the *eat-4* mutants expressing EAT-4 in AWC and RIA but not in AFD neurons (*eat-4 (AWC+,RIA+)*) completely masked the defect of *glc-3* mutants (Figure 33). These results suggest that GLC-3 glutamate receptors in AIY neurons receive EAT-4 mediated glutamate signals from AFD neurons.

Recently, ODR-3 G-alpha dependent heterotrimeric G protein coupled signaling was found to mediate thermosensory signal transduction in AWC neurons, and EAT-16 RGS (regulator of G protein signaling) suppressed the G protein coupled signaling in AWC (Figure 4B; Kuhara et al, 2008). *odr-3(n1605)* mutants and *eat-16(nj8)* mutants migrated toward warmer and colder temperature than the cultivation temperature, respectivery, in the population TTX assay (Figure 34; Kuhara et al, 2008). *glc-3 odr-3* double mutants migrated much warmer temperature than both *glc-3* and *odr-3* single mutants after cultivation at 17°C and 20°C, implicating the additive effect of *odr-3* and *glc-3* mutation (Figure 34). Similarly, thermotactic defect of *eat-16(nj8)* mutants and the *eat-4(ky5)* mutants expressing EAT-4 in AFD and RIA (*eat-4 (AFD+,RIA+)*) influenced additively on the defect of *glc-3* mutants after cultivation at 17°C, 20°C and 23°C (Figure 34). These results implicate GLC-3 independent EAT-4 mediated glutamatergic neurotransmission in AWC. Altogether, our genetic analyses suggest that GLC-3/GluCl is required for reception of EAT-4/VGLUT dependent glutamate signals from AFD neurons.

We conducted calcium imaging to verify that EAT-4 dependent glutamate transmission from AFD thermosensory neurons is mediated by GLC-3 in AIY

interneurons (Figure 35). FRET ratios in AIY neurons of the double mutants (*eat-4 (AWC+,RIA+); glc-3*) constructed from the *eat-4* mutants expressing EAT-4 in AWC and RIA (*eat-4 (AWC+,RIA+)*) and *glc-3* mutants changed more than that of wild-type animals (9.8% ± 0.8% for double mutants and 7% ± 0.7% for wild-type animals at 90S), similar to those in both single mutants (10% ± 0.6% for transgenic *eat-4* mutants and 10% ± 0.8% for *glc-3* mutants at 90S) (Figure 35 A and B), thereby indicating the same hyper-responsiveness of double mutants to thermal stimuli as both single mutants. By contrast, FRET ratios in AIY neurons of the double mutants (*eat-4 (AFD+,RIA+); glc-3*) constructed from the *eat-4* mutants expressing EAT-4 in AFD and RIA (*eat-4 (AFD+,RIA+)*) and *glc-3* mutants showed the change in-between those in both single mutants (7.6% ± 0.4% for double mutants, 3.3% ± 0.9% for transgenic *eat-4* mutants, and 10% ± 0.8% for *glc-3* mutants at 90S) (Figure 35 C and D). These physiological results are consistent with the results obtained by genetic analysis, further implicating the molecular model that GLC-3 inhibits AIY interneurons upon receiving EAT-4 dependent glutamate signals from AFD neurons.

Discussion

EAT-4/VGLUT dependent glutamatergic neurotransmission in the thermotaxis neural circuit

In the current model for temperature sensing, thermal stimuli are transduced in AFD through three functionally redundant guanylyl cyclases and cGMP-gated channels (Figure 4A; Inada et al, 2006; Komatsu et al, 1996) and in AWC through heterotrimeric G protein signaling and cGMP-gated channels (Figure 4B; Kuhara et al, 2008). In this study, our results suggest a model for signaling pathways downstream of temperature sensing (Figure 36). After temperature sensing in AFD and AWC sensory neurons, thermosensory information is transmitted to postsynaptic interneuron AIY through EAT-4/VGLUT dependent glutamatergic neurotransmission. EAT-4 dependent glutamate signals from AFD inhibit AIY through activation of inhibitory glutamate receptor GLC-3/GluCl, thereby inducing migration toward colder temperature. By contrast, EAT-4 dependent glutamate signals from AWC stimulate AIY to induce migration toward warmer temperature. Hence, we demonstrated that the bidirectional regulation of AIY through EAT-4 dependent glutamate transmissions from AFD and AWC is essential for terminal behavioral phenotypes.

Previous reports showed that AFD and AWC differ in contribution for thermotaxis; AFD-ablated animals exhibited severe defect (Kuhara et al, 2008;

Mori & Ohshima, 1995), whereas AWC-ablated animals exhibited slight defect in thermotaxis (Biron et al, 2008; Kuhara et al, 2008). These results suggested that thermotaxis is regulated by the orchestrated information in major thermosensory neuron AFD and supportive thermosenosry neuron AWC. Consistent with these previous results, our behavioral and calcium imaging results demonstrated that contributions of inhibitory glutamate signals from AFD and excitatory glutamate signals from AWC are not equivalent. For IT (isothermal tracking) behavior, EAT-4 dependent glutamate transmission from AFD was indispensable, while that from AWC was not necessary (Figure 15). In addition, transgenic *eat-4* mutants expressing EAT-4 in AFD, AWC, and RIA showed strong tendency to migrate toward colder temperature except for the case where the introduction dose of *AFDp::eat-4 cDNA* to the *eat-4* mutants was reduced to less than one tenth of *AWCp::eat-4 cDNA* (Figure 17). Further, glutamate transmission from AFD inhibits AIY activity in response to both warming and cooling and that from AWC stimulates AIY activity in response to only warming (Figure 21 and 25), suggesting that the contribution of inhibitory glutamate signals from AFD is larger than that of excitatory glutamate signals from AWC. Our study also showed that well-balanced glutamate signals from AFD and AWC could drive nearly normal responsiveness of AIY to temperature changes and eventual normal thermotaxis (Figure 17 and 26). Taken together, glutamate signals from AFD and AWC are implied to be the critical factor for mediating the orchestration of major information in AFD and supportive information in AWC. Also, our study demonstrated that GLC-3 receives EAT-4 dependent glutamate signals from AFD, although glutamate receptors that

receive glutamate signals from AWC remained to be identified. The failure of finding excitatory glutamate receptors may possibly be caused by the difference in contribution between AFD and AWC for thermotaxis, thus reflecting the biased detection ability of thermotaxis defect toward AFD over AWC.

Signal transduction from RIA interneurons to postsynaptic motor neurons

The RIA interneuron, known as one of the most pivotal interneurons in *C. elegans*, integrates signals processed in the thermotaxis neural circuit and emits outputs to downstream neurons (Figure 3; Mori & Ohshima, 1995; Tanizawa et al, 2006). Given those previous reports, our work revealed that multiple transmissions include EAT-4 dependent glutamate from RIA are involved in communicating processed information in the circuit to downstream neurons, thereby generating ultimate thermotactic outputs (Figure 15 and 36). Although there are no solid evidences as to which neurons downstream of RIA are main component neurons in the circuit, RIA is heavily connected with numerous presynapses to SMD and RMD head motorneurons that regulate turning behavior (Figure 37; Gray et al, 2005; White et al, 1986). Considering that temperature regulates turn frequency and run duration (Zariwala et al, 2003), it is quite likely that SMD and RMD control turn frequency, depending on thermal information transmitted by RIA. We expect that inspection of glutamate transmission from RIA to SMD or RMD, including identification of glutamate receptors functioning in SMD or RMD for thermotaxis, reveal the information processing that consequently generates a variety of thermotactic behavioral

outputs.

Information processing in the simple circuit composed of AFD, AWC, and AIY neurons

Mori and Ohshima (1995) proposed the neural circuit for thermotaxis, in which AFD thermosensory neurons transmit excitatory signal to AIY interneurons. Consistent with this proposal, Clark et al, (2006) showed with calcium imaging that AIY of animals lacking AFD did not respond to temperature changes. Given these results and our results on EAT-4, one can propose that the neural signals transmitted from AFD to AIY are of at least two kinds, EAT-4 dependent inhibitory signals and EAT-4 independent excitatory signals. In the present study, we further showed that the thermotactic abnormality of *gcy-23 gcy-8 gcy-18* triple mutants with defective AFD function is considerably different from that of the *eat-4* mutants expressing EAT-4 in AWC and RIA but not in AFD (*eat-4 (AWC+,RIA+)*) (Figure 33), and that AIY of *eat-4* mutants are hyper-responsive to temperature change than wild-type animals (Figure 21), thereby undoubtedly implicating EAT-4 independent excitatory signals from AFD to AIY. Recent electrophysiological study showing that AFD responds to both cooling and warming (Ramot et al, 2008) is consistent with these results.

Our results also suggest that AWC transmit excitatory signals to AIY through EAT-4 dependent glutamatergic neurotransmission (Figure 21), although we previously reported that hyper-responsiveness of AWC to temperature change

induced lower-responsiveness of AIY (Kuhara et al, 2008). It is probable that AWC transmits EAT-4 independent inhibitory signals in addition to EAT-4 dependent excitatory glutamate signals to AIY, which is reminiscent of the regulation of behavioral response to odorants, where AWC releases both glutamate and neuropeptide NLP-1 to postsynaptic AIA interneurons (Chalasani et al, 2010).

AWC senses odorants as well as temperature (Bargmann et al, 1993; Kuhara et al, 2008). How does *C. elegans* distinguish these qualitatively different signals within a sensory neuron? Similar to thermal signal, olfactory signal is transduced through G protein signaling and cGMP-gated channels in AWC, and is further transmitted to AIY through EAT-4 dependent glutamatergic neurotransmission (Chalasani et al, 2007; Coburn & Bargmann, 1996; L'Etoile & Bargmann, 2000; Roayaie et al, 1998). Intriguingly, olfactory signal from AWC inhibits AIY upon reception of glutamate signal by GLC-3/GluCl (Chalasani et al, 2007), whereas, as shown in this study, thermal signal from AWC stimulates AIY through putative glutamate receptors other than GLC-3/GluCl. Hence, our results demonstrated that segregation of different sensory signals such as olfactory and thermosensory signals is mediated through not only distinct signal transductions in a sensory neuron, but also discrete neurotransmissions in downstream neural circuits.

We demonstrated one of the simplest neural circuits consisting of two different sensory neurons and a single postsynaptic interneuron, where AFD and AWC

sensory neurons utilize the same EAT-4/VGLUT dependent glutamatergic neurotransmission to inhibit or stimulate the postsynaptic neuron AIY, respectively. The balance between inhibition and stimulation of the AIY activity significantly affected thermotactic behavior. Strong EAT-4 dependent glutamatergic transmission from AFD enhanced the tendency for animals to migrate toward colder temperature than the cultivation temperature, while weak EAT-4 dependent transmission from AFD relative to AWC weakened the tendency to migrate colder temperature and rather strengthened the tendency to migrate toward warmer temperature than the cultivation temperature. Thus, two synaptic transmissions encoding opposite information flows regulate neural activities to generate various behavioral outputs. Recently, from the network theory perspective, it was proposed that elucidation of information processing in simple network motifs reveal information processing in neural network of vertebrates (Milo et al, 2002). Studies on synaptic transmission in the simple neural circuit consisting of AFD, AWC, and AIY should shed light onto information processing underlying vertebrate intertwined neural networks.

Materials and methods

Strains and genetics

The techniques used for culturing and handling *C. elegans* were essentially as described by Brenner (1974). We used the following strains: wild-type *C. elegans* variety Bristol strain (N2), IK604 *eat-4(ky5)* III, IK600 *eat-4(nj2)* III, IK602 *eat-4(nj6)* III, KP4 *glr-1(n2461)* III, IK703 *avr-14(ad1302)* I, IK708 *glc-3(ok321)* V, IK732 *mgl-1(tm1811)* X, IK712 *mgl-2(tm355)* I, IK706 *mgl-3(tm1766)* IV, IK726 *mgl-2(tm355)* I; *mgl-1(tm1811)* X, IK728 *mgl-3(tm1766)* IV; *mgl-1(tm1811)* X, IK724 *mgl-2(tm355)* I; *mgl-3(tm1766)* IV, IK736 *mgl-2(tm355)* I; *mgl-3(tm1766)* IV; *mgl-1(tm1811)* X, CB1265 *unc-104(e1265)* II, IK589 *ttx-7(nj50)* I, IK597 *gcy-23(nj37) gcy-8(oy44) gcy-18(nj38)* IV, MT3644 *odr-3(n1605)* V, IK839 *eat-16(nj8)* I, IK813 *gcy-23(nj37) gcy-8(oy44) gcy-18(nj38)* IV; *glc-3(ok321)* V, IK815 *glc-3(ok321) odr-3(n1605)* V, IK840 *eat-16(nj8)* I; *glc-3(ok321)* V, IK818 eat-4*(ky5); Ex[gcy-8p::eat-4* cDNA, *glr-3p::eat-4* cDNA, *ges-1p::NLS-GFP]* designated as *eat-4 (AFD+,RIA+)*, IK819 *eat-4(ky5); Ex[odr-3p::eat-4* cDNA, *glr-3p::eat-4* cDNA, *ges-1p::NLS-GFP]* designated as *eat-4 (AWC+,RIA+)*, IK820 *eat-4 (AFD+,RIA+)* III*; glc-3(ok321)* V, IK822 *eat-4 (AWC+, RIA+)* III*; glc-3(ok321)* V, and many transgenic strains derived from them. *eat-4(nj2)* and *eat-4(nj6)* were isolated in genetic screens as described by Okochi et al, (2005). The isolated *eat-4* mutants were outcrossed to wild-type animals more than six times before the analyses.

The individual TTX assay

The individual thermotaxis (TTX) assay was performed using a 9-cm agar plate and a vial containing frozen acetic acid, as described by Mori and Ohshima (1995) and Mohri et al, (2005). The L4 larvae (12-24 animals per 6-cm plate) were cultured with food (*E. coli* strain OP50) at 20°C for 8-16 hours under uncrowded condition. In this study, we used a 45-ml glass vial (Wheaton) for creating the radial temperature gradient on the assay plate, where fully matured, actively egg-laying adult animals were allowed to move freely for 60 minutes. The results of the assays were calculated as the percentages of animals showing isothermal tracking (IT).

The thermotaxis assay on a radial thermal gradient shown in Figure5A and 13 was performed as the individual TTX assay with some modification. The L4 larvae were cultured with food (*E. coli* strain OP50) at the designated temperature (17°C, 20°C, or 23°C). The results of thermotaxis assays were calculated as the percentages of animals that migrated to their cultivation temperature.

The population TTX assay

The population TTX assay was performed as previously reported (Ito et al, 2006). Equipment for establishing the linear thermal gradient was used as essentially described by Hedgecock and Russell (1975). A stable, linear thermal gradient was established on a 60-cm long aluminum platform, one end of which

was placed in a water bath at 5°C and the opposite end in a water bath at 35°C. TTX plate (13.5 cm×6 cm, 1.8 cm height) containing 10 ml of TTX medium (3g/l NaCl, 20g/l Bacto Agar, 25mM KPO_4) with 2% agar was placed on the aluminum platform such that temperature gradient could be established along the agar surface of 13.5cm long. The extra space between the bottom of the TTX plate and the aluminum platform was filled with water to increase thermal conductivity as much as possible. The center of the 13.5 cm long-agar surface in TTX plate was adjusted at 20°C and the TTX plate was maintained for 15 min before a linear thermal gradient ranging from approximately 17°C to 23°C was established on the agar surface. Uncrowded and well-fed animals were used for the TTX assay. A single adult animal was placed on a 6-cm plate containing 14 ml of nematode growth medium (NGM) with 2% agar, on which *E. coli* OP50 was seeded; the animal and its progeny were cultured at respective temperature. The animals were collected with 1ml of NG buffer (0. 3% NaCl, 1 mM $CaCl_2$, 1 mM $MgSO_4$, 25 mM potassium phosphate, pH 6.0) kept at 20°C and were washed twice with NG buffer at 20°C. Approximately 50–200 animals were placed at the center of the TTX plate. Excess water surrounding the animals was removed with tissue paper. After 60 minutes, the animals were immobilized by placing TTX plates at 4°C over night, and the animals in each of the eight regions were scored (Figure 2A). The TTX index was calculated as shown in Figure 2C.

Counting bends

Counting bends was performed as described by Segalat et al. (1995). Animals cultured with OP50 at 20°C were analyzed at room temperature (about 22 to 24°C) on 6cm agar plates (2% agar, 1mM $CaCl_2$, 1mM $MgSO_4$, 25mM pH 6.0 potassium phosphate) containing OP50. Two minutes after transfer to agar plates, the number of body bends was counted for one minute.

Molecular Biology

The *eat-4* genomic fragment including 2.4 kb or 5.5 kb of the promoter region and 2 kb of the downstream region was amplified by PCR from N2 genome. The *full length eat-4::gfp* translational fusion gene fragment, which was amplified by PCR from N2 genome and pPD95.75, contains 5.5 kb fragment upstream of *eat-4* gene, *eat-4* gene (4.5 kb) including all exons and introns, gfp (0.9 kb), and 2 kb fragment downstream of *eat-4* gene.

For cell-specific rescue experiments, *cell-specific promoter::eat-4* cDNA construct, *cell-specific promoter::avr-14* cDNA constructs, *cell-specific promoter::mgl-3* cDNA construct, and *cell-specific promoter::glc-3* cDNA construct were generated. *eat-4* cDNA was PCR-amplified by using tagged primers from yk32h2 EST clone that contains *eat-4* cDNA lacking initial 7 bp, and was cloned into pPD49.26 to generate pNR8. One type of *avr-14* cDNAs (*avr-14a* cDNA)were PCR-amplified by using tagged primers from yk1522g07 EST clone that contains full-length *avr-14a* cDNA with putative sixth intron, and was cloned into pPD49.26 to

generate pNR57. The other type of *avr-14* cDNAs (*avr-14b* cDNA) were PCR-amplified by using tagged primers from yk1522g07 EST clone and yk1592d04 EST clone that contains *avr-14b* cDNA lacking three exons, and was cloned into pPD49.26 to generate pNR59. *mgl-3* cDNA was made artificially in accordance with putative *mgl-3* cDNA shown in the *C. elegans* genome database by GenScript Corporation, USA, and was cloned into pPD49.26 to generate pNR94. *glc-3* cDNA was PCR-amplified from yk1649c11 EST clone that contains full-length *glc-3* cDNA, and was cloned into pPD49.26 to generate pNR56. The resultant plasmids were confirmed to contain the intact cDNA by sequencing. All plasmids used for cell-specific rescue experiments were generated by inserting cell-specific promoter fragments into pNR8, pNR57, pNR59, pNR94 or pNR56. All cell-specific promoter constructs were previously generated by PCR to contain only non-coding region. Before conducting the rescue experiments, expression patterns of *cell-specific promoter::gfp* constructs were verified by examining GFP fluorescence. Cell-specific promoters are 0.7 kb of *gcy-8p* for AFD, 2.3 kb of *odr-3p* for AWC which also induces expression slightly in AWB, 0.8 kb of *ttx-3p* for AIY, 1.9 kb of *glr-3p* for RIA, 1.4 kb of *lin-11p* for AIZ which also induces expression in ADF, AVJ, AVH, AVG, ADL and RIC, 2.1 kb of *osm-6p* for sensory neurons, 5.3 kb of *glr-1p* for motor and command neurons, and 1.4 kb of *unc-14p* for all neurons.

For calcium imaging of AIY, *ttx-3p::yc3.60* construct was generated. yellow cameleon 3.60 was amplified from YC3.60/pcDNA3 (Nagai et al, 2004) and cloned into pPD49.26 to generate pNR46. *ttx-3p* fragment was inserted into

pNR46 to generate *ttx-3p::yc3.60* (pNR86). The resultant plasmid was confirmed to contain the intact *ttx-3p::yc3.60* by sequencing.

Transgenic animals

Germline transformation was performed by co-injecting experimental DNA (0.2-100 ng/ul) and an injection marker pKDK66 *ges-1p::NLS-GFP* (50 ng/ul) or pNAS88 *ges-1p::NLS TagRFP* (50 ng/ul) into the gonad (Mello et al, 1991). Multiple independent transgenic lines were established for each experimental DNA. For comparison of phenotypes on different genetic backgrounds, transgenic arrays were transferred by intercrossing.

***In vivo* calcium imaging and data analysis**

In vivo calcium imaging was performed essentially according to previous reports with some modifications (Kimura et al, 2004; Kuhara et al, 2008). After cultivated at 20°C, well-fed animals expressing *ttx-3p::yc3.60* were glued onto a 1.5% agar pad on glass, immersed in M9 buffer, and covered by cover glass. The agar pad and M9 buffer were kept at the initial imaging temperature. Sample preparation was completed within 2 min. The sample was then placed onto a peltier-based thermocontroller (Tokai Hit, Japan) on the stage of an Olympus BX61WI at the initial imaging temperature for 2 min, and fluorescence was introduced into a Dual-View (Molecular devices, USA) optics systems. Cyan fluorescent protein (CFP; F480) and yellow fluorescent protein (YFP; F535)

images were simultaneously captured by an EM-CCD camera C9100-13 ImagEM (Hamamatsu Photonics). Images were taken with a 500-ms exposure time with 2×2 binning. The temperature on the agar pad was monitored by a thermometer system, DCM-20 (Tokai Hit and Hamamatsu Photonics). For each imaging experiment, fluorescence intensities of F535 and F480 were measured using MetaMorph imaging analysis system (Molecular Device). Since a computer regulates all the recorded images and the outcome of the analysis, any intention of a researcher should be excluded. Relative increases or decreases in the intracellular calcium concentration were measured as increases or decreases in the YFP/CFP fluorescence ratio of the cameleon protein (Ratio Change).

Oligonucleotide primers and usage of them

For detection of *eat-4(nj2)* mutation by PCR

nri005: GCTTGTCAGAAGACAAGTGC

nri017: ACAAAAAATCTCAAAAGAAACTCACTTGGCGAGTGGAGCT

PCR extension time: 40sec

To detect *nj2* mutation, digest PCR fragments with SacI.

For detection of *eat-4(nj6)* mutation by PCR

nri019: TCACTTTACTGGAGTCACTTTTTATGCTGTCTATGCCTGC

nri021: TTTACCTGGAGCCGCCTGAG

PCR extension time: 40sec

To detect *nj6* mutation, digest PCR fragments with PstI.

For detection of *eat-4(ky5)* mutation by PCR

nri005: GCTTGTCAGAAGACAAGTGC

nri006: CGATGCAATTTCGGTGCAGC

nri014: GTTATCTTGACCGGAGAACC

PCR extension time: 60sec

Two amount of nri014 (10uM), one amount of nri005 and nri006 (5uM) are mixed and used for PCR.

For detection of *avr-14(ad1302)* mutation by PCR

nri099: TTCGAGAAGTTGGCAAGTCG

nri100: TGAATCGGCAGGTTCAGGAG

PCR extension time: 40sec

To detect *ad1302* mutation, digest PCR fragments with XbaI.

For detection of *glc-3(ok321)* mutation by PCR

nri097: TCAAAATACAGGGGTAGGCG

nri098: ACAATTCCTGGAACTCACGG

PCR extension time: 180sec

For detection of *mgl-1(tm1811)* mutation by PCR

nri107: CATCATCTGGACATATCGCT

nri108: AATGCACCGAGGCTGAATTA

PCR extension time: 150sec

For detection of *mgl-2(tm355)* mutation by PCR

nri105: ACATAGCCTTCAAGCCGAGA

nri106: GGATTGGATCTGATGGATGG

PCR extension time: 40sec

For detection of *mgl-3(tm1766)* mutation by PCR

nri091: TGCTGGAAGTCAAGTCAGTG

nri092: CCACCAGACAACCTGCAAGC

nri093: CCACAACAGTGGAATGCGAC

PCR extension time: 180sec

Two amount of nri093 (10uM), one amount of nri091 and nri092 (5uM) are mixed and used for PCR.

Statistics

All error bars in the Figures indicate standard error of mean (SEM). Results of behavioral experiments were treated as parametric data. The statistical analysis for all behavioral experiments was performed by one-way analysis of variance (ANOVA) for multiple comparisons. Comparisons between each result were followed by post hoc Tukey-Kramer test, except for data sets including results of “0 %”. Results of calcium imaging were treated as nonparametric data. The statistical analysis for all calcium imaging was performed by Steel-Dwass tests.

A single asterisk (*), double asterisk (**), and nonsignificant (n.s.) in the Figures indicate $p < 0.05$, $p < 0.01$, and $p > 0.05$, respectively.

Acknowledgments

I want to express my greatest thanks to I. Mori for her guidance throughout my work. I thank A. Kuhara for various methods, protocols, and appropriate suggestions; F. Nakamura for a part of outcrosses and TTX assays; Y. Okochi for isolation of *eat-4(nj2)* and *eat-4(nj6)* mutants; H. Inada for sharing unpublished results; M. Okumura for various technical advices; Y. Tanizawa for *glc-3* promoter; N. Nishio for *ges-1p::NLS TagRFP* and sharing unpublished results of TTX assays; A. Miyawaki for yc3.60 construct; A. Fire for pPD plasmids; J. McGree for *ges-1* promoter; L. Avery for *eat-4(ky5)* mutant; S. Mitani at the National Bioresource Project (Japan) and *Caenorhabditis* Genetic Center for strains; the *C. elegans* Sequence Consortium for updating the *C. elegans* genome information; all members of Mori laboratory for comments on my study and stimulating discussion. This study was supported by the Japan Society for the Promotion of Science.

Finally, let me express my heartfelt appreciation to my family and all friends for their extensive support.

References

Bargmann C, Hartwieg E, Horvitz H (1993) Odorant-selective genes and neurons mediate olfaction in C. elegans. *Cell* **74:** 515-527

Bellocchio E, Reimer R, Fremeau RJ, Edwards R (2000) Uptake of glutamate into synaptic vesicles by an inorganic phosphate transporter. *Science* **289:** 957-960

Biron D, Wasserman S, Thomas J, Samuel A, Sengupta P (2008) An olfactory neuron responds stochastically to temperature and modulates Caenorhabditis elegans thermotactic behavior. *Proc Natl Acad Sci U S A* **105:** 11002-11007

Brenner S (1974) The genetics of Caenorhabditis elegans. *Genetics* **77:** 71-94

Brockie P, Maricq A (2003) Ionotropic glutamate receptors in Caenorhabditis elegans. *Neurosignals* **12:** 108-125

Chalasani S, Chronis N, Tsunozaki M, Gray J, Ramot D, Goodman M, Bargmann C (2007) Dissecting a circuit for olfactory behaviour in Caenorhabditis elegans. *Nature* **450:** 63-70

Chalasani S, Kato S, Albrecht D, Nakagawa T, Abbott L, Bargmann C (2010) Neuropeptide feedback modifies odor-evoked dynamics in Caenorhabditis elegans olfactory neurons. *Nat Neurosci* **13:** 615-621

Chalfie M, Tu Y, Euskirchen G, Ward WW, Prasher DC (1994) Green fluorescent protein as a marker for gene expression. *Science* **263:** 802-805

Clark D, Biron D, Sengupta P, Samuel A (2006) The AFD sensory neurons encode multiple functions underlying thermotactic behavior in Caenorhabditis elegans. *J Neurosci* **26:** 7444-7451

Clark D, Gabel C, Lee T, Samuel A (2007) Short-term adaptation and temporal processing in the cryophilic response of Caenorhabditis elegans. *J Neurophysiol* **97:** 1903-1910

Coburn C, Bargmann C (1996) A putative cyclic nucleotide-gated channel is required for sensory development and function in C. elegans. *Neuron* **17:** 695-706

de Bono M, Maricq A (2005) Neuronal substrates of complex behaviors in C. elegans. *Annu Rev Neurosci* **28:** 451-501

Dent J, Davis M, Avery L (1997) avr-15 encodes a chloride channel subunit that mediates inhibitory glutamatergic neurotransmission and ivermectin sensitivity in Caenorhabditis elegans. *EMBO J* **16:** 5867-5879

Dent JA, Smith MM, Vassilatis DK, Avery L (2000) The genetics of ivermectin resistance in Caenorhabditis elegans. *Proc Natl Acad Sci U S A* **97:** 2674-2679

Di Maio V (2008) Regulation of information passing by synaptic transmission: a short review. *Brain Res* **1225:** 26-38

Dillon J, Hopper N, Holden-Dye L, O'Connor V (2006) Molecular characterization of the metabotropic glutamate receptor family in Caenorhabditis elegans. *Biochem Soc Trans* **34:** 942-948

Gomez M, De Castro E, Guarin E, Sasakura H, Kuhara A, Mori I, Bartfai T, Bargmann C, Nef P (2001) Ca2+ signaling via the neuronal calcium sensor-1 regulates associative learning and memory in C. elegans. *Neuron* **30:** 241-248

Gray J, Hill J, Bargmann C (2005) A circuit for navigation in Caenorhabditis elegans. *Proc Natl Acad Sci U S A* **102:** 3184-3191

Hall D, Hedgecock E (1991) Kinesin-related gene unc-104 is required for axonal transport of synaptic vesicles in C. elegans. *Cell* **65:** 837-847

Hart A, Sims S, Kaplan J (1995) Synaptic code for sensory modalities revealed by C. elegans GLR-1 glutamate receptor. *Nature* **378:** 82-85

Hedgecock E, Russell R (1975) Normal and mutant thermotaxis in the nematode

Caenorhabditis elegans. *Proc Natl Acad Sci U S A* **72:** 4061-4065

Hills T, Brockie P, Maricq A (2004) Dopamine and glutamate control area-restricted search behavior in Caenorhabditis elegans. *J Neurosci* **24:** 1217-1225

Hobert O, Mori I, Yamashita Y, Honda H, Ohshima Y, Liu Y, Ruvkun G (1997) Regulation of interneuron function in the C. elegans thermoregulatory pathway by the ttx-3 LIM homeobox gene. *Neuron* **19:** 345-357

Horoszok L, Raymond V, Sattelle D, Wolstenholme A (2001) GLC-3: a novel fipronil and BIDN-sensitive, but picrotoxinin-insensitive, L-glutamate-gated chloride channel subunit from Caenorhabditis elegans. *Br J Pharmacol* **132:** 1247-1254

Inada H, Ito H, Satterlee J, Sengupta P, Matsumoto K, Mori I (2006) Identification of guanylyl cyclases that function in thermosensory neurons of Caenorhabditis elegans. *Genetics* **172:** 2239-2252

Ito H, Inada H, Mori I (2006) Quantitative analysis of thermotaxis in the nematode Caenorhabditis elegans. *J Neurosci Methods* **154:** 45-52

Kerr R, Lev-Ram V, Baird G, Vincent P, Tsien R, Schafer W (2000) Optical imaging of calcium transients in neurons and pharyngeal muscle of C. elegans. *Neuron* **26:** 583-594

Kimura K, Miyawaki A, Matsumoto K, Mori I (2004) The C. elegans thermosensory neuron AFD responds to warming. *Curr Biol* **14:** 1291-1295

Komatsu H, Mori I, Rhee J, Akaike N, Ohshima Y (1996) Mutations in a cyclic nucleotide-gated channel lead to abnormal thermosensation and chemosensation in C. elegans. *Neuron* **17:** 707-718

Kuhara A, Inada H, Katsura I, Mori I (2002) Negative regulation and gain control of sensory neurons by the C. elegans calcineurin TAX-6. *Neuron* **33:** 751-763

Kuhara A, Okumura M, Kimata T, Tanizawa Y, Takano R, Kimura K, Inada H, Matsumoto K, Mori I (2008) Temperature sensing by an olfactory neuron in a circuit controlling behavior of C. elegans. *Science* **320:** 803-807

L'Etoile N, Bargmann C (2000) Olfaction and odor discrimination are mediated by the C. elegans guanylyl cyclase ODR-1. *Neuron* **25:** 575-586

Lee R, Sawin E, Chalfie M, Horvitz H, Avery L (1999) EAT-4, a homolog of a mammalian sodium-dependent inorganic phosphate cotransporter, is necessary for glutamatergic neurotransmission in caenorhabditis elegans. *J Neurosci* **19:** 159-167

Mello C, Kramer J, Stinchcomb D, Ambros V (1991) Efficient gene transfer in C.elegans: extrachromosomal maintenance and integration of transforming sequences. *EMBO J* **10:** 3959-3970

Milo R, Shen-Orr S, Itzkovitz S, Kashtan N, Chklovskii D, Alon U (2002) Network motifs: simple building blocks of complex networks. *Science* **298:** 824-827

Miyawaki A, Llopis J, Heim R, McCaffery J, Adams J, Ikura M, Tsien R (1997) Fluorescent indicators for Ca2+ based on green fluorescent proteins and calmodulin. *Nature* **388:** 882-887

Mohri A, Kodama E, Kimura K, Koike M, Mizuno T, Mori I (2005) Genetic control of temperature preference in the nematode Caenorhabditis elegans. *Genetics* **169:** 1437-1450

Mori I, Ohshima Y (1995) Neural regulation of thermotaxis in Caenorhabditis elegans. *Nature* **376:** 344-348

Nagai T, Yamada S, Tominaga T, Ichikawa M, Miyawaki A (2004) Expanded dynamic range of fluorescent indicators for Ca(2+) by circularly permuted yellow fluorescent proteins. *Proc Natl Acad Sci U S A* **101:** 10554-10559

Nakajima Y, Iwakabe H, Akazawa C, Nawa H, Shigemoto R, Mizuno N, Nakanishi S (1993) Molecular characterization of a novel retinal metabotropic glutamate receptor mGluR6 with a high agonist selectivity for L-2-amino-4-phosphonobutyrate. *J Biol Chem* **268:** 11868-11873

Nakanishi S (1994) Metabotropic glutamate receptors: synaptic transmission, modulation, and plasticity. *Neuron* **13:** 1031-1037

Ni B, Rosteck PJ, Nadi N, Paul S (1994) Cloning and expression of a cDNA encoding a brain-specific Na(+)-dependent inorganic phosphate cotransporter. *Proc Natl Acad Sci U S A* **91:** 5607-5611

Nonet ML (1999) Visualization of synaptic specializations in live C. elegans with synaptic vesicle protein-GFP fusions. *J Neurosci Methods* **89:** 33-40

Okochi Y, Kimura K, Ohta A, Mori I (2005) Diverse regulation of sensory signaling by C. elegans nPKC-epsilon/eta TTX-4. *EMBO J* **24:** 2127-2137

Otsuka A, Jeyaprakash A, García-Añoveros J, Tang L, Fisk G, Hartshorne T, Franco R, Born T (1991) The C. elegans unc-104 gene encodes a putative kinesin heavy chain-like protein. *Neuron* **6:** 113-122

Ramot D, MacInnis B, Goodman M (2008) Bidirectional temperature-sensing by a single thermosensory neuron in C. elegans. *Nat Neurosci* **11:** 908-915

Rankin C, Wicks S (2000) Mutations of the caenorhabditis elegans brain-specific inorganic phosphate transporter eat-4 affect habituation of the tap-withdrawal response without affecting the response itself. *J Neurosci* **20:** 4337-4344

Roayaie K, Crump J, Sagasti A, Bargmann C (1998) The G alpha protein ODR-3 mediates olfactory and nociceptive function and controls cilium morphogenesis in C. elegans olfactory neurons. *Neuron* **20:** 55-67

Satterlee JS, Sasakura H, Kuhara A, Berkeley M, Mori I, Sengupta P (2001) Specification of thermosensory neuron fate in C. elegans requires ttx-1, a homolog of otd/Otx. *Neuron* **31:** 943-956

Sulston J, Horvitz H (1977) Post-embryonic cell lineages of the nematode, Caenorhabditis elegans. *Dev Biol* **56:** 110-156

Sulston J, Schierenberg E, White J, Thomson J (1983) The embryonic cell lineage of the nematode Caenorhabditis elegans. *Dev Biol* **100:** 64-119

Ségalat L, Elkes D, Kaplan J (1995) Modulation of serotonin-controlled behaviors by Go in Caenorhabditis elegans. *Science* **267:** 1648-1651

Takamori S, Rhee J, Rosenmund C, Jahn R (2000) Identification of a vesicular glutamate transporter that defines a glutamatergic phenotype in neurons. *Nature* **407:** 189-194

Tanizawa Y, Kuhara A, Inada H, Kodama E, Mizuno T, Mori I (2006) Inositol monophosphatase regulates localization of synaptic components and behavior in the mature nervous system of C. elegans. *Genes Dev* **20:** 3296-3310

Wenick A, Hobert O (2004) Genomic cis-regulatory architecture and trans-acting regulators of a single interneuron-specific gene battery in C. elegans. *Dev Cell* **6:** 757-770

White J, Southgate E, Thomson J, Brenner S (1986) The Structure of the Nervous System of the Nematode Caenorhabditis elegans. *Phil Trans Royal Soc London Series B, Biol Scien* **314:** 1-340

Yates D, Portillo V, Wolstenholme A (2003) The avermectin receptors of Haemonchus contortus and Caenorhabditis elegans. *Int J Parasitol* **33:** 1183-1193

Zariwala H, Miller A, Faumont S, Lockery S (2003) Step response analysis of thermotaxis in Caenorhabditis elegans. *J Neurosci* **23:** 4369-4377

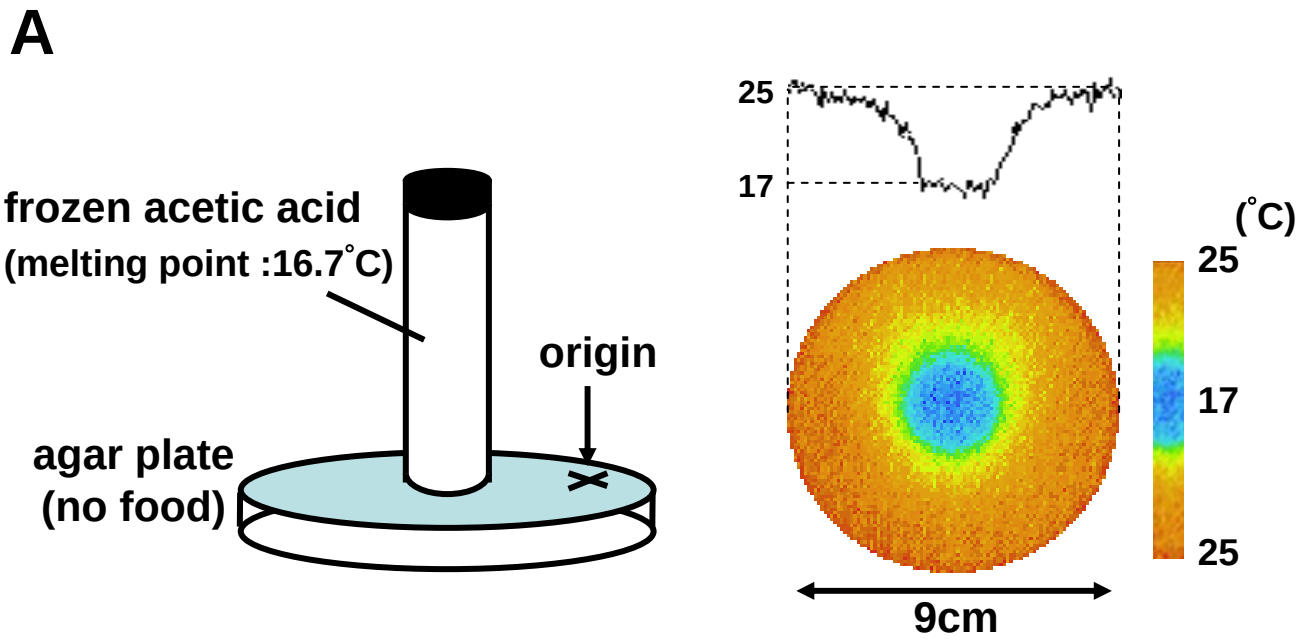

Figure 1. Individual TTX assay
(A) Procedures for individual TTX assay. A stable radial thermal gradient with 17˚C at the center and 25˚C at the periphery (9cm-diameter) was established by using a glass vial containing frozen acetic acid and keeping room temperature at 25℃. Adult animals were individually placed on a radial thermal gradient (origin) and were allowed to move freely for 60 minutes.
(B) Thermotaxis tracks of wild-type animals after cultivation at 23˚C, 20˚C, and 17˚C on a radial thermal gradient. Most wild-type animals migrated to their cultivation temperature and moved isothermally on a radial thermal gradient.

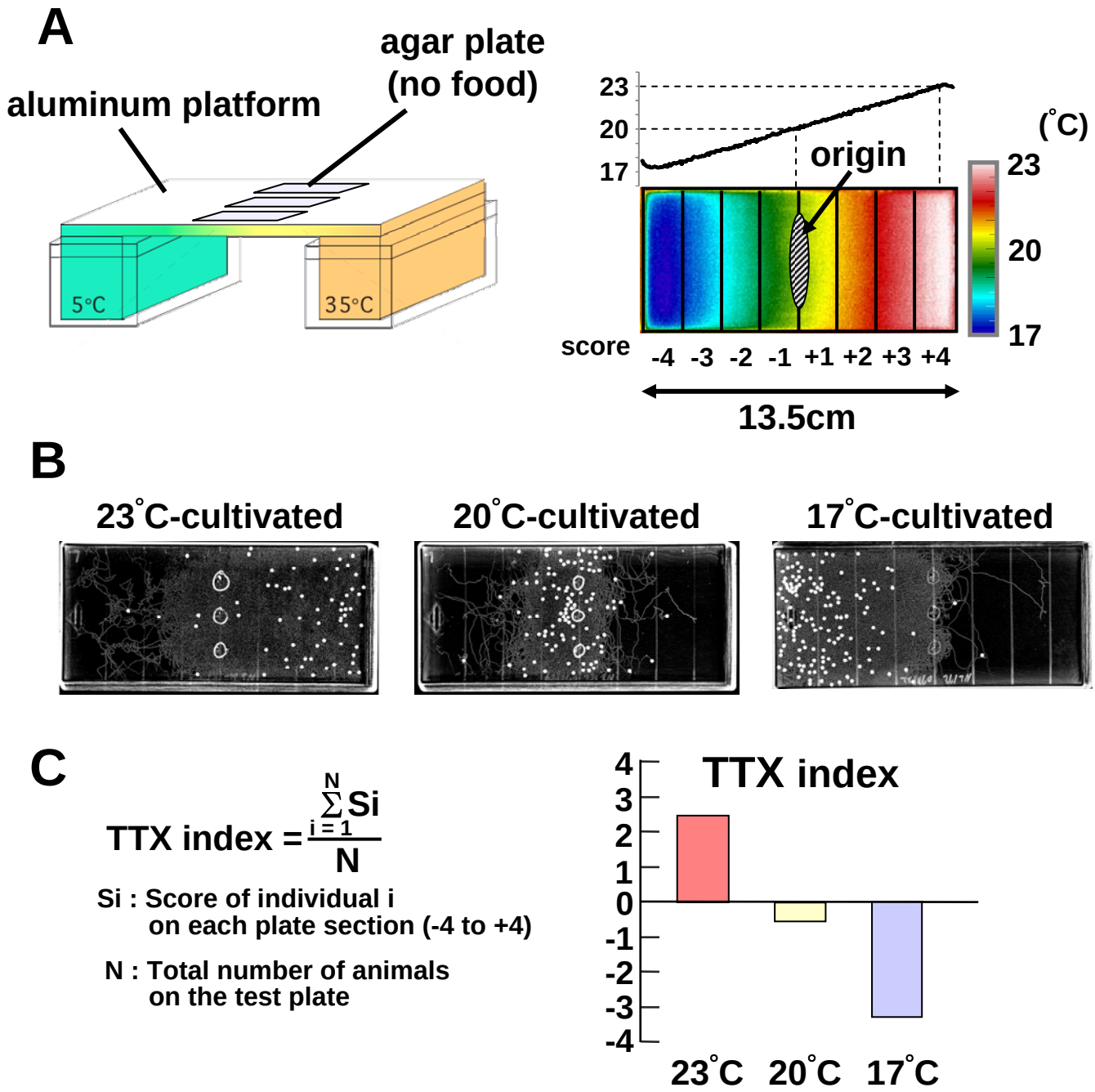

Figure 2. Population TTX assay

(A) Procedures for population TTX assay. A stable linear thermal gradient from 17°C to 23°C (13.5cm) was established on a 60-cm long aluminum platform, one end of which was placed in a water bath at 5°C and the opposite end in a water bath at 35°C. About 50-200 animals were placed on the agar surface of 20°C (origin) and allowed to move freely for 60 minutes. The steepness of the temperature gradient was stably kept at 0.45°C/cm.

(B) Thermotaxis tracks of wild-type animals after cultivation at 23°C, 20°C, and 17°C on a linear thermal gradient. Most wild-type animals migrated to their cultivation temperature (white dots).

(C) The thermotactic behavior was quantified as TTX index. Red bars, yellow bars, and blue bars represent TTX indices of animals cultivated at 23°C, 20°C, and 17°C, respectively.

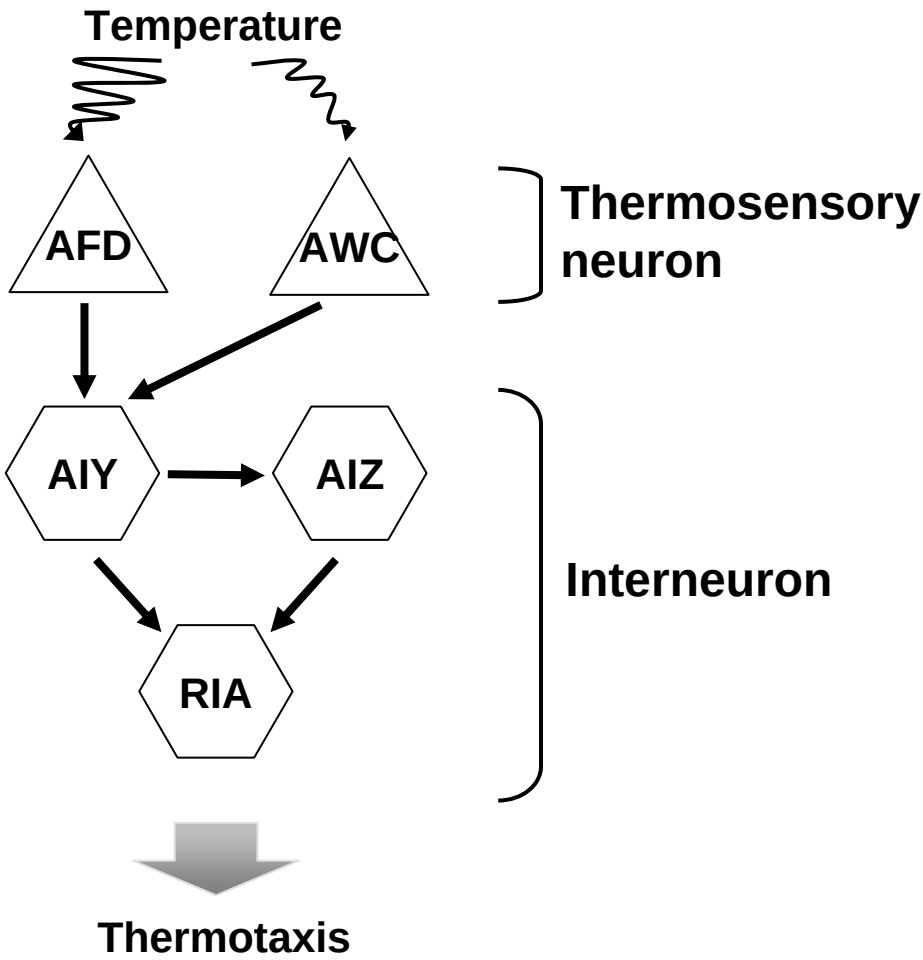

Figure 3. The neural circuit model for thermotaxis
Temperature is sensed by AFD and AWC sensory neurons, thermal information from AFD and AWC is conveyed to AIY interneuron, and the subsequent neural information from AIY is further conveyed to AIZ and RIA interneuron. Black arrows between neurons represent chemical synapses.

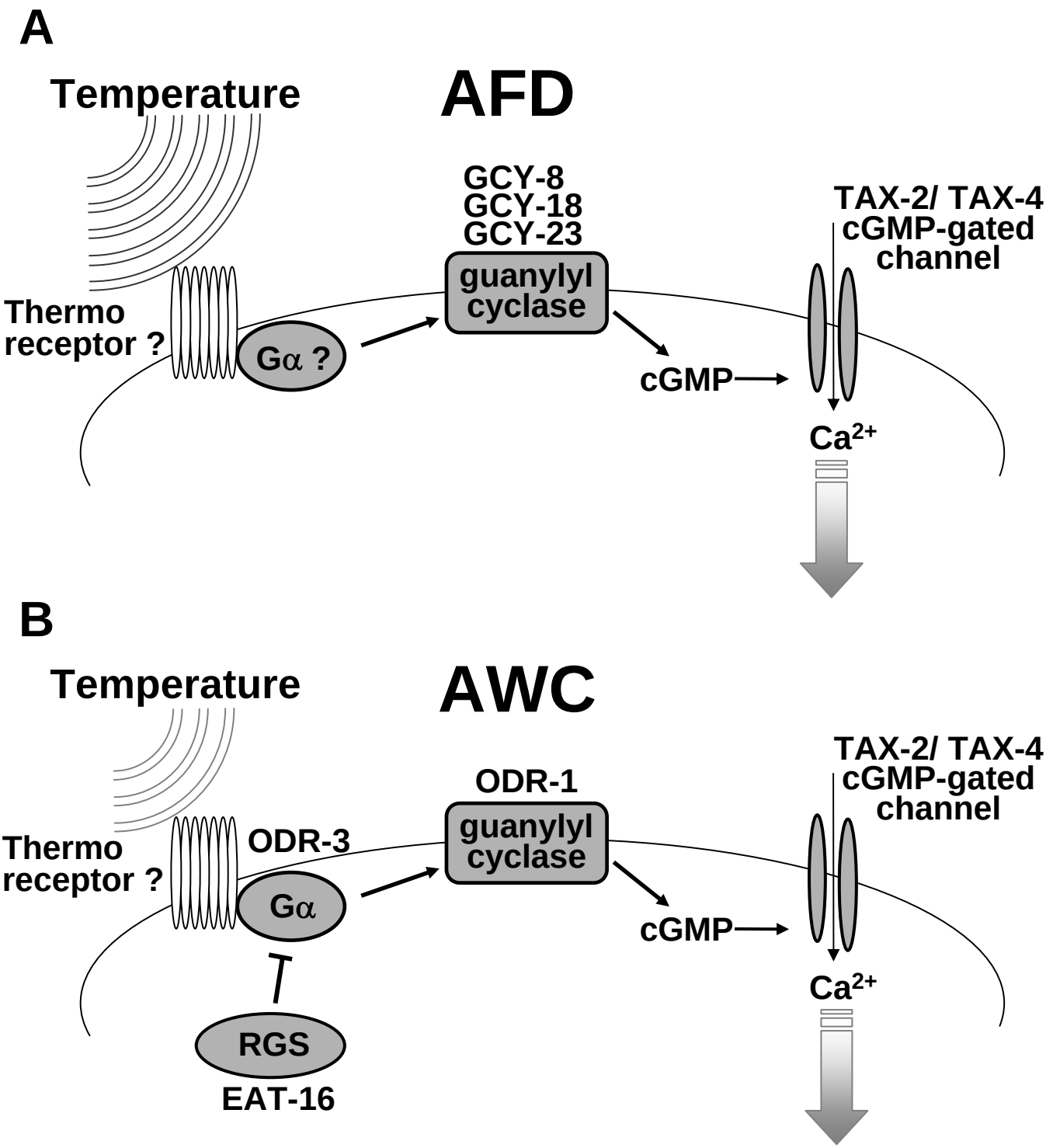

Figure 4. Temperature sensing signal transduction in thermosensory neurons
(A) The model of signal transduction in AFD. Three guanylyl cyclases, GCY-8, GCY-18 and GCY-23 redundantly produce cGMP, and TAX-2/TAX-4 cGMP-dependent cation channel increase internal calcium concentration.
(B) The model of signal transduction in AWC. ODR-1 guanylyl cyclase produces cGMP through activation of ODR-3 G-alpha, and TAX-2/TAX-4 increases internal calcium concentration. This G protein coupled signaling is suppressed by EAT-16 RGS.

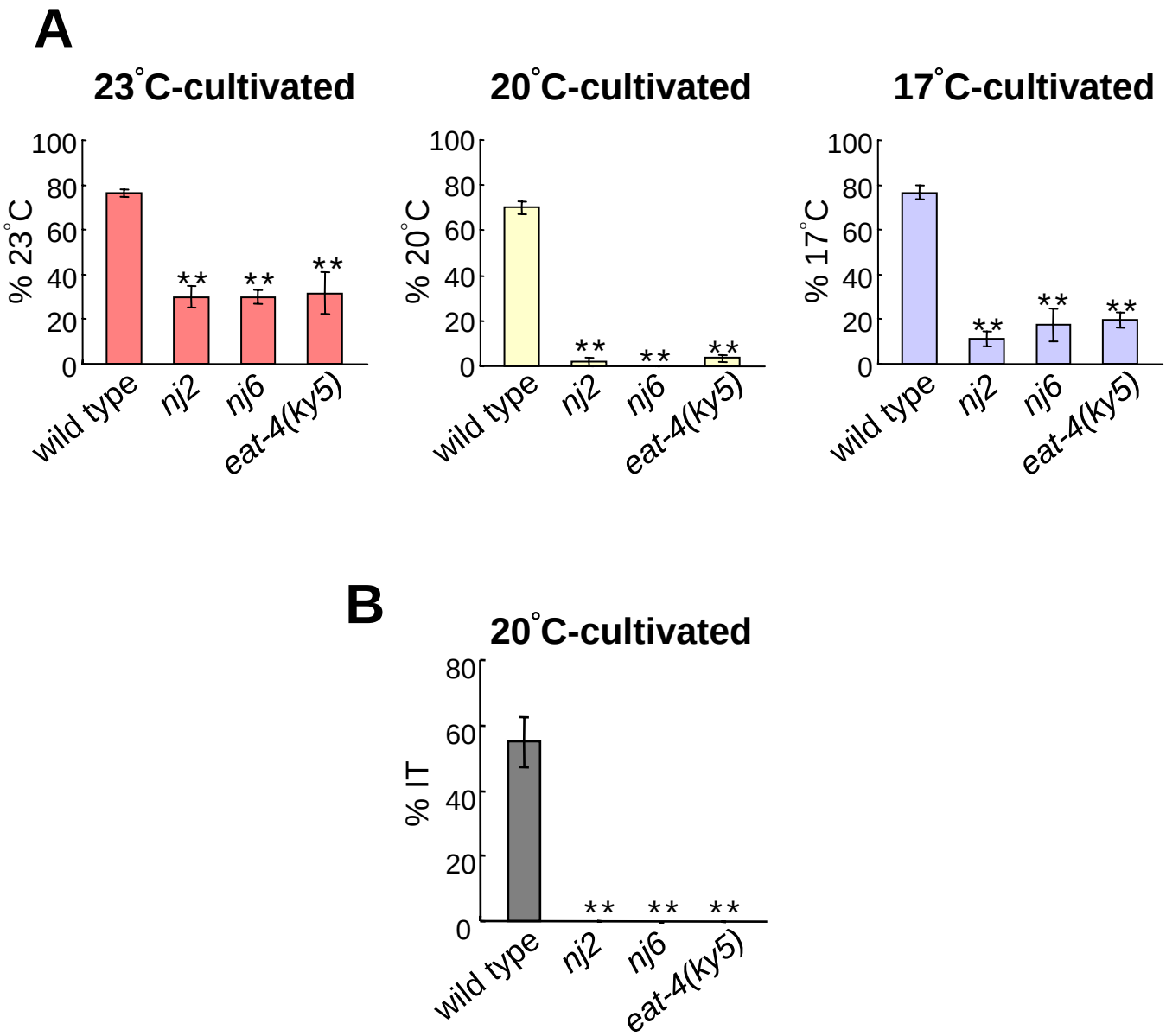

Figure 5. Thermotaxis defects of *nj2*, *nj6*, and *eat-4(ky5)* mutants in the individual TTX assay.

(A) Fraction of animals that migrated to their cultivation temperature after cultivated at 23˚C (red) , 20˚C (yellow) , or 17˚C (blue). n > 60 animals for each genotype. Error bar indicates SEM. Double asterisk at 23˚C-cultivated and 17˚C-cultivated both indicate $p < 0.01$ in post hoc Tukey-Kramer test for a comparison with wild-type animals. Double asterisk at 20˚C-cultivated indicates $p < 0.01$ in ANOVA for a comparison with wild-type animals.

(B) Fraction of animals that moved isothermally after cultivated at 20˚C. n = 60 animals for both strains. Error bar indicates SEM. Double asterisk indicates $p < 0.01$ in ANOVA for a comparison with wild-type animals.

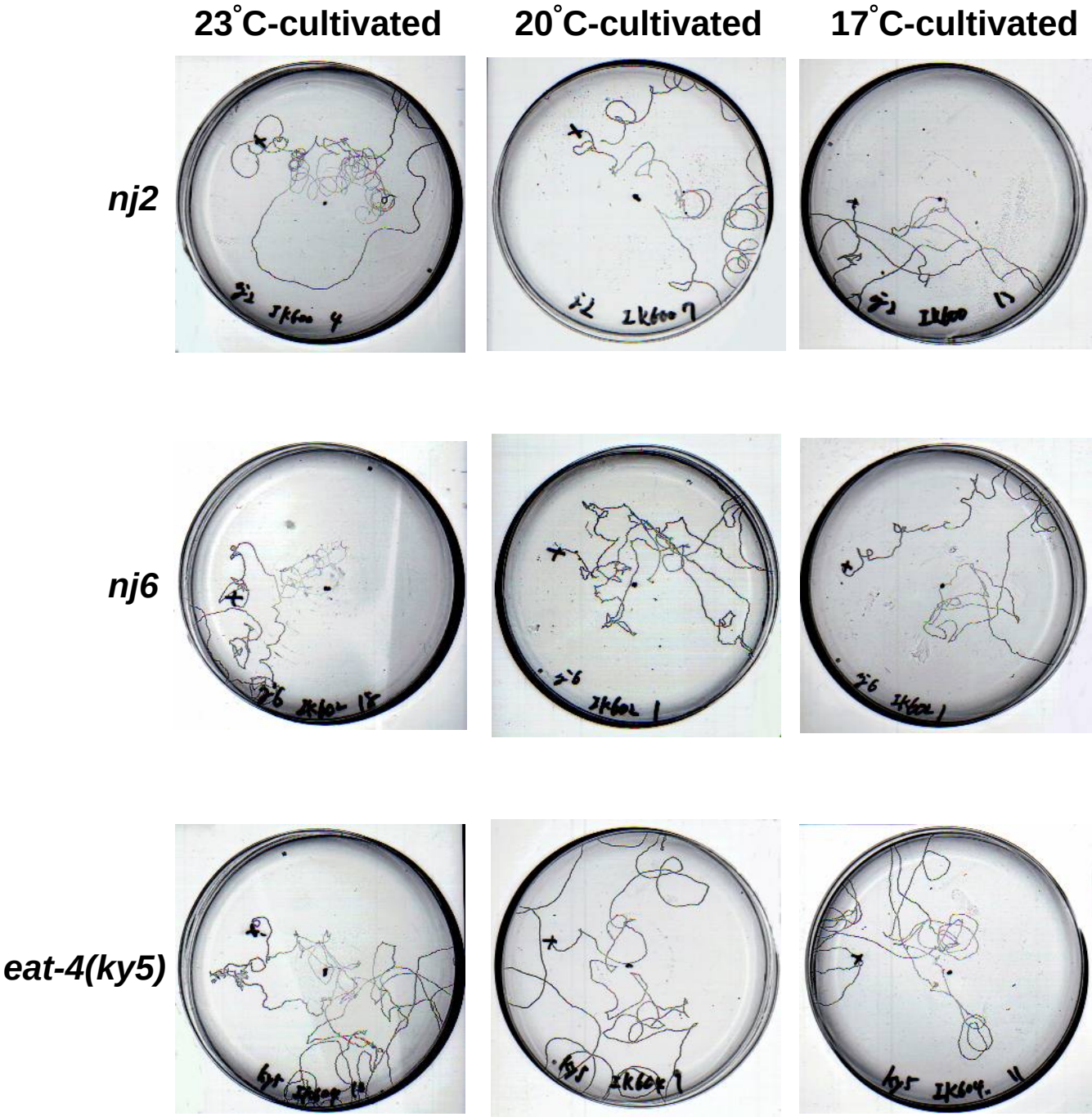

Figure 6. Thermotaxis tracks of *nj2*, *nj6*, and *eat-4(ky5)* mutants on a radial thermal gradient.
All mutants moved randomly after cultivated at 23°C , 20°C , or 17°C.

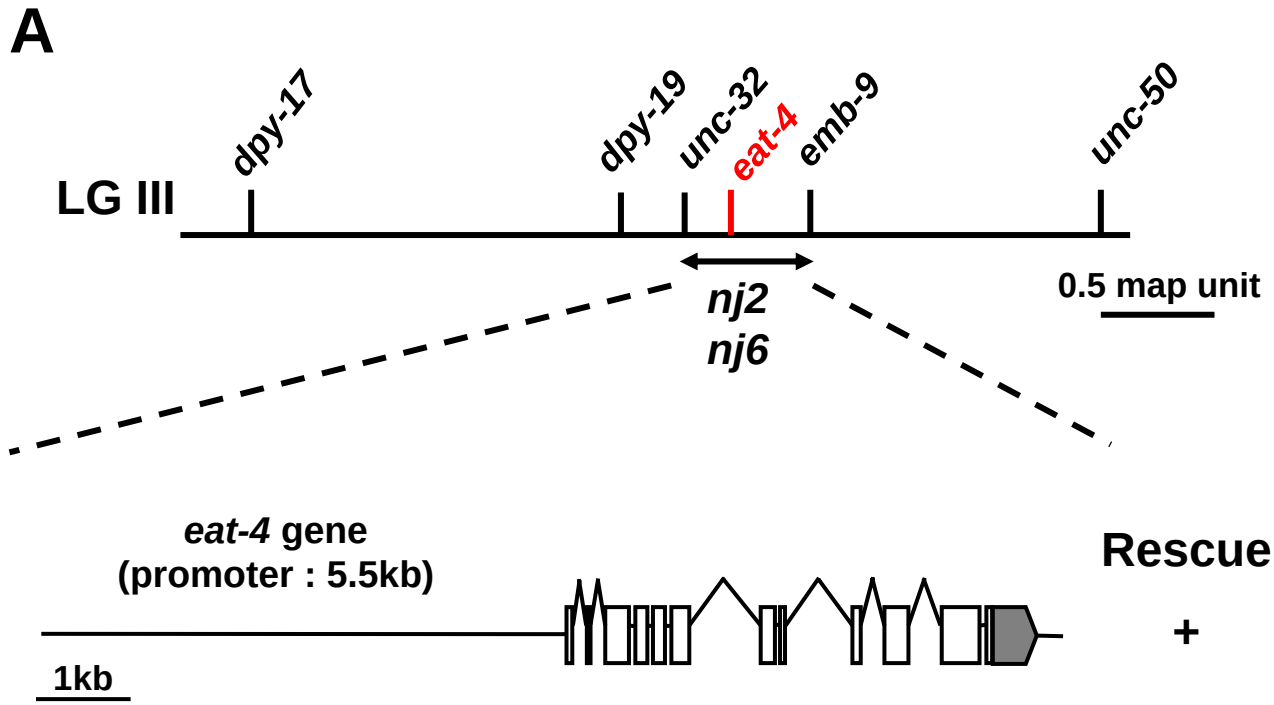

Figure 7. The result of genetic mapping of *nj2* and *nj6* mutations.
(A) *nj2* and *nj6* mutations were mapped to the region including *eat-4* gene by multi-factor crosses. The thermotaxis defects of *nj2* and *nj6* mutants were restored by introducing *eat-4* gene.
(B) Thermotaxis tracks of *nj2* and *nj6* transgenic mutants carrying *eat-4* gene fragment after cultivated at 20°C. These transgenic mutants moved isothermally on a radial thermal gradient.

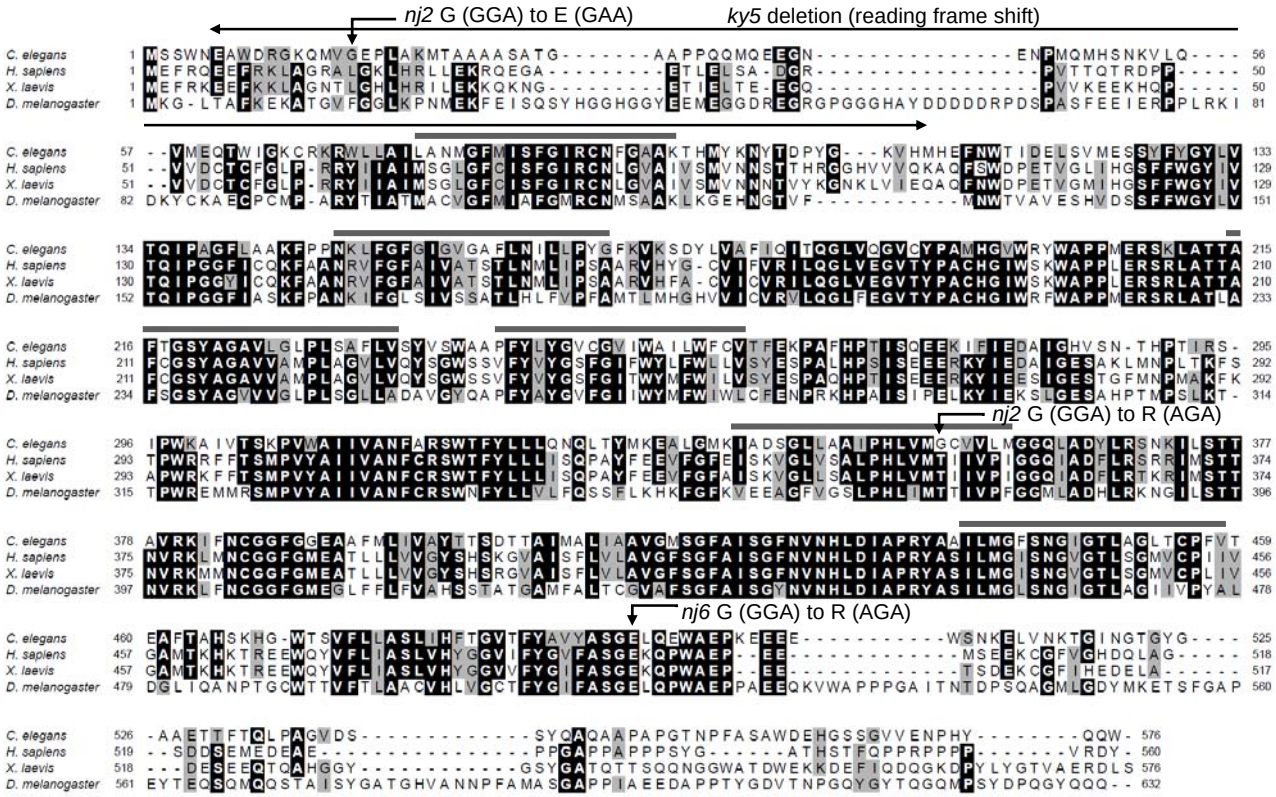

Figure 8. Comparison of sequences of EAT-4 and VGLUTs in other species. Black and gray boxes highlight identical and similar residues, respectively. Gray bars are putative transmembrane segments predicted in the previous report (Ni et al, 1994). Single arrows indicate the mutation sites of *nj2* and *nj6*. Deletion of *ky5* is indicated by a double-headed arrow.

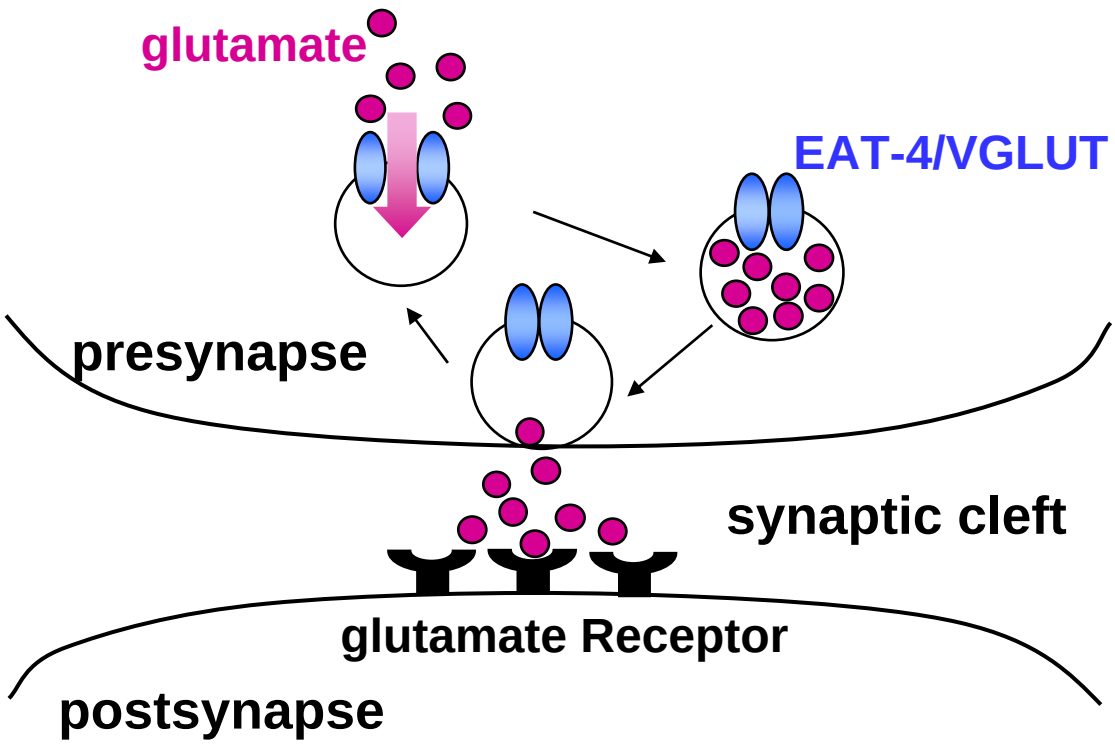

Figure 9. Function of EAT-4 .
EAT-4 is a *C. elegans* homolog of mammalian vesicular glutamate transporter (VGLUT) that concentrates glutamate into synaptic vesicles.

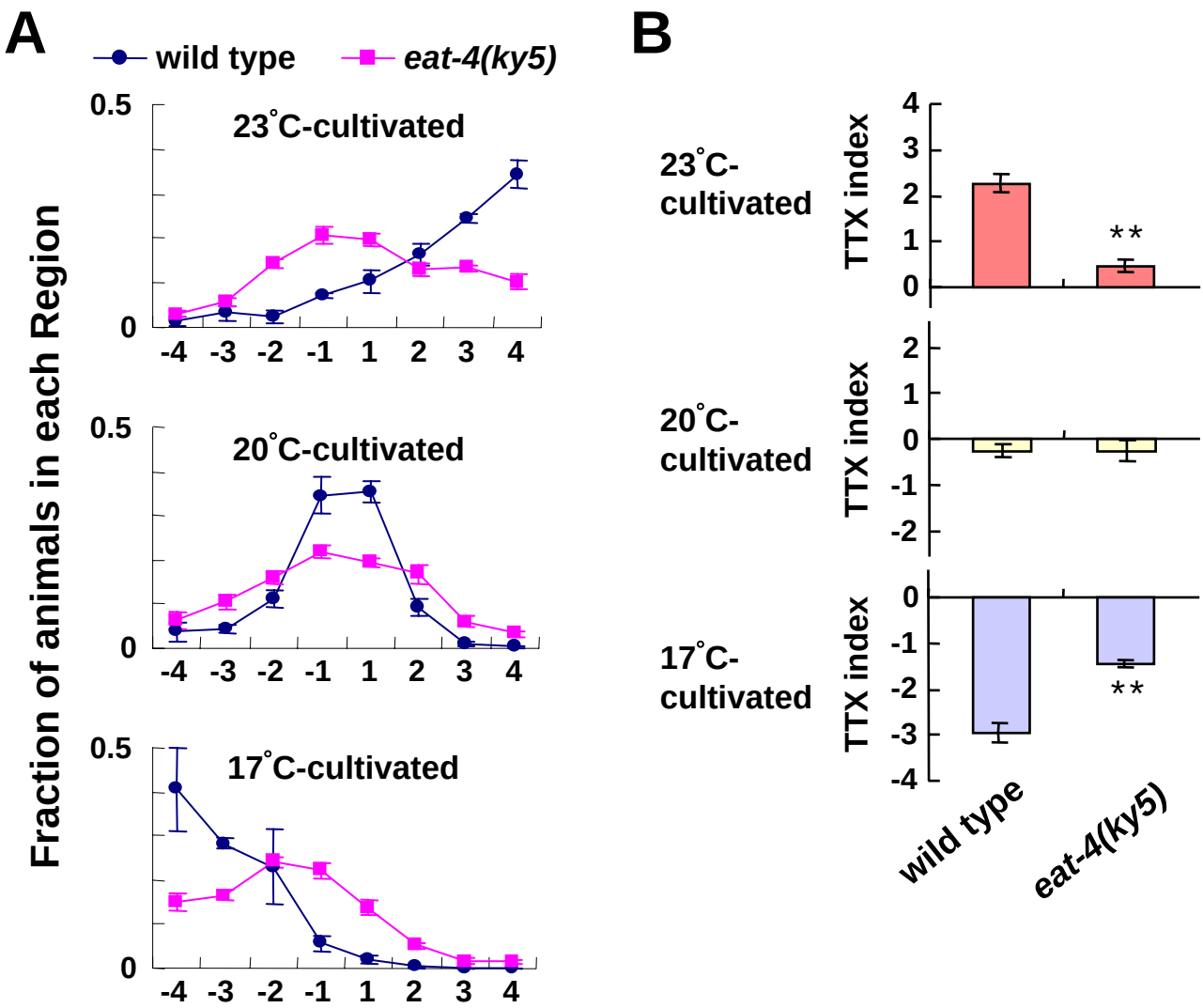

Figure 10. Thermotaxis defects of *eat-4(ky5)* mutants in the population TTX assay.
(A) Distributions of wild-type animals and *eat-4(ky5)* mutants cultivated at 23˚C, 20˚C, and 17˚C in the population thermotaxis assay.
(B) TTX indices of wild-type animals and *eat-4(ky5)* mutants. Red bars, yellow bars, and blue bars represent TTX indices of animals cultivated at 23˚C, 20˚C, and 17˚C, respectively. n = 3 or more assays. Error bar indicates SEM. Double asterisk indicates $p < 0.01$ in post hoc Tukey-Kramer tests for a comparison with wild-type animals.

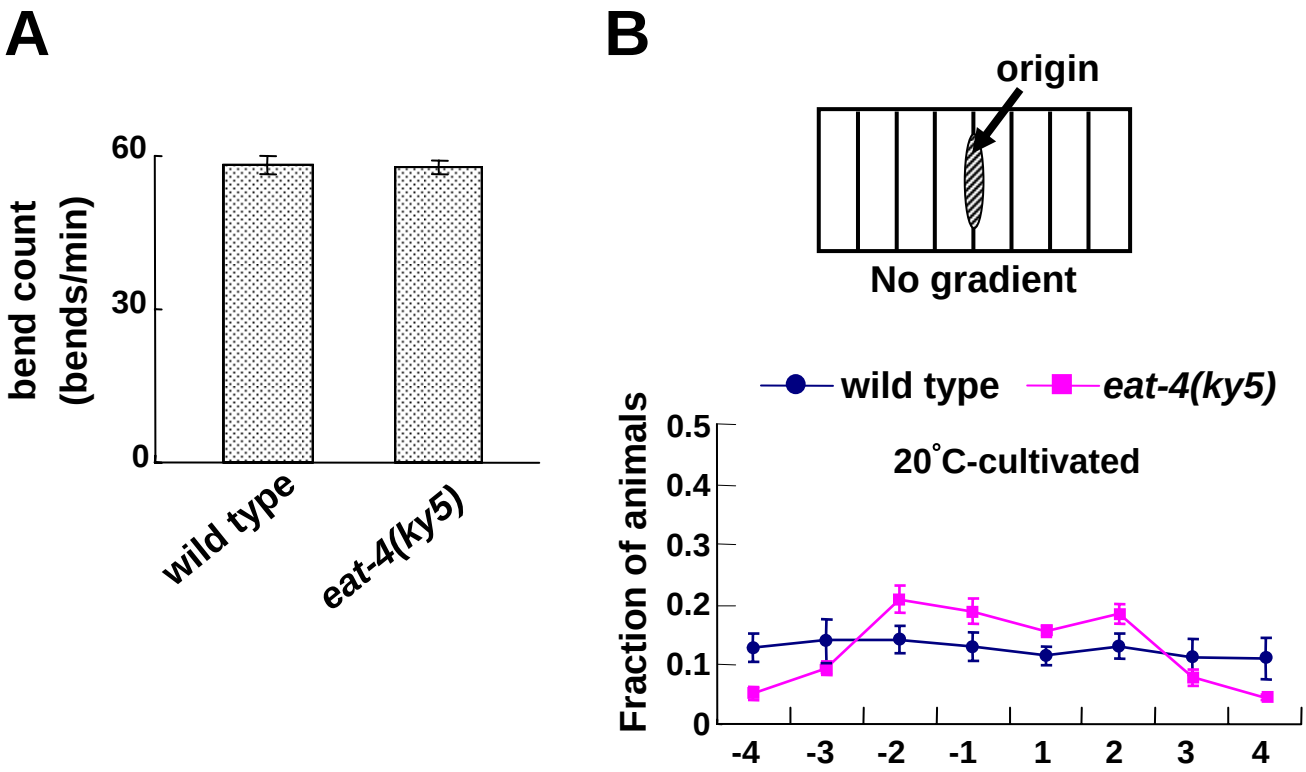

Figure 11. Assay for motor activity of *eat-4(ky5)* mutants.
(A) Bend counts per minute of wild-type animals and *eat-4(ky5)* mutants. n = 10 animals for each genotype. Error bar indicates SEM. $p > 0.05$ in post hoc Tukey-Kramer test.
(B) Distribution of wild-type animals and *eat-4(ky5)* mutants on TTX plates without the temperature gradient. Animals cultivated at 20°C were placed at the center line of the plate and left for 60 min (top). n = 3 or more assays. Error bar indicates SEM.

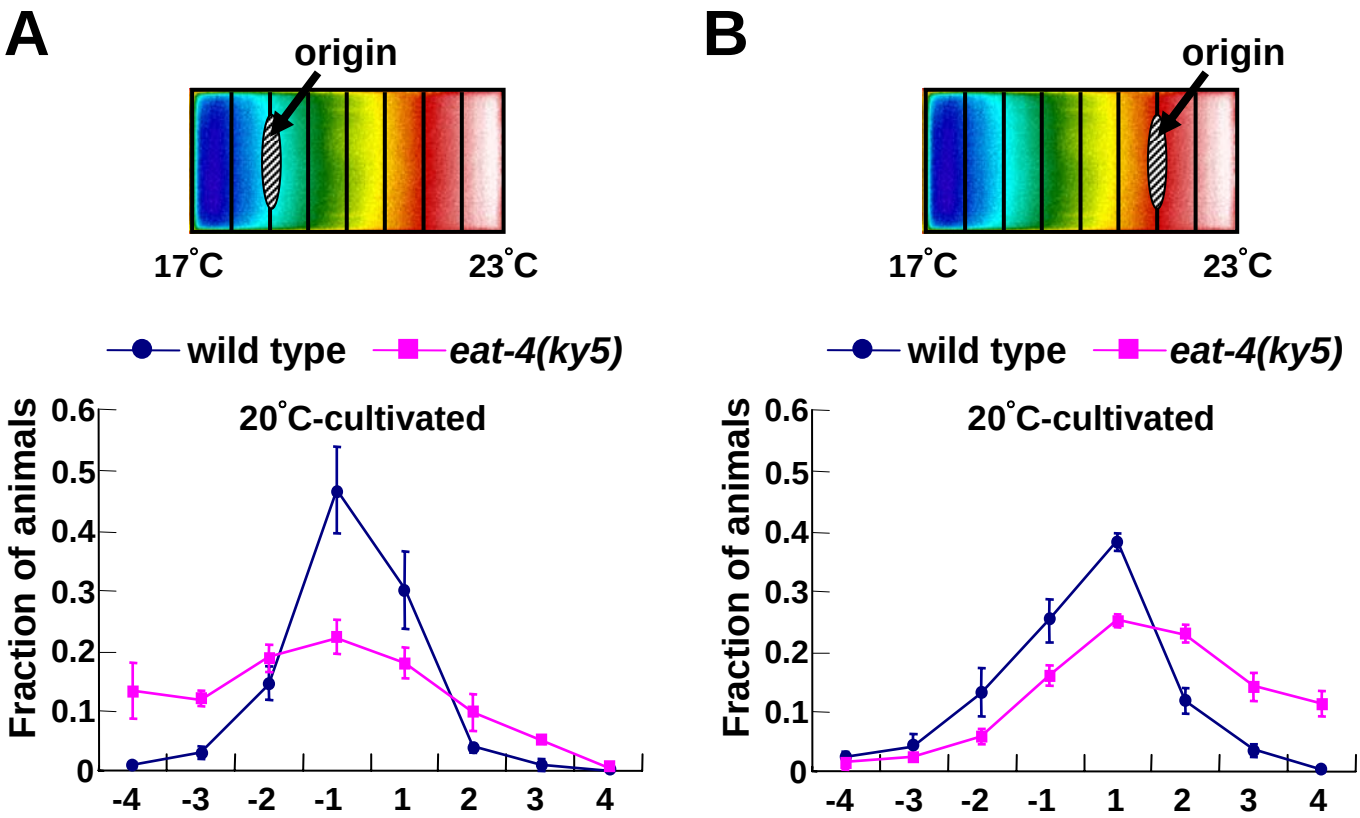

Figure 12. Distribution of wild-type animals and *eat-4(ky5)* mutants on the linear temperature gradient after placed at different points from 20˚C.
Animals cultivated at 20˚C were placed at the lower temperature point (A) or higher temperature point (B) than 20˚C and left for 60 min (top). Most of wild-type migrated around 20˚C. *eat-4(ky5)* showed a greater tendency to move in the opposing direction from 20˚C than wild-type. n = 3 or more assays. Error bar indicates SEM.

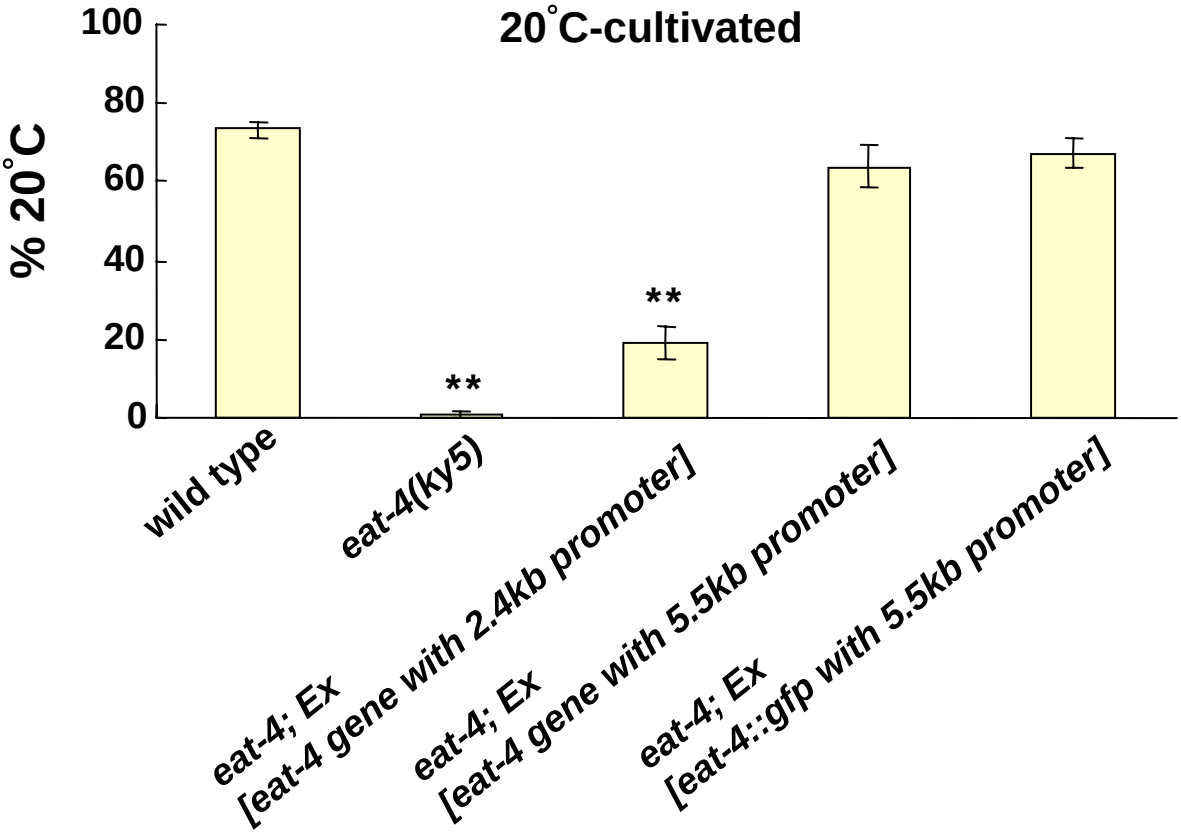

Figure 13. Analysis for activities of two *eat-4* promoters by the individual TTX assay. Fraction of wild-type animals and *eat-4* transgenic mutants containing genomic *eat-4* gene or *eat-4::gfp* that migrated to their cultivation temperature after cultivated at 20°C in the individual TTX assay. n > 60 animals for each genotype. Error bar indicates SEM. Double asterisk indicates $p < 0.01$ in post hoc Tukey-Kramer tests for a comparison with wild-type animals.

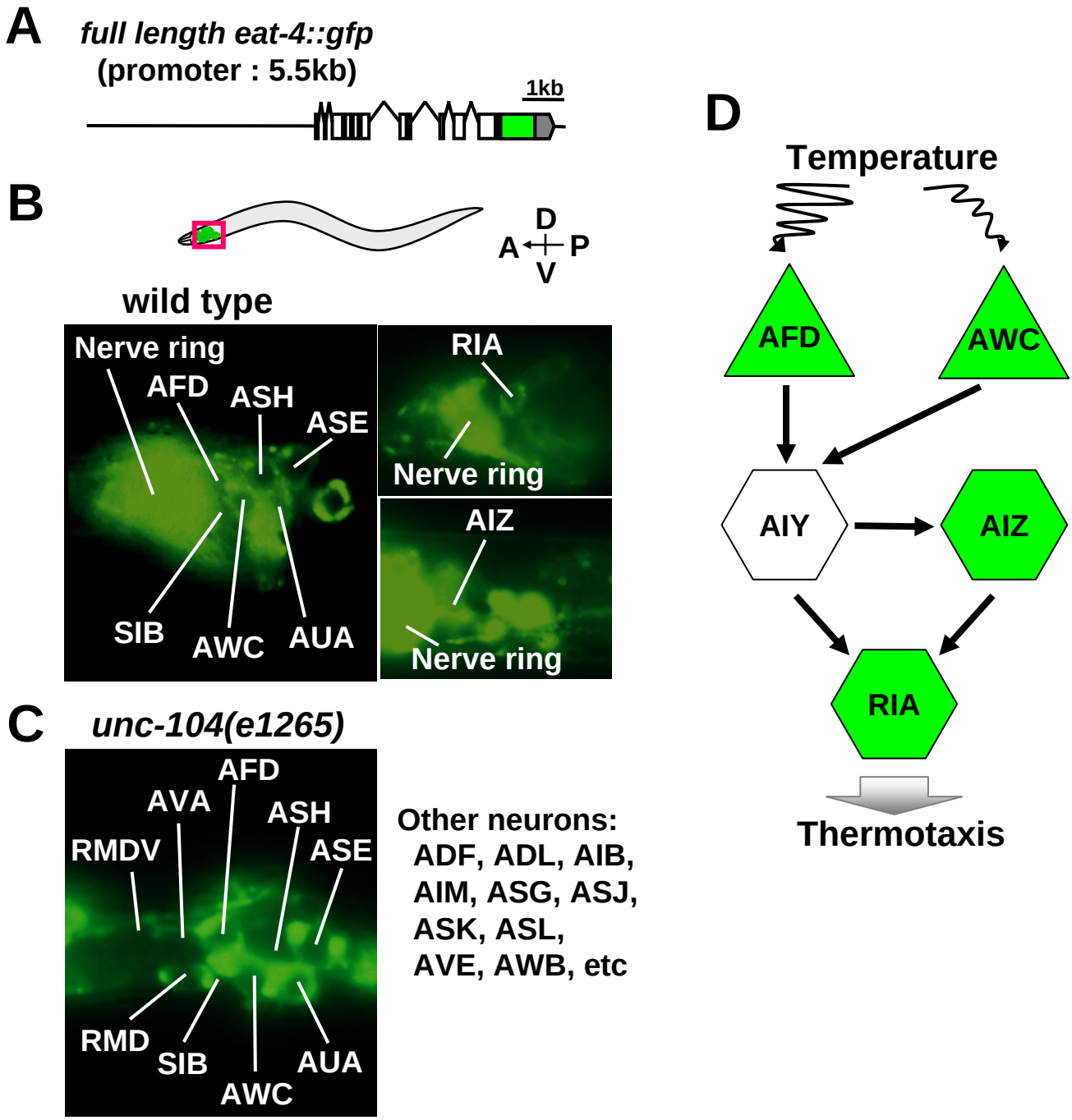

Figure 14. Expression pattern of EAT-4.
(A) The *full length eat-4::gfp* fusion gene with 5.5kb of promoter region.
(B, C) The expression of *full length eat-4::gfp* in the head of wild-type animals (B), and of *unc-104(e1265)* mutants (C). Anterior is to the left and dorsal is up (top). (B) Fluorescence was observed in nerve ring and cell body of many neurons including AFD, AWC (left panel), RIA (top right panel), and AIZ neurons (bottom right panel) in wild-type. (C) Fluorescence was not observed in nerve ring but in cell body of many neurons including AFD, AWC in *unc-104(e1265)* mutants.
(D) Neurons expressing the *full length eat-4::gfp* in the thermotaxis neural circuit are colored green.

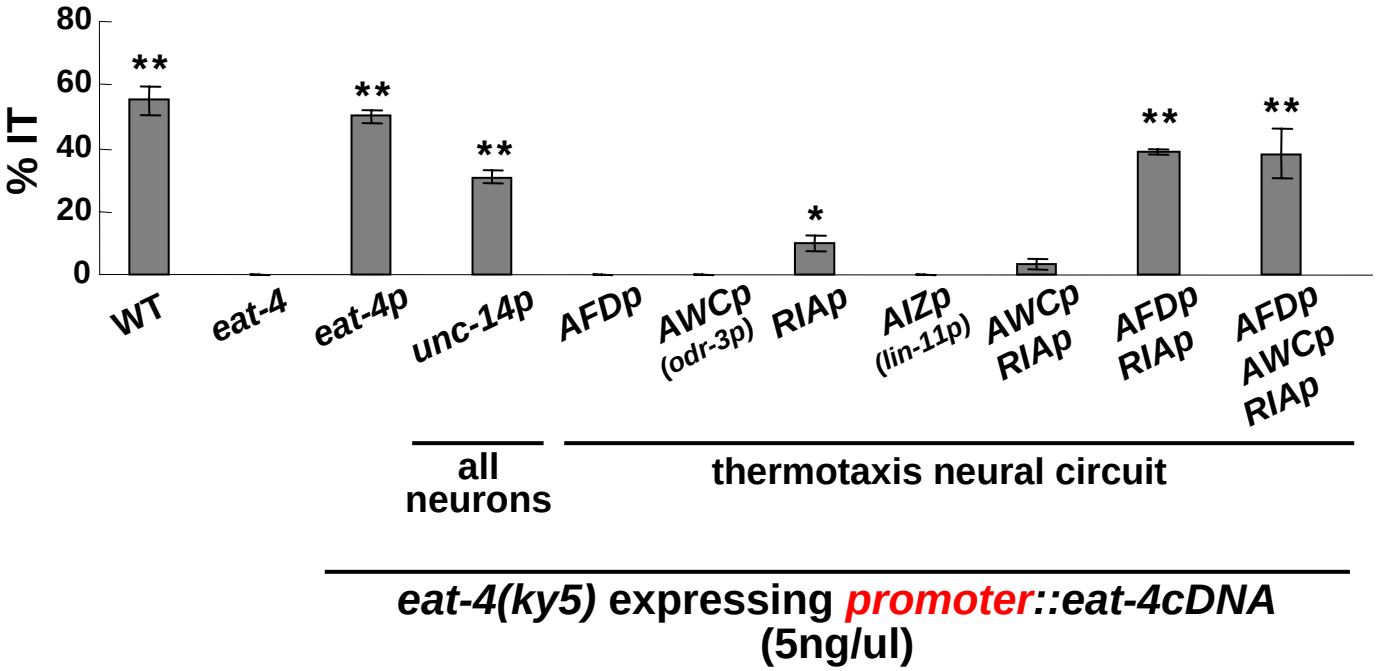

Figure 15. Cell-specific rescue experiments of *eat-4(ky5)* mutants in the individual TTX assay.
Rescue experiments for defective isothermal tracking (IT behavior) of *eat-4(ky5)* mutants by introducing cell-specific *promoters::eat-4 cDNA* at 5ng/ul. Gray bars represent fraction of animals that moved isothermally. n = 58 or more animals. Error bar indicates SEM. Single and double asterisk indicate $p < 0.05$ and 0.01, respectively, in ANOVA for a comparison with *eat-4(ky5)* mutants.

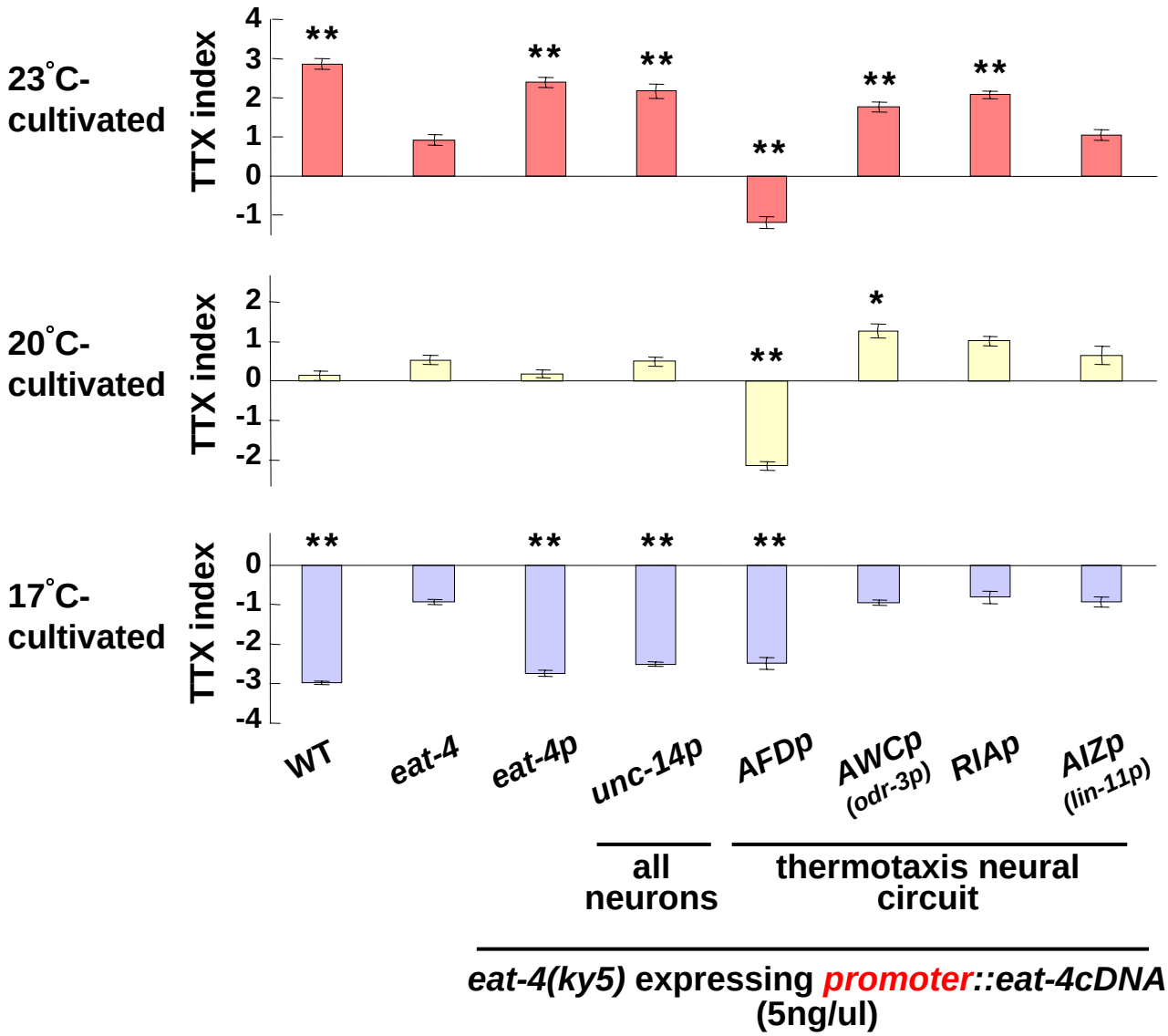

Figure 16. Cell-specific rescue experiments of *eat-4(ky5)* mutants in the population TTX assay.
Rescue experiments for defective migration to cultivation temperature of *eat-4(ky5)* mutants by introducing individual cell-specific *promoters::eat-4 cDNA* at 5ng/ul. Red bars, yellow bars, and blue bars represent TTX indices of animals cultivated at 23˚C, 20˚C, and 17˚C, respectively. n = 3 or more assays. Error bar indicates SEM. Single asterisk and double asteris indicate $p < 0.05$ and $p < 0.01$ respectively in post hoc Tukey-Kramer tests for a comparison with *eat-4(ky5)* mutants.

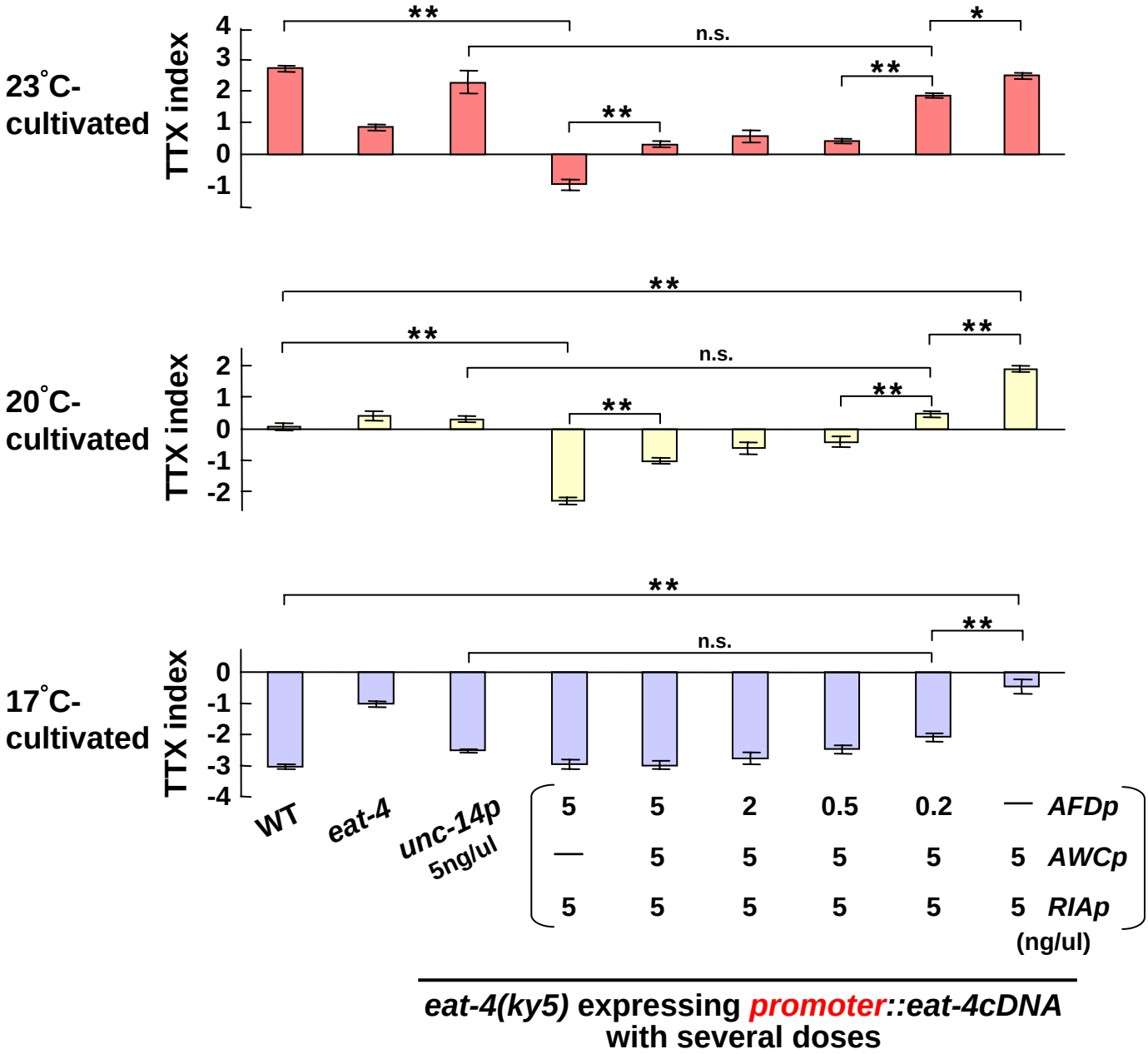

Figure 17. Rescue experiments of *eat-4(ky5)* mutants with simultaneous expression of EAT-4 in AFD, AWC, and RIA in the population TTX assay. Rescue experiments for defective migration to cultivation temperature of *eat-4(ky5)* mutants by introducing *AFDp::eat-4 cDNA*, *AWCp::eat-4 cDNA*, and *RIAp::eat-4 cDNA* simultaneously at several doses. n = 3 or more assays. Error bar indicates SEM. Single asterisk, double asterisk, and n.s. indicate $p < 0.05$, $p < 0.01$, and $p > 0.05$ respectively, in post hoc Tukey-Kramer tests for a comparison of each genotype.

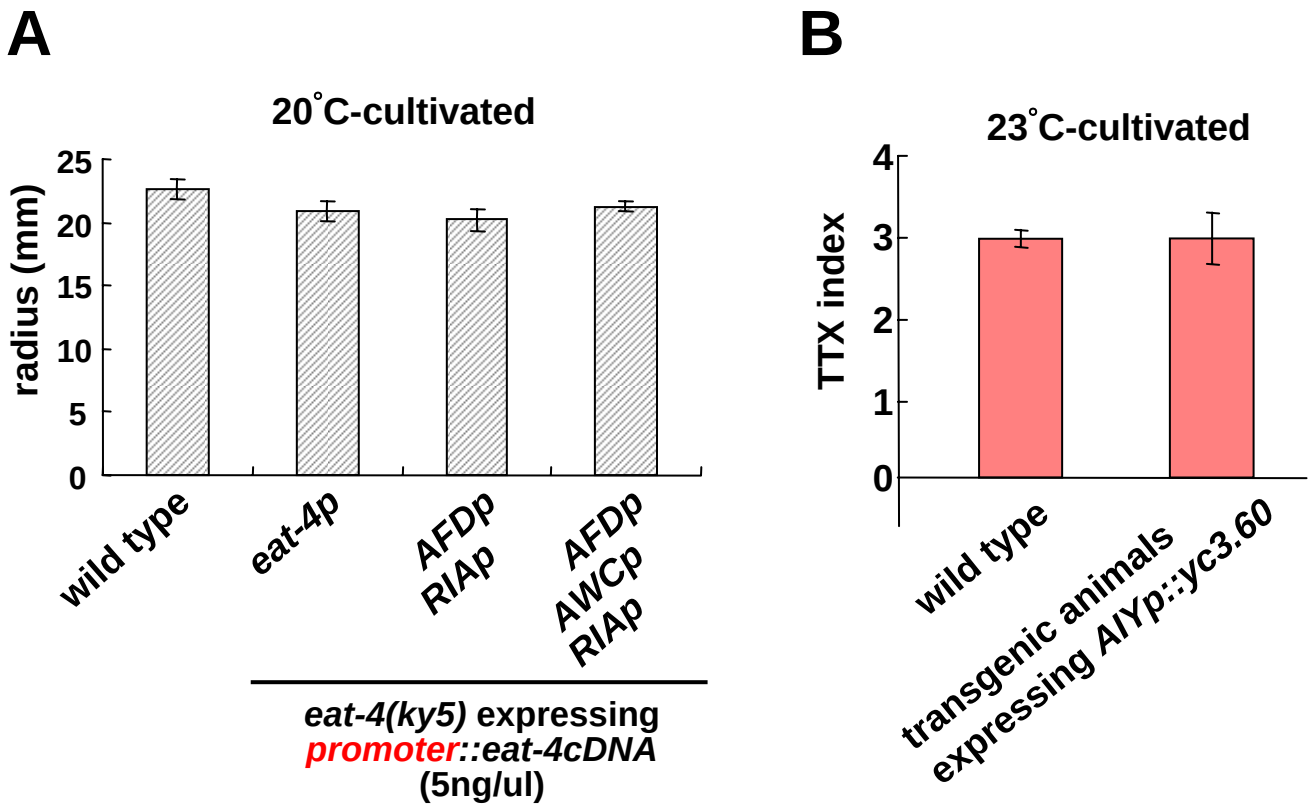

Figure 18. Radius of isothermal tracks of *eat-4* transgenic animals on the individual TTX assay plates and the population thermotaxis assays of transgenic animals containing *AIYp::yc3.60* after cultivated at 23˚C.

(A) We measured radius of isothermal tracks of animals that moved isothermally as shown in Figure 15. Radius of all *eat-4* transgenic mutants showing normal fraction of isothermal tracks did not differ from that of wild-type animals ($p > 0.05$ in post hoc Tukey-Kramer test). n = 3 assays. Error bar indicates SEM.

(B) *AIYp::yc3.60* did not affect the normal thermotaxis of wild-type ($p > 0.05$ in post hoc Tukey-Kramer test). n = 3 assays. Error bar indicates SEM.

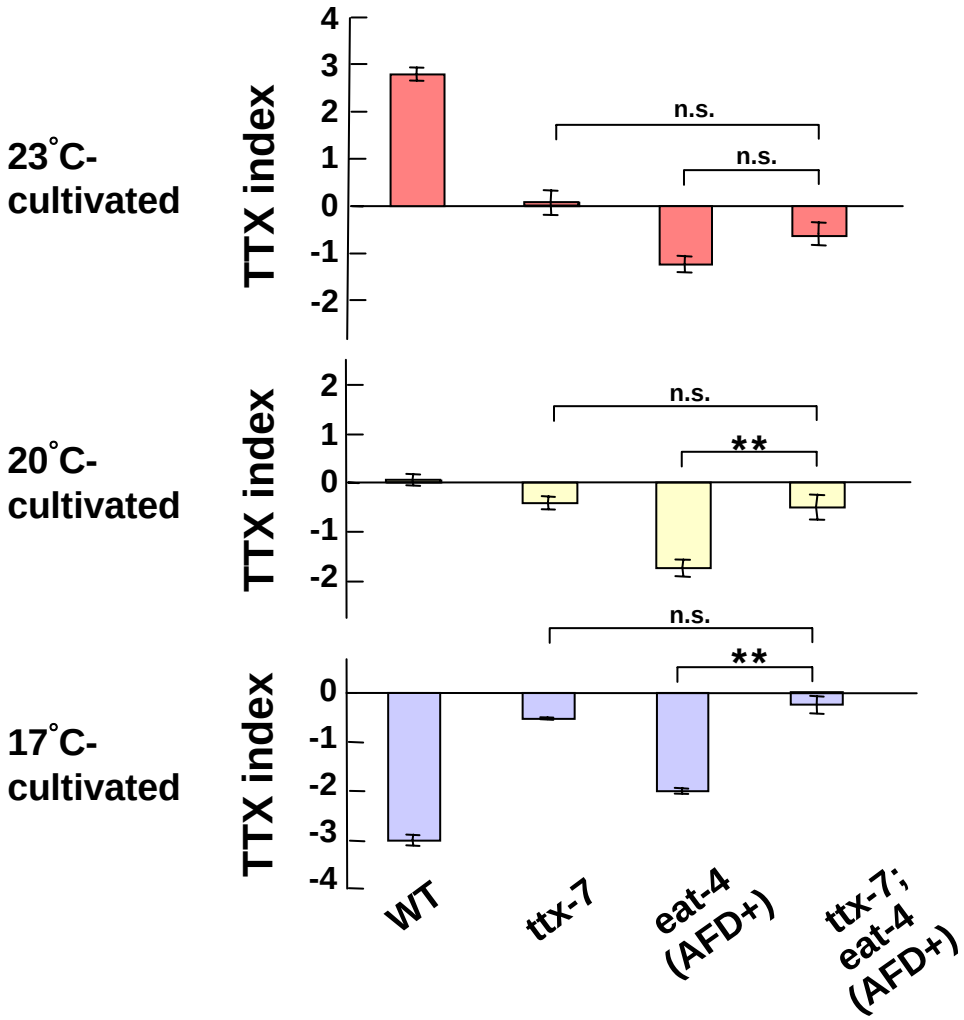

Figure 19. The population thermotaxis assay of *eat-4* transgenic mutants carrying genetically abnormal function in RIA.
eat-4 (AFD+) represents the transgenic *eat-4(ky5)* mutants expressing EAT-4 in AFD. Thermotactic defect of *ttx-7(nj50)* mutants completely masked the defect of *eat-4 (AFD+)*. n = 3 or more assays. Error bar indicates SEM. Double asterisk and n.s. indicate $p < 0.01$ and $p > 0.05$, respectively, in post hoc Tukey-Kramer tests for a comparison of each genotype.

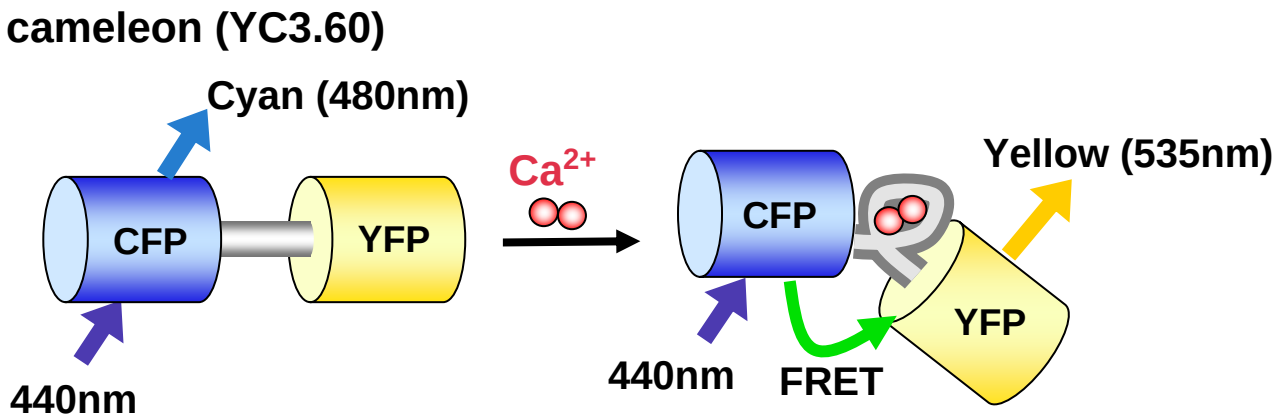

Figure 20. Schematic structure of cameleon YC3.60.
The color of fluorescence emitted by cameleon changes from cyan to yellow with fluorescence resonance energy transfer (FRET) which is mediated by the binding of Ca^{2+} to cameleon.

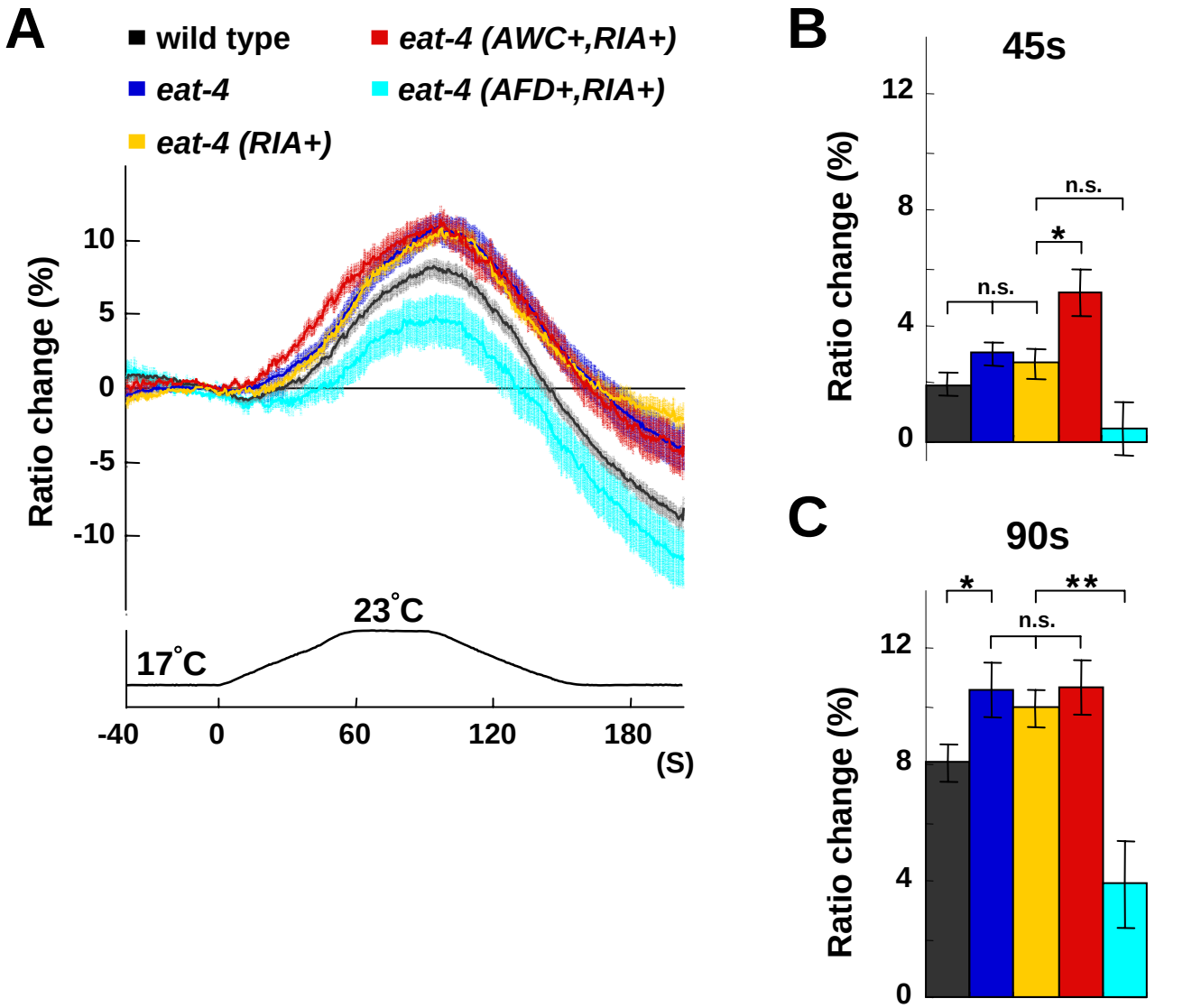

Figure 21. *in vivo* calcium imaging of AIY according to warming in *eat-4(ky5)* mutants and the *eat-4(ky5)* transgenic animals after cultivated at 20˚C.

(A) The intracellular calcium concentration change was measured as the YFP/CFP fluorescence change (Ratio change) of cameleon (yc3.6). *eat-4 (AWC+, RIA+)*, *eat-4 (AFD+, RIA+)*, and *eat-4 (RIA+)* represent the transgenic *eat-4(ky5)* mutants expressing EAT-4 in AWC and RIA but not in AFD, in AFD and RIA but not in AWC, and in RIA but not in AFD and AWC, respectively (top). Response curves represent the average of Ratio change according to temperature change. Temperature change along time is shown at the bottom of the response curve. 0s is the time starting temperature change from 17˚C to 23˚C (bottom). (B, C) The average of Ratio changes to temperature stimuli at 45s (B) and at 90s (C) regarding the results shown in Figure 21A. The color of bars in the graphs corresponds to the color of response curves described in Figure 21A. n = 18 or more animals. Error bar indicates SEM. Single asterisk, double asterisk, and n.s. indicate $p < 0.05$, $p < 0.01$, and $p > 0.05$, respectively, in Steel-Dwass tests for a comparison of each genotype.

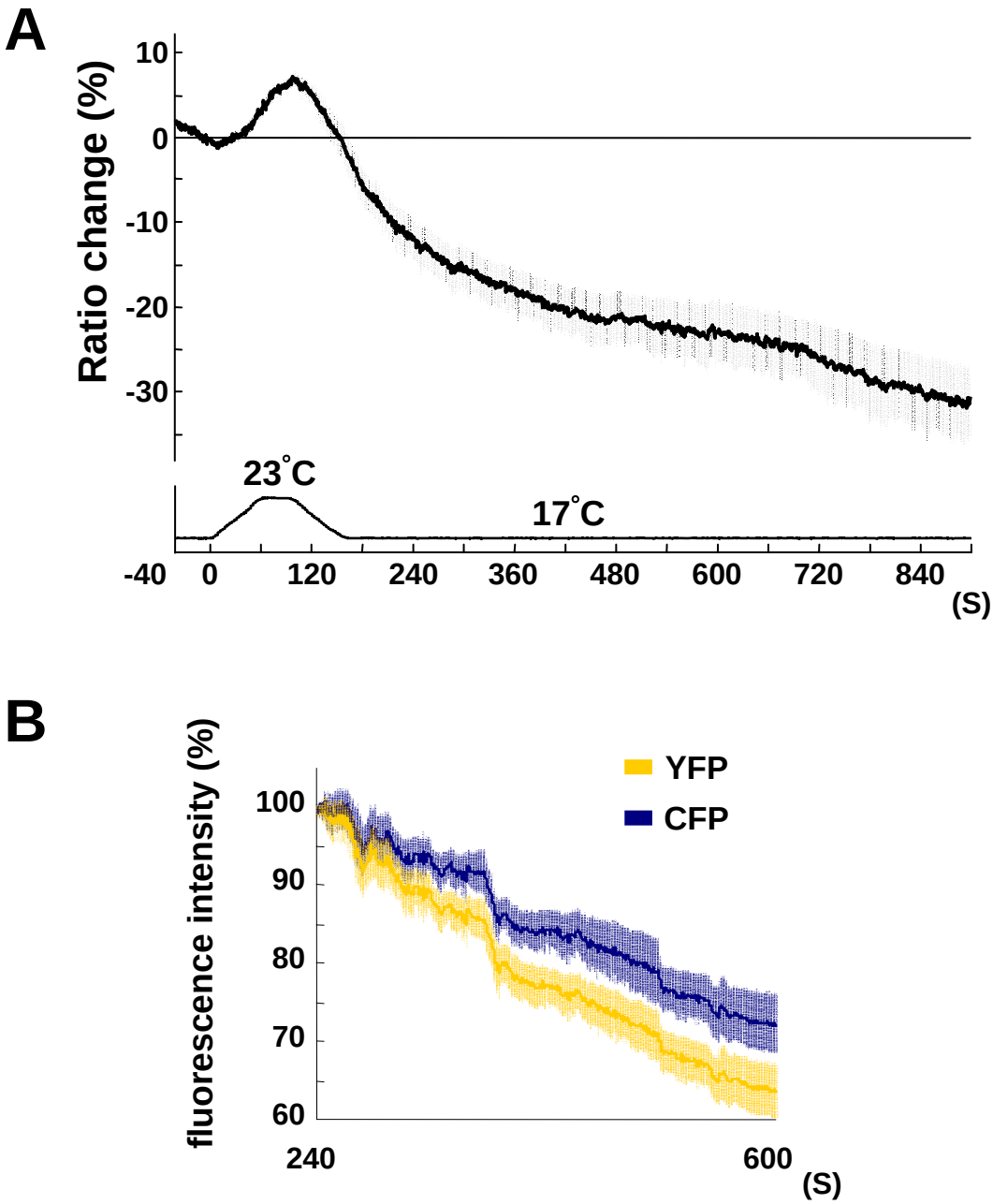

Figure 22. long-term *in vivo* calcium imaging of AIY in 20˚C-cultivated wild-type animals
(A) Ratio change of yc3.6 in AIY of wild-type animals in response to warming. By providing same temperature change as shown in Figure 21, we monitored ratio change until 900s. After the temperature change from 17˚C to 23˚C, FRET ratios continued to decrease gradually. n = 11 animals. Error bar indicates SEM.
(B) Change of fluorescence intensities of YFP (yellow) and CFP (blue) in yc3.6 from 240s to 600s in Figure 22A. We set the average intensities of YFP and CFP at 240s as 100%. Fluorescence intensities of YFP decrease faster than that of CFP. n = 7 animals. Error bar indicates SEM.

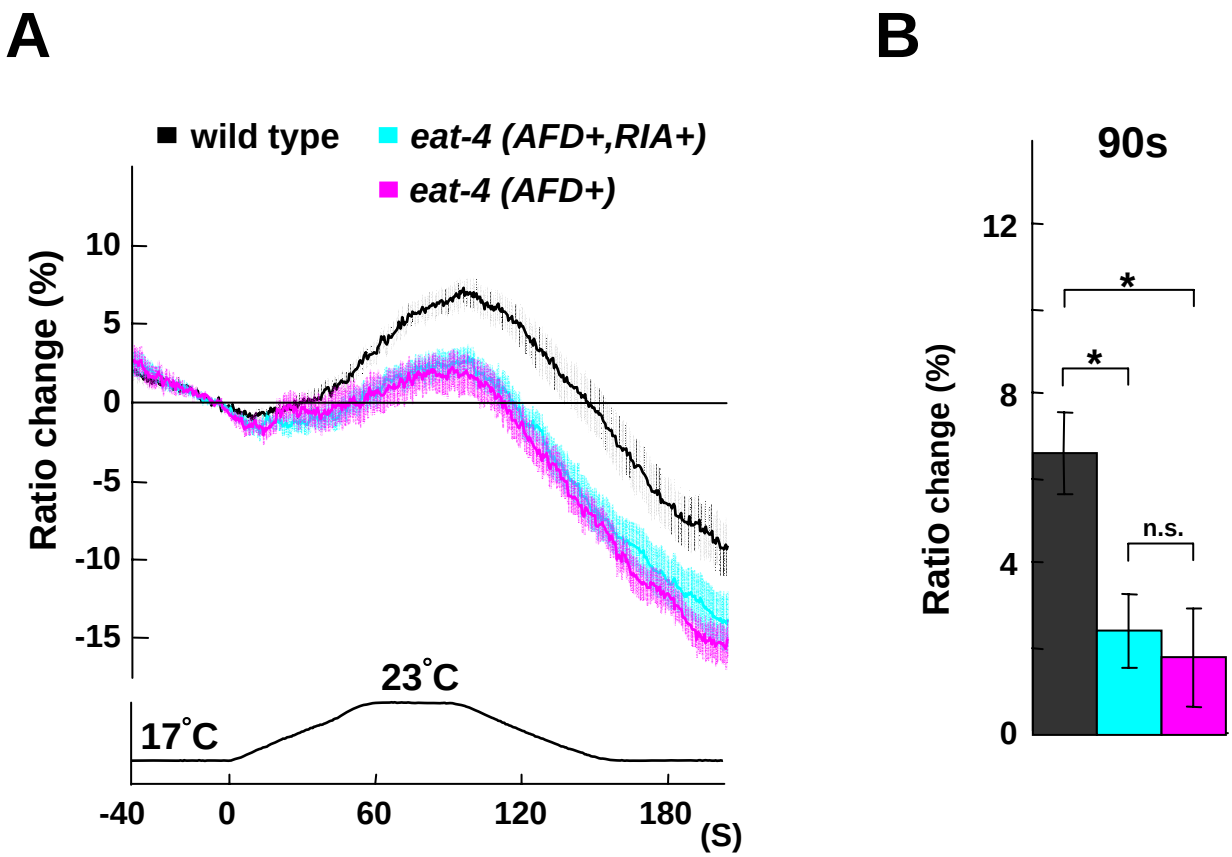

Figure 23. *in vivo* calcium imaging of AIY in 20˚C-cultivated *eat-4(ky5)* transgenic animals
(A) Ratio change of yc3.6 in AIY of *eat-4* transgenic animals in response to temperature change. *eat-4 (AFD+, RIA+)* and *eat-4 (AFD+)* represent the transgenic *eat-4(ky5)* mutants expressing EAT-4 in both AFD and RIA, and in AFD but not in RIA, respectively (top). (B) The average of Ratio changes to temperature stimuli at 90s concerning the results shown in Figure 23A. The color of bars in the graphs corresponds to the color of response curves described in Figure 23A. n = 15 animals. Error bar indicates SEM. Single asterisk and n.s. indicate $p < 0.05$ and $p > 0.05$, respectively, in Steel-Dwass tests for a comparison of each genotype.

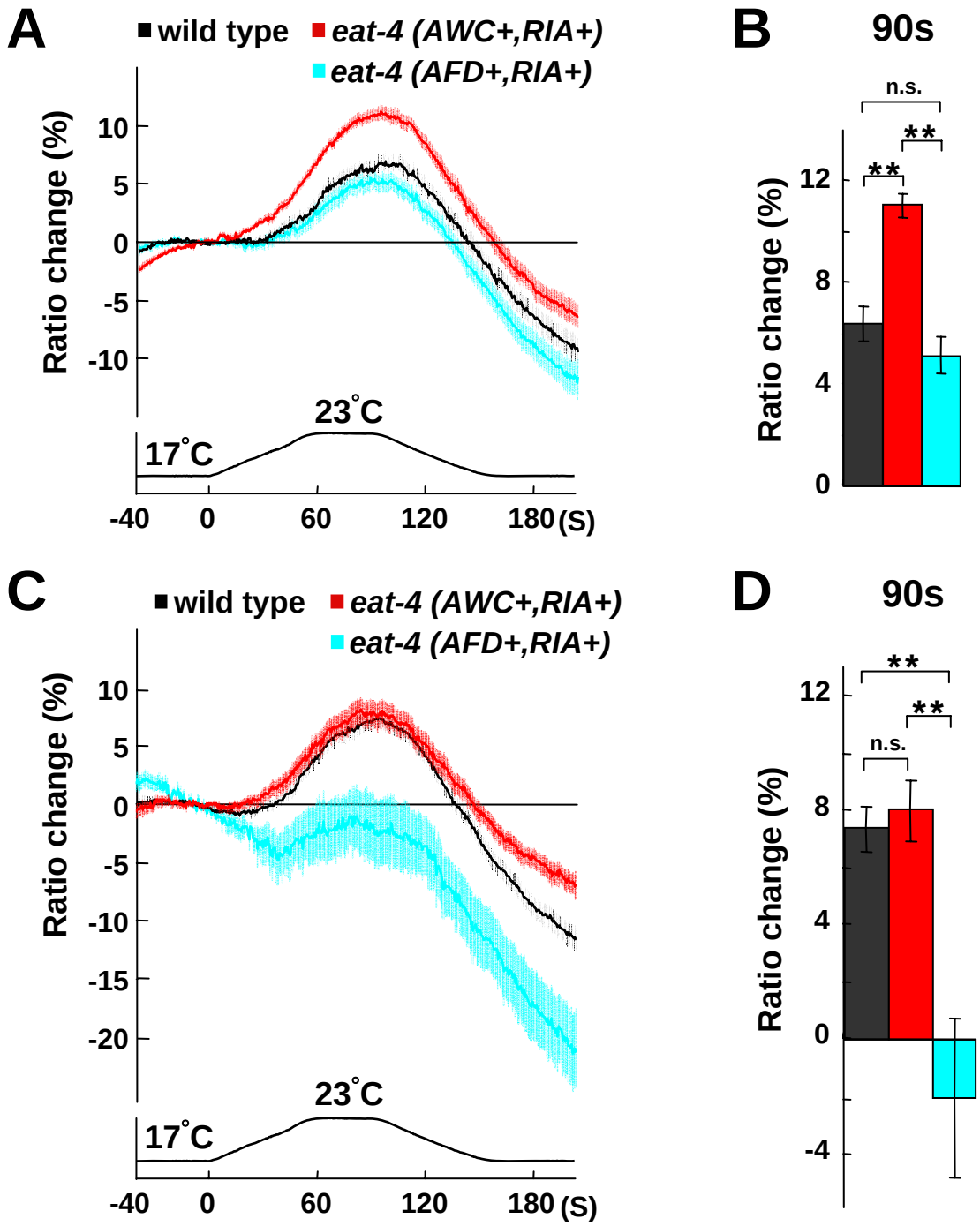

Figure 24. *in vivo* calcium imaging of AIY in 17˚C- and 23˚C-cultivated *eat-4(ky5)* transgenic animals shown in Figure 21.

(A) Ratio change of yc3.6 in AIY of 17˚C-cultivated animals in response to warming.

(B) The average of Ratio changes to temperature stimuli at 90s concerning the results shown in Figure 23A.

(C) Ratio change of yc3.6 in AIY of 23˚C-cultivated animals in response to warming.

(D) The average of Ratio changes to temperature stimuli at 90s concerning the results shown in Figure 24C.

(A, B, C, D) n = 21 or more animals. Error bar indicates SEM. Double asterisk and n.s. indicate $p < 0.01$ and $p > 0.05$, respectively, in Steel-Dwass tests for a comparison of each genotype.

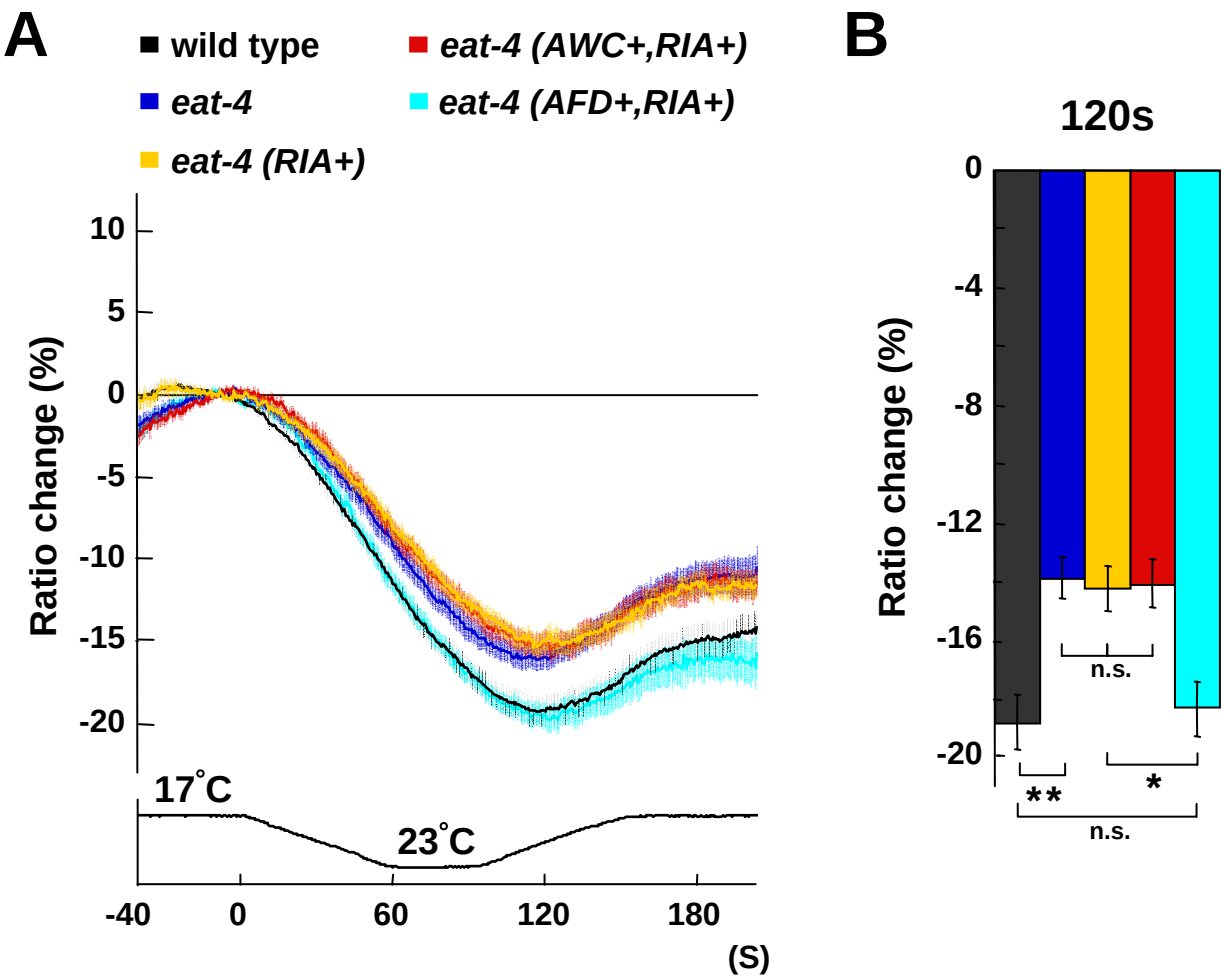

Figure 25. *in vivo* calcium imaging of AIY according to cooling in *eat-4(ky5)* mutants and the *eat-4(ky5)* transgenic animals after cultivated at 20˚C.

(A) Ratio change of yc3.6 in AIY in response to temperature change from 23˚C to 17˚C.

(B) The average of Ratio changes to temperature stimuli at 120s for the results shown in Figure 23. n = 18 or more animals. Error bar indicates SEM. Single asterisk, double asterisk, and n.s. indicate $p < 0.05$, $p < 0.01$, and $p > 0.05$, respectively, in Steel-Dwass tests for a comparison of each genotype.

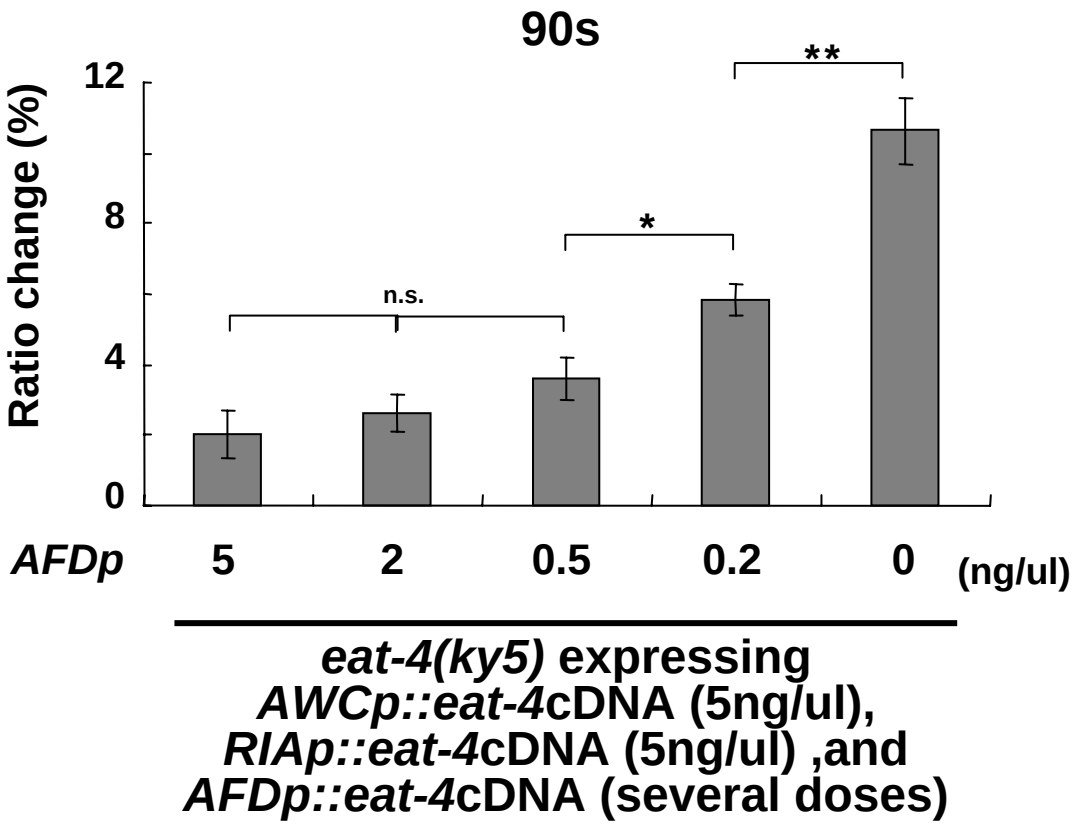

Figure 26. *in vivo* calcium imaging of AIY according to warming in 20˚C-cultivated *eat-4(ky5)* transgenic animals expressing EAT-4 in AFD, AWC and RIA.
The average of Ratio changes of *eat-4(ky5)* expressing EAT-4 in AFD, AWC and RIA simultaneously by introducing several doses of *AFDp::eat-4 cDNA* with 5ng/ul of *AWCp::eat-4 cDNA* and *RIAp::eat-4 cDNA* at 90s. n = 18 or more animals. Error bar indicates SEM. Single asterisk, double asterisk, and n.s. indicate $p < 0.05$, $p < 0.01$, and $p > 0.05$, respectively, in Steel-Dwass tests for a comparison of each genotype.

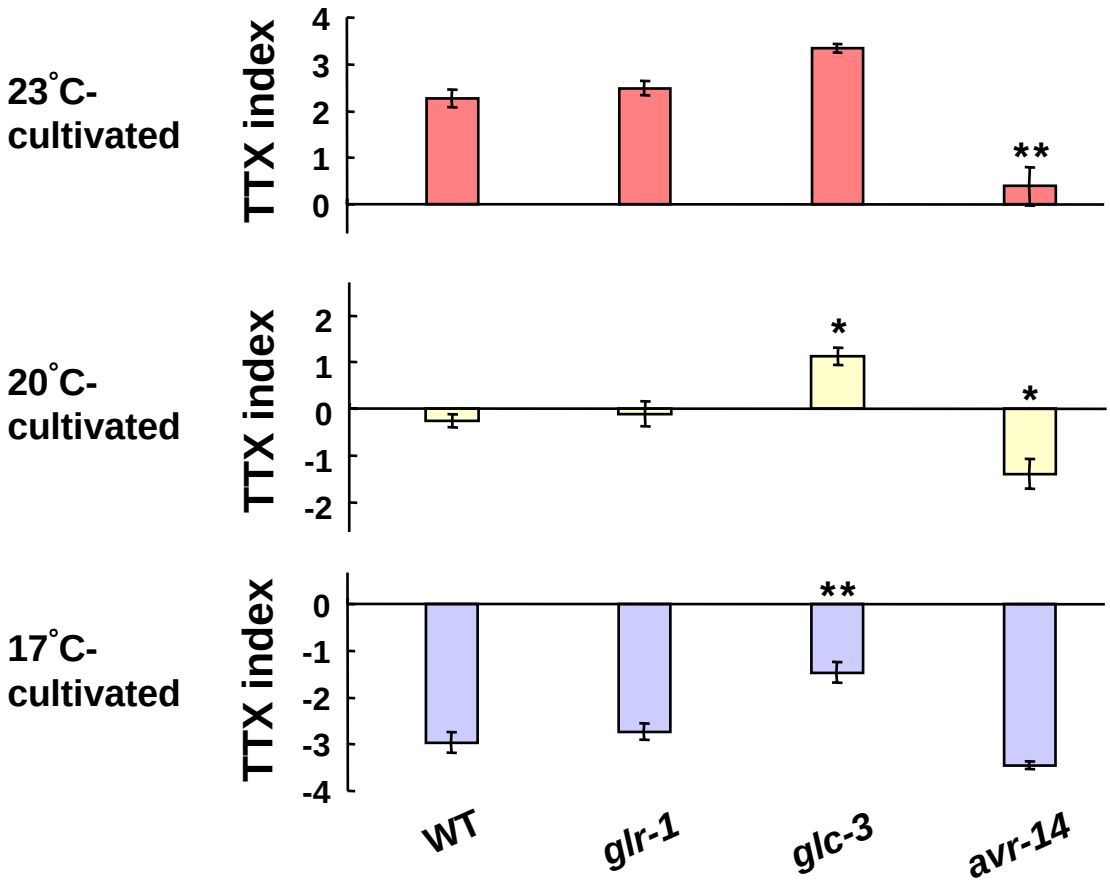

Figure 27. The population TTX assay of *glr-1*, *glc-3*, and *avr-14* mutants.
Red bars, yellow bars, and blue bars represent TTX indices of animals cultivated at 23°C, 20°C, and 17°C, respectively. n = 3 or more assays. Error bar indicates SEM. Single asterisk and double asteris indicate $p < 0.05$ and $p < 0.01$ respectively in post hoc Tukey-Kramer tests for a comparison with wild type animals.

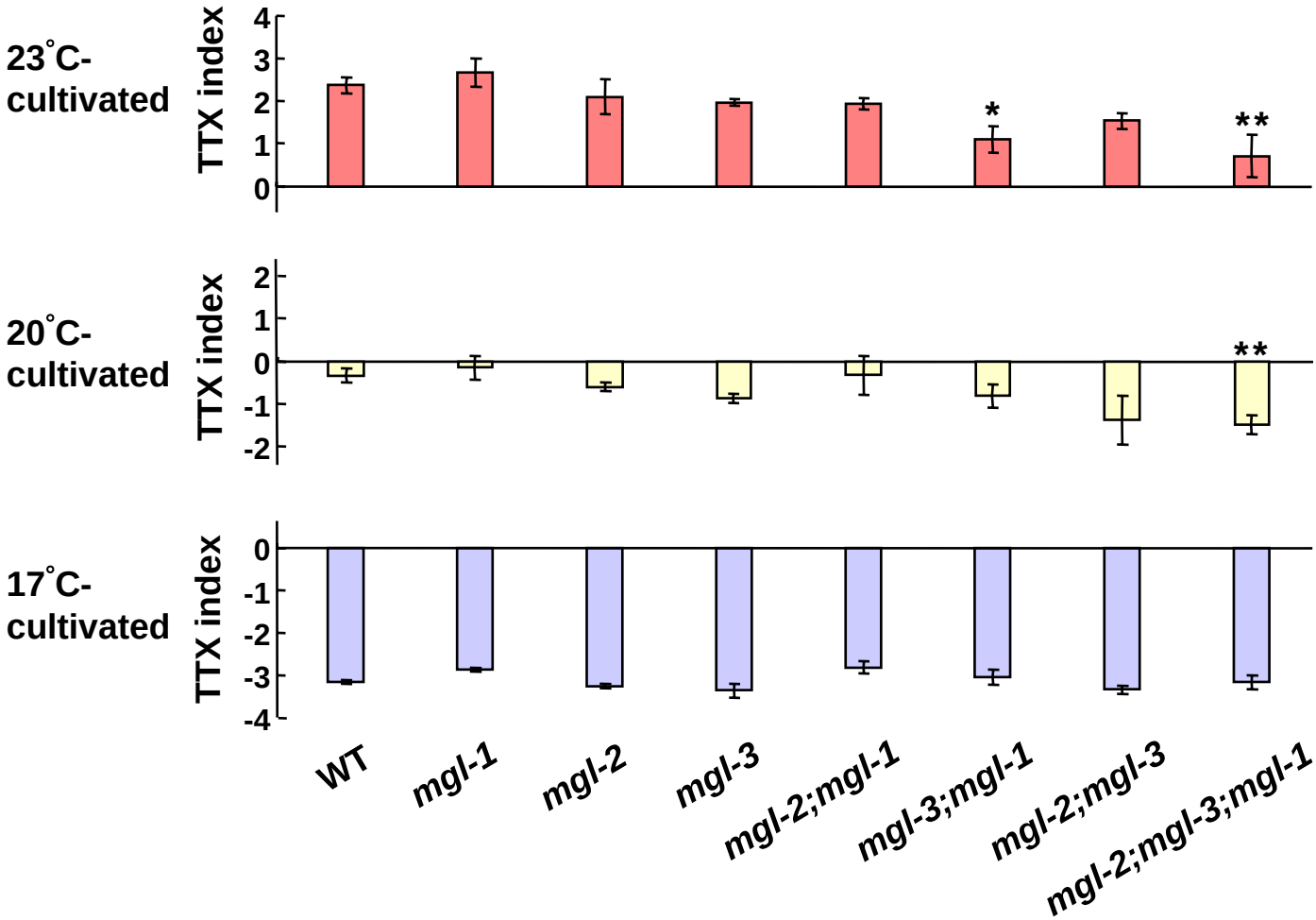

Figure 28. The population TTX assay of mGluR mutants.
TTX indices of *mgl-1*, *mgl-2*, and *mgl-3* mutants, and these double or triple mutants cultivated at 23˚C, 20˚C, and 17˚C. n = 3 or more assays. Error bar indicates SEM. Single asterisk and double asteris indicate $p < 0.05$ and $p < 0.01$ respectively in post hoc Tukey-Kramer tests for a comparison with wild type animals.

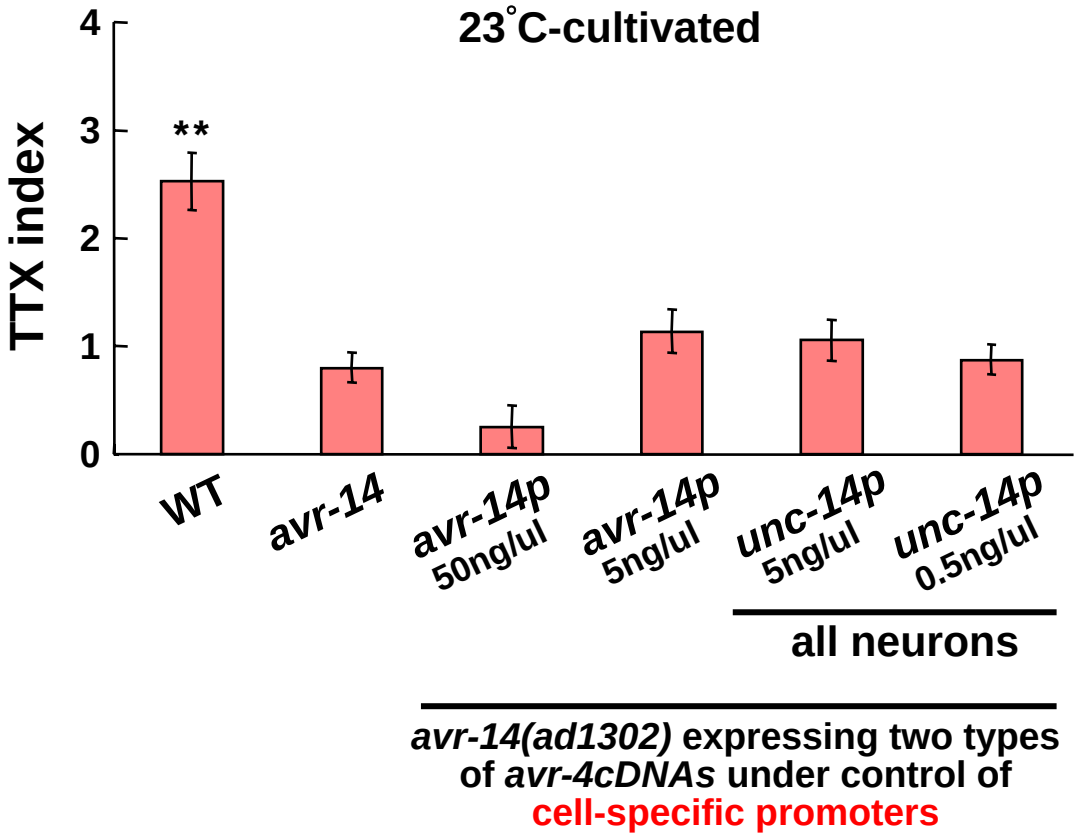

Figure 29. Cell-specific rescue experiments of *avr-14(ad1302)* mutants in the population TTX assay.
Rescue experiments for cryophilic movement of 23°C-cultivated *avr-14(ad1302)* mutants by introducing cell-specific *promoters::eat-4 cDNAs* at several doses. Red bars represent TTX indices of animals. n = 3 or more assays. Error bar indicates SEM. Double asteris indicate $p < 0.01$ in post hoc Tukey-Kramer tests for a comparison with *avr-14(ad1302)* mutants.

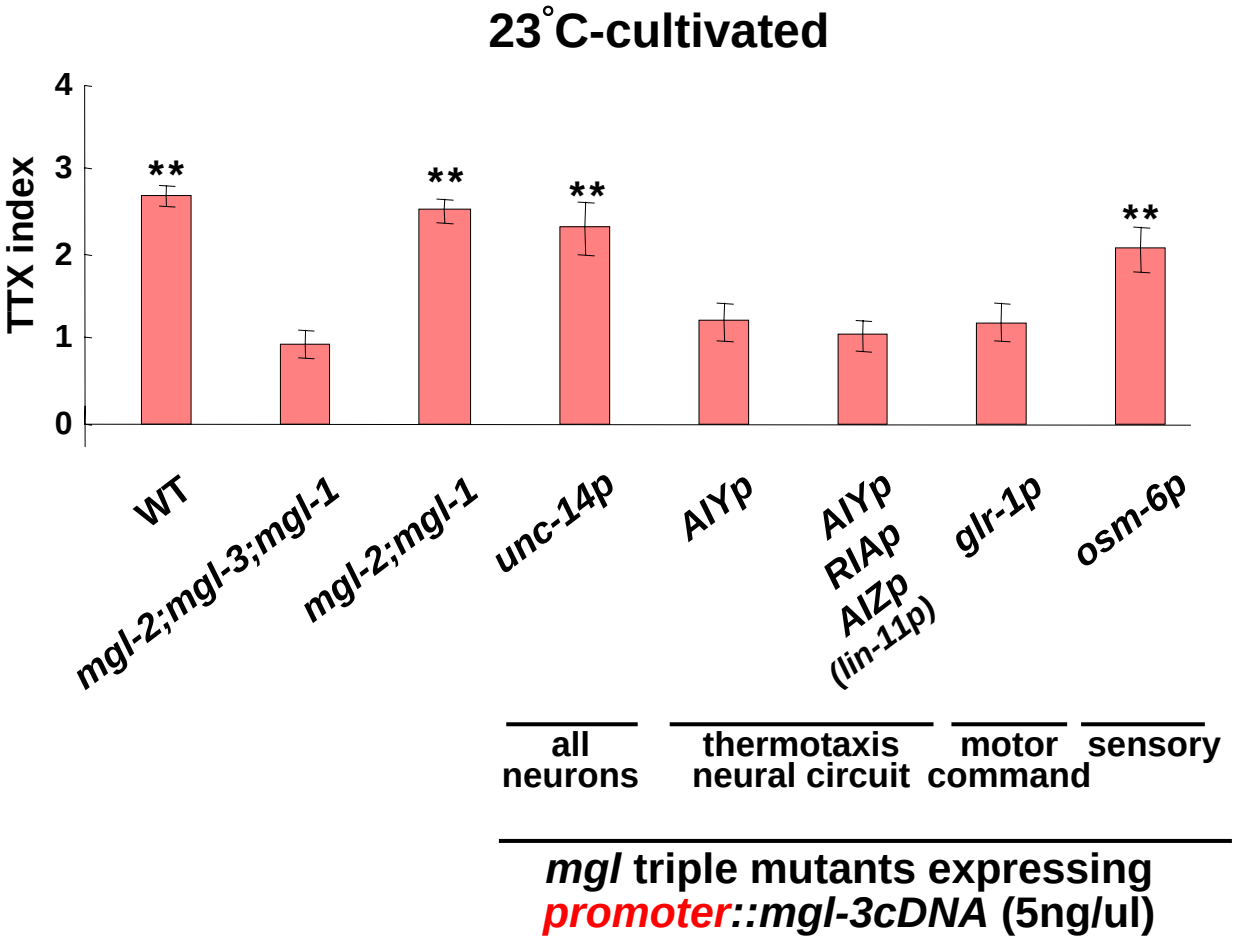

Figure 30. Cell-specific rescue experiments of *mgl-2(tm355); mgl-3(tm1766); mgl-1(tm1811)* triple mutants in the population TTX assay.
Rescue experiments for cryophilic movement of 23°C-cultivated *mgl* triple mutants by introducing cell-specific *promoters::mgl-3 cDNAs* at 5ng/ul. Red bars represent TTX indices of animals. n = 3 or more assays. Error bar indicates SEM. Double asteris indicate $p < 0.01$ in post hoc Tukey-Kramer tests for a comparison with *mgl-2(tm355); mgl-3(tm1766); mgl-1(tm1811)* triple mutants.

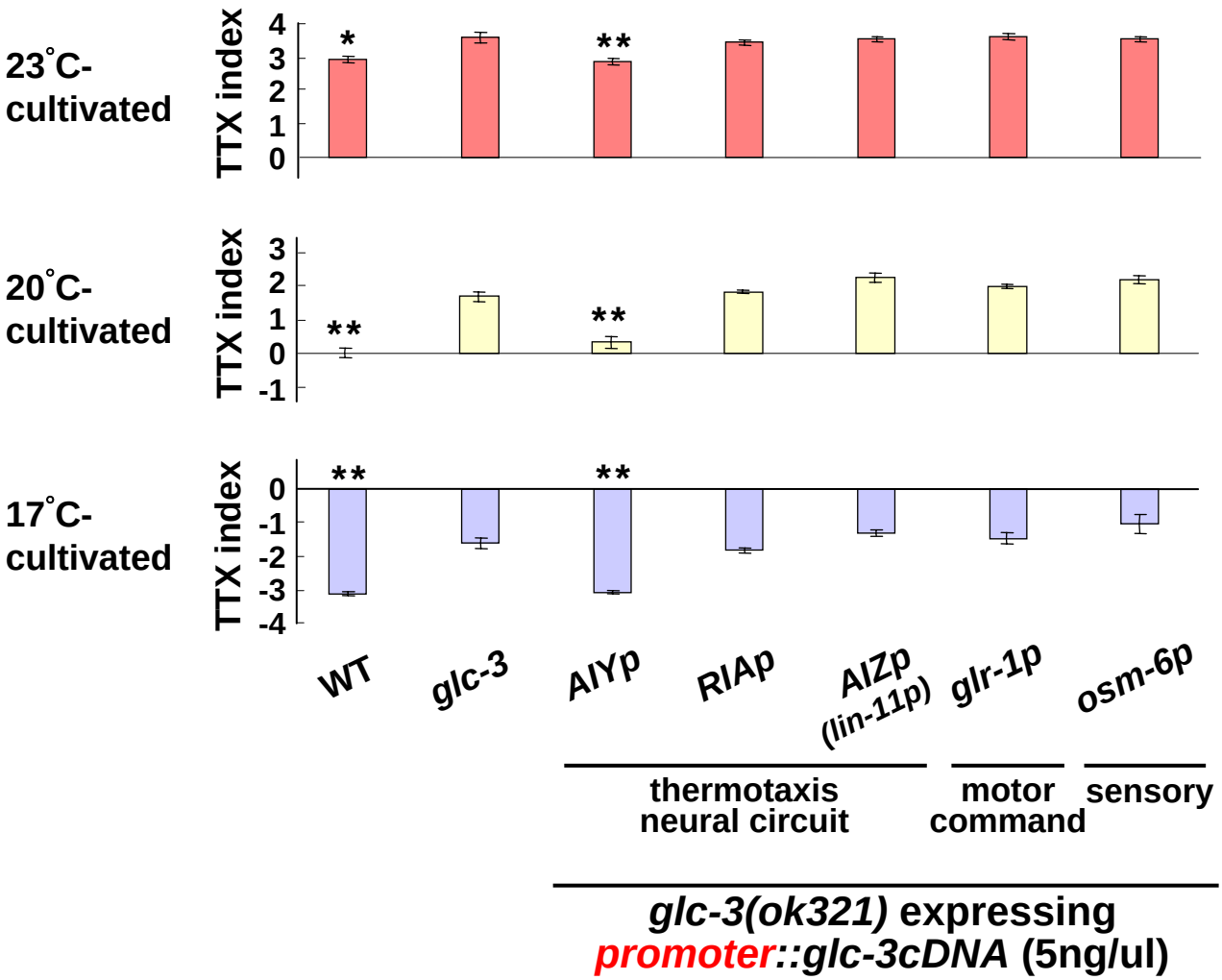

Figure 31. Cell-specific rescue experiments of *glc-3(ok321)* mutants in the population TTX assay.
Rescue experiments for thermophilic movement of *glc-3(ok321)* mutants by introducing cell-specific *promoters::glc-3 cDNAs* at 5ng/ul. Red bars, yellow bars, and blue bars represent TTX indices of animals cultivated at 23˚C, 20˚C, and 17˚C, respectivel. n = 3 or more assays. Error bar indicates SEM. Double asteris indicate $p < 0.01$ in post hoc Tukey-Kramer tests for a comparison with *glc-3(ok321)* mutants.

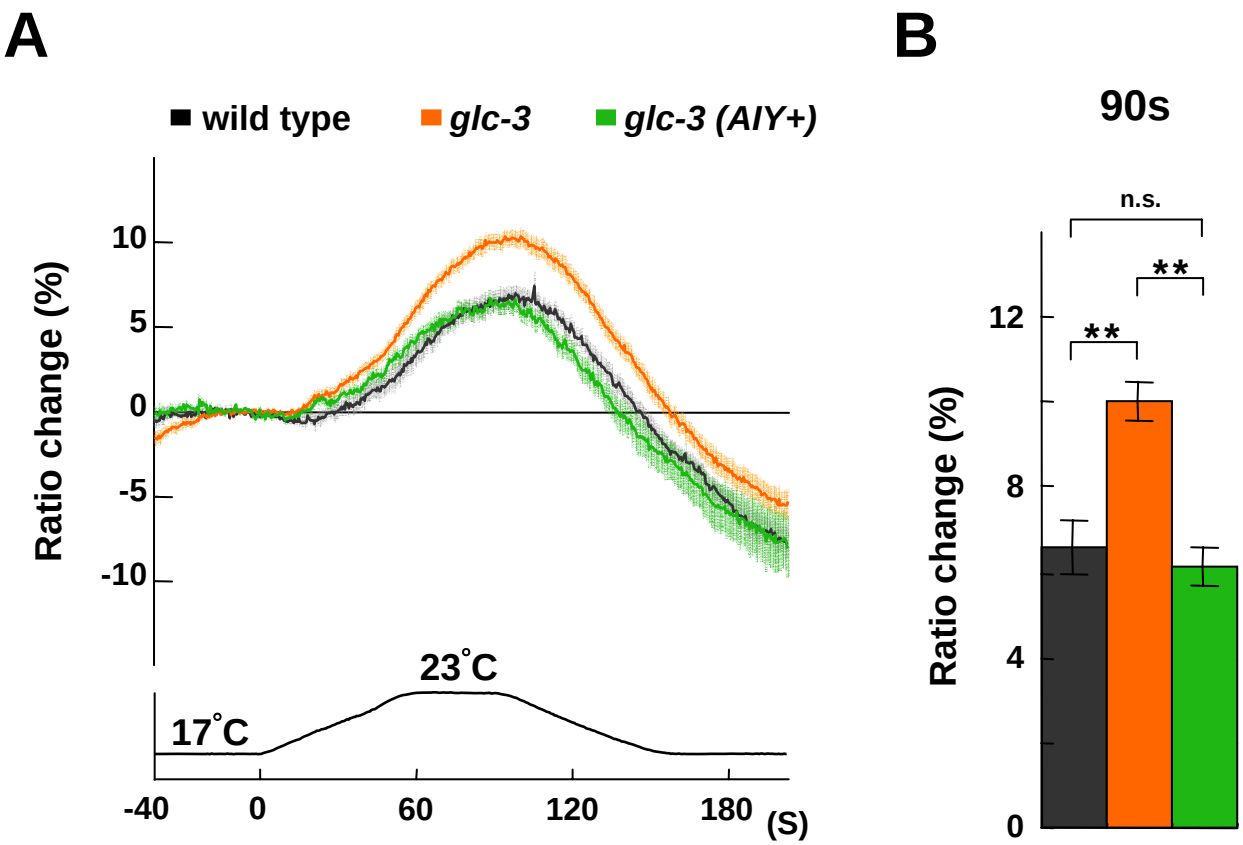

Figure 32. *in vivo* calcium imaging of AIY in 20˚C-cultivated *glc-3(ok321)* mutants and the *glc-3(ok321)* transgenic animals.
(A) Ratio change of yc3.6 in AIY according to temperature change. *glc-3 (AIY+)* represents the transgenic *glc-3(ok321)* mutants expressing GCL-3 in AIY. (B) The average of Ratio changes to temperature stimuli at 90s regarding the results shown in Figure 31A. n = 24 or more animals. Error bar indicates SEM. Double asterisk and n.s. indicates $p < 0.01$ and $p > 0.05$, respectively, in Steel-Dwass tests for a comparison with wild-type animals.

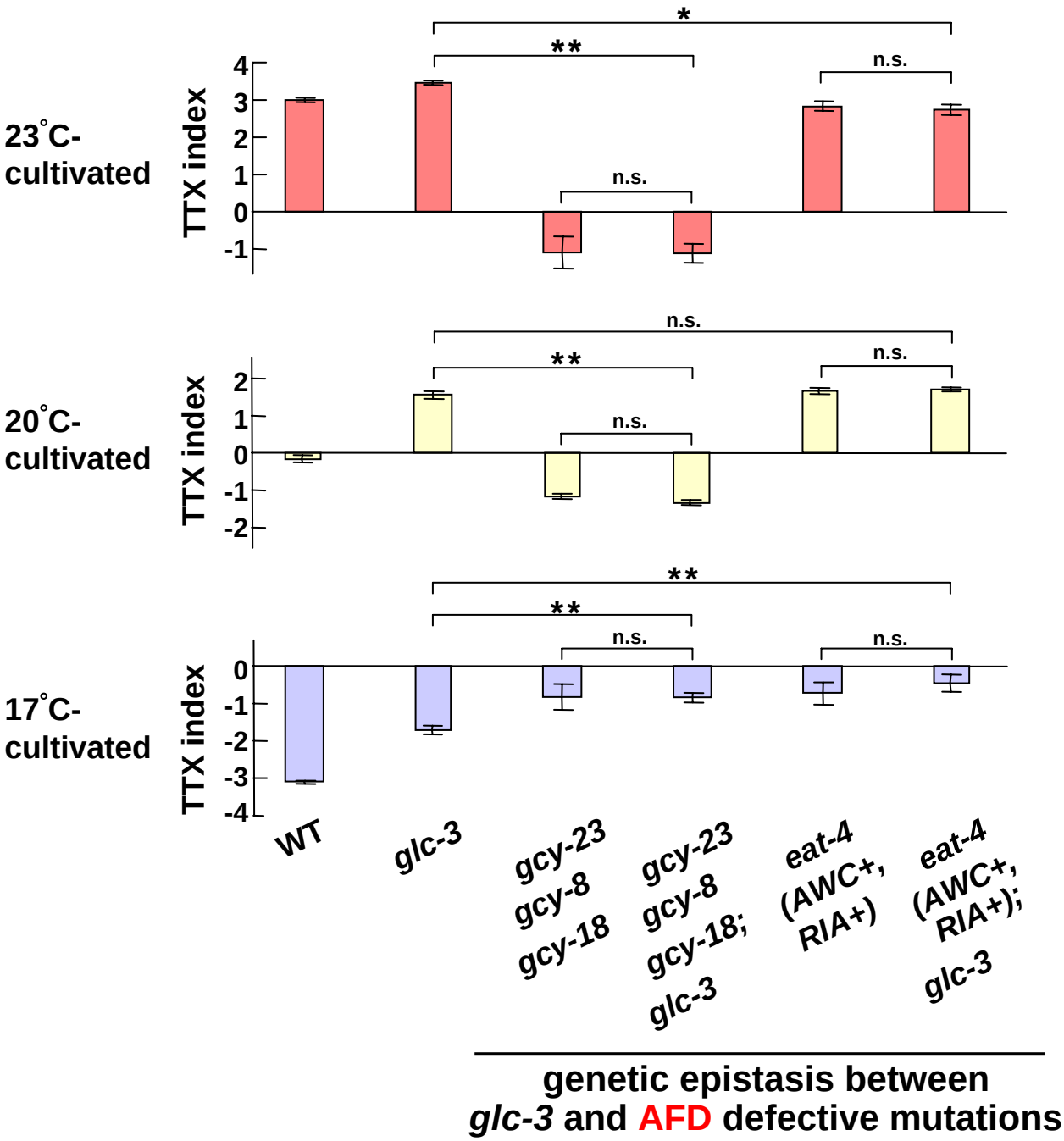

Figure 33. Analysis of genetic epistasis between *glc-3* and AFD-defective mutants. The population thermotaxis assays of AFD defective mutants, and *glc-3* mutants in the background of abnormal neural signaling in AFD. n = 3 or more assays. Error bar indicates SEM. Single asterisk, double asterisk and n.s. indicate $p < 0.05$, $p < 0.01$, and $p > 0.05$, respectively, in post hoc Tukey-Kramer tests for a comparison of each genotype.

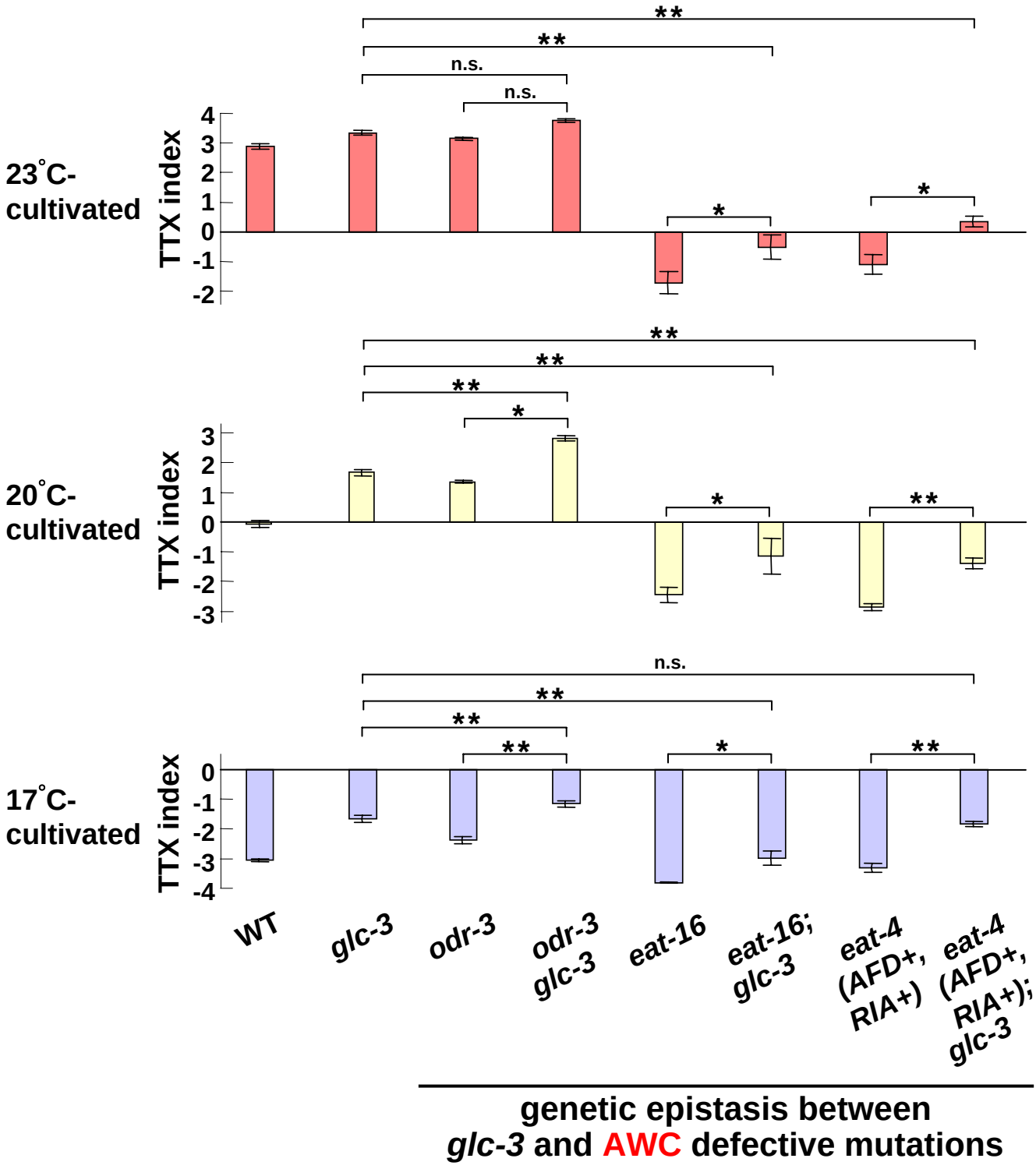

Figure 34. Analysis of genetic epistasis between *glc-3* and AWC-defective mutants. The population thermotaxis assays of AWC defective mutants, and *glc-3* mutants in the background of abnormal neural signaling in AWC. n = 3 or more assays. Error bar indicates SEM. Single asterisk, double asterisk and n.s. indicate $p < 0.05$, $p < 0.01$, and $p > 0.05$, respectively, in post hoc Tukey-Kramer tests for a comparison of each genotype.

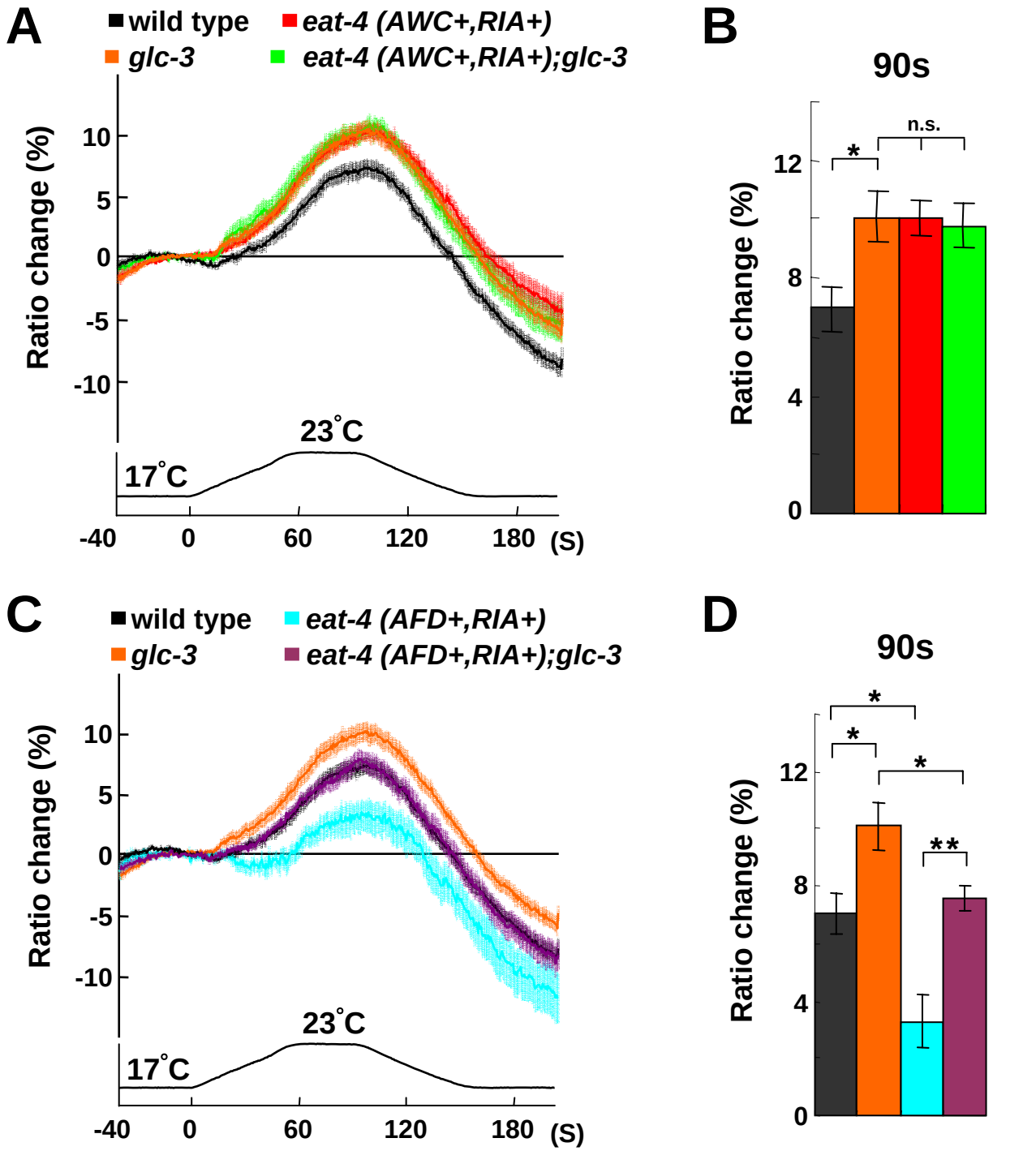

Figure 35. Effect of AFD or AWC defect on activity of AIY in *glc-3(ok321)* mutants.
(A, B) *in vivo* calcium imaging of AIY in *eat-4 (AWC+,RIA+); glc-3* and each single mutants. (A) Ratio change of yc3.6 in AIY according to temperature change. (B) The average of Ratio changes to temperature stimuli at 90s regarding the results shown in Figure 35A.
(C, D) *in vivo* calcium imaging of AIY in *eat-4 (AFD+,RIA+); glc-3* and each single mutants. (C) Ratio change of yc3.6 in AIY according to temperature change. (D) The average of Ratio changes to temperature stimuli at 90s regarding the results shown in Figure 35C.
(A, B, C, D) n = 22 or more animals. Error bar indicates SEM. Single asterisk, double asterisk and n.s. indicate $p < 0.05$, $p < 0.01$, and $p > 0.05$, respectively, in post hoc Tukey-Kramer tests for a comparison of each genotype.

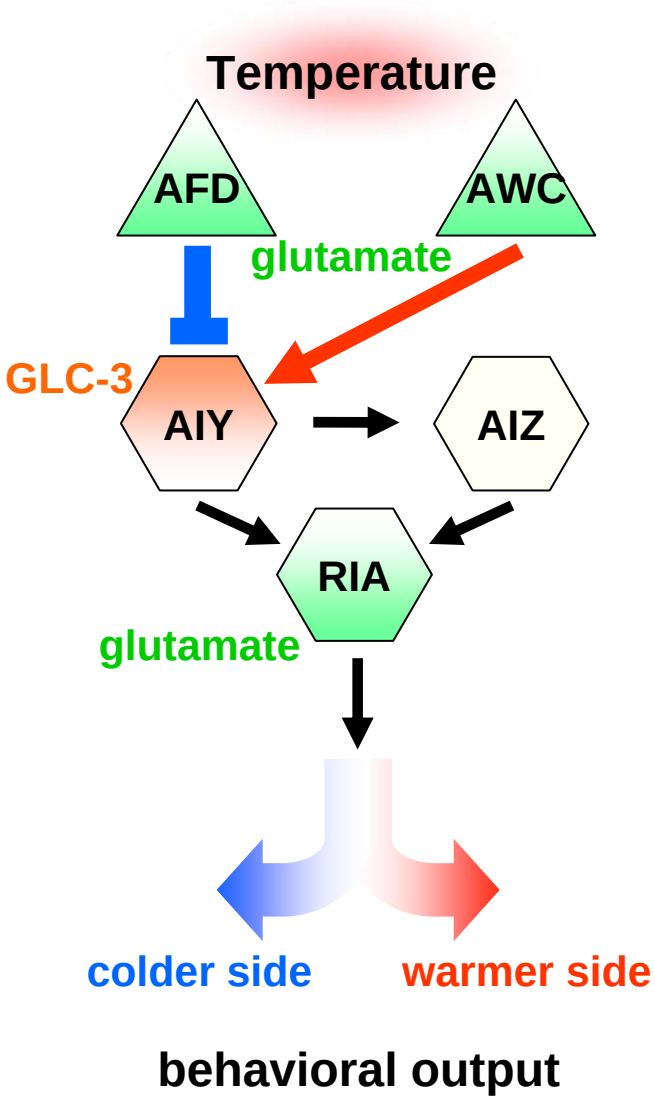

Figure 36. A model for glutamatergic neurotransmission in the thermotaxis neural circuit.
AFD, AWC, and RIA release glutamate in EAT-4 dependent manner (green). GLC-3 acts in AIY (orange). EAT-4 dependent glutamate signals from AFD inhibit the activity of AIY through activation of GLC-3 inhibitory glutamate receptors, and induce eventual migration to colder side (blue). By contrast, EAT-4 dependent glutamate signals from AWC stimulate the activity of AIY, and induce eventual migration to warmer side (red).

A

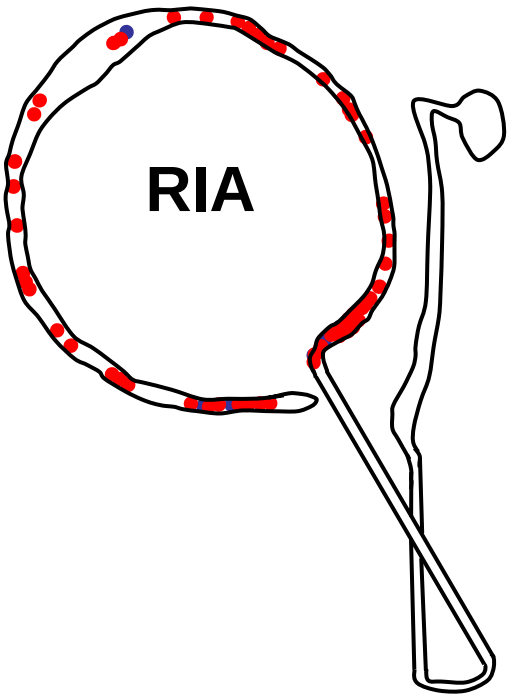

(White *et al*., 1986 modified)

B

downstream neurons of RIA	percentage of total presynapses in RIA
SMD	40%
RMD	50%
RIV	8%
SIA	1%
RIA	1%

Figure 37. Postsynaptic neurons of RIA.
(A) Schematic structure of RIA interneurons. RIA has a single neurite. All dots represent presynapses in the neurite of RIA. Of those, red dots represent presynapses connecting to SMD or RIA head motor neurons.
(B) Percentages of precynapses connecting to each neurons in RIA.

Ionotropic (channel)	
AMPA/KA type	***glr-1 glr-2 glr-3 glr-4 glr-5 glr-6 glr-7 glr-8***
NMDA type	***nmr-1 nmr-2***
Cl^- channel type	***glc-1 glc-2 glc-3 glc-4 avr-14 avr-15***
metabotropic	***mgl-1 mgl-2 mgl-3***

Table 1. Glutamate receptors in *C. elegans*.
Four classes of glutamate receptors are predicted in *C. elegans.*

Appendix

pNR8 (*eat-4* cDNA)

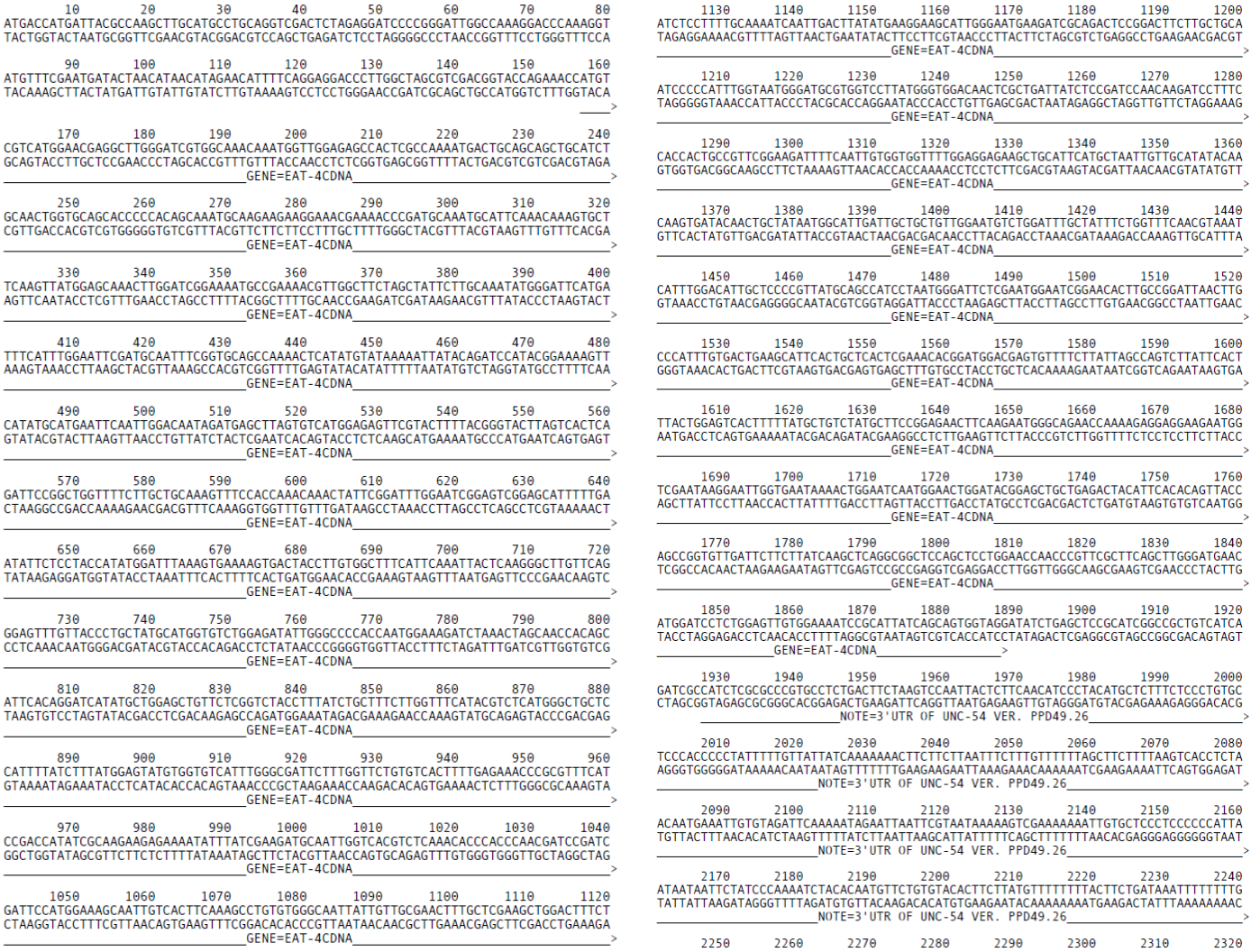


NOTE=3'UTR OF UNC-54 VER. PPD49.26
NOTE=3'UTR OF ____

pNR57 (*avr-14a* cDNA)

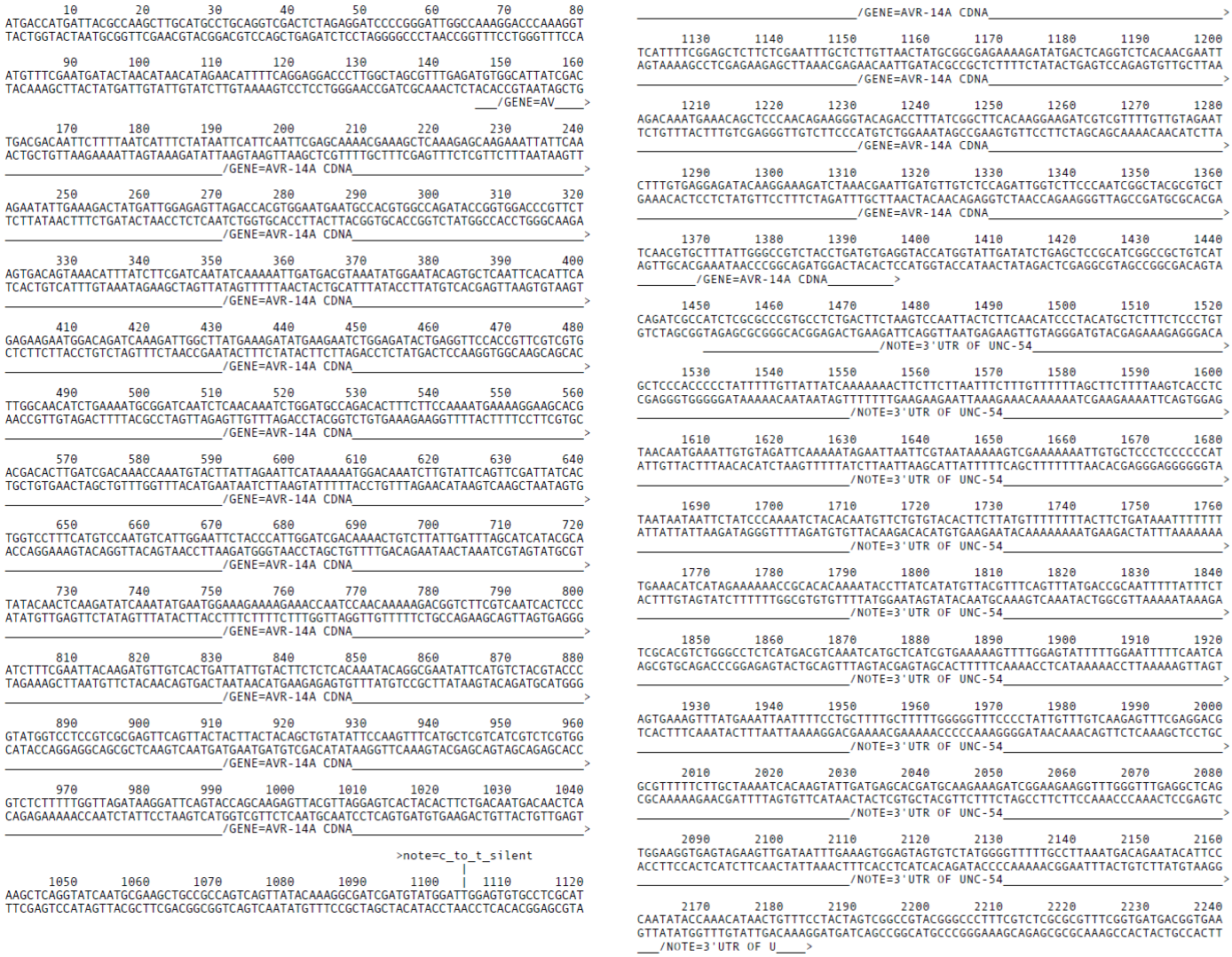

```
      2250      2260      2270      2280      2290      2300      2310      2320
AACCTCTGACACATGCAGCTCCCGGAGACGGTCACAGCTTGTCTGTAAGCGGATGCCGGGAGCAGACAAGCCCGTCAGGG
TTGGAGACTGTGTACGTCGAGGGCCTCTGCCAGTGTCGAACAGACATTCGCCTACGGCCCTCGTCTGTTCGGGCAGTCCC

      2330      2340      2350      2360      2370      2380      2390      2400
CGCGTCAGCGGGTGTTGGCGGGTGTCGGGGCTGGCTTAACTATGCGGCATCAGAGCAGATTGTACTGAGAGTGCACCATA
GCGCAGTCGCCCACAACCGCCCACAGCCCCGACCGAATTGATACGCCGTAGTCTCGTCTAACATGACTCTCACGTGGTAT

      2410      2420      2430      2440      2450      2460      2470      2480
TGCGGTGTGAAATACCGCACAGATGCGTAAGGAGAAAATACCGCATCAGGCGGCCTTAAGGGCCTCGTGATACGCCTATT
ACGCCACACTTTATGGCGTGTCTACGCATTCCTCTTTTATGGCGTAGTCCGCCGGAATTCCCGGAGCACTATGCGGATAA

      2490      2500      2510      2520      2530      2540      2550      2560
TTTATAGGTTAATGTCATGATAATAATGGTTTCTTAGACGTCAGGTGGCACTTTTCGGGGAAATGTGCGCGGAACCCCTA
AAATATCCAATTACAGTACTATTATTACCAAAGAATCTGCAGTCCACCGTGAAAAGCCCCTTTACACGCGCCTTGGGGAT

      2570      2580      2590      2600      2610      2620      2630      2640
TTTGTTTATTTTTCTAAATACATTCAAATATGTATCCGCTCATGAGACAATAACCCTGATAAATGCTTCAATAATATTGA
AAACAAATAAAAAGATTTATGTAAGTTTATACATAGGCGAGTACTCTGTTATTGGGACTATTTACGAAGTTATTATAACT

      2650      2660      2670      2680      2690      2700      2710      2720
AAAAGGAAGAGTATGAGTATTCAACATTTCCGTGTCGCCCTTATTCCCTTTTTTGCGGCATTTTGCCTTCCTGTTTTTGC
TTTTCCTTCTCATACTCATAAGTTGTAAAGGCACAGCGGGAATAAGGGAAAAAACGCCGTAAAACGGAAGGACAAAAACG

      2730      2740      2750      2760      2770      2780      2790      2800
TCACCCAGAAACGCTGGTGAAAGTAAAAGATGCTGAAGATCAGTTGGGTGCACGAGTGGGTTACATCGAACTGGATCTCA
AGTGGGTCTTTGCGACCACTTTCATTTTCTACGACTTCTAGTCAACCCACGTGCTCACCCAATGTAGCTTGACCTAGAGT

      2810      2820      2830      2840      2850      2860      2870      2880
ACAGCGGTAAGATCCTTGAGAGTTTTCGCCCCGAAGAACGTTTTCCAATGATGAGCACTTTTAAAGTTCTGCTATGTGGC
TGTCGCCATTCTAGGAACTCTCAAAAGCGGGGCTTCTTGCAAAAGGTTACTACTCGTGAAAATTTCAAGACGATACACCG

      2890      2900      2910      2920      2930      2940      2950      2960
GCGGTATTATCCCGTATTGACGCCGGGCAAGAGCAACTCGGTCGCCGCATACACTATTCTCAGAATGACTTGGTTGAGTA
CGCCATAATAGGGCATAACTGCGGCCCGTTCTCGTTGAGCCAGCGGCGTATGTGATAAGAGTCTTACTGAACCAACTCAT

      2970      2980      2990      3000      3010      3020      3030      3040
CTCACCAGTCACAGAAAAGCATCTTACGGATGGCATGACAGTAAGAGAATTATGCAGTGCTGCCATAACCATGAGTGATA
GAGTGGTCAGTGTCTTTTCGTAGAATGCCTACCGTACTGTCATTCTCTTAATACGTCACGACGGTATTGGTACTCACTAT

      3050      3060      3070      3080      3090      3100      3110      3120
ACACTGCGGCCAACTTACTTCTGACAACGATCGGAGGACCGAAGGAGCTAACCGCTTTTTTGCACAACATGGGGGATCAT
TGTGACGCCGGTTGAATGAAGACTGTTGCTAGCCTCCTGGCTTCCTCGATTGGCGAAAAAACGTGTTGTACCCCCTAGTA

      3130      3140      3150      3160      3170      3180      3190      3200
GTAACTCGCCTTGATCGTTGGGAACCGGAGCTGAATGAAGCCATACCAAACGACGAGCGTGACACCACGATGCCTGTAGC
CATTGAGCGGAACTAGCAACCCTTGGCCTCGACTTACTTCGGTATGGTTTGCTGCTCGCACTGTGGTGCTACGGACATCG

      3210      3220      3230      3240      3250      3260      3270      3280
AATGGCAACAACGTTGCGCAAACTATTAACTGGCGAACTACTTACTCTAGCTTCCCGGCAACAATTAATAGACTGGATGG
TTACCGTTGTTGCAACGCGTTTGATAATTGACCGCTTGATGAATGAGATCGAAGGGCCGTTGTTAATTATCTGACCTACC

      3290      3300      3310      3320      3330      3340      3350      3360
AGGCGGATAAAGTTGCAGGACCACTTCTGCGCTCGGCCCTTCCGGCTGGCTGGTTTATTGCTGATAAATCTGGAGCCGGT
TCCGCCTATTTCAACGTCCTGGTGAAGACGCGAGCCGGGAAGGCCGACCGACCAAATAACGACTATTTAGACCTCGGCCA

      3370      3380      3390      3400      3410      3420      3430      3440
GAGCGTGGGTCTCGCGGTATCATTGCAGCACTGGGGCCAGATGGTAAGCCCTCCCGTATCGTAGTTATCTACACGACGGG
CTCGCACCCAGAGCGCCATAGTAACGTCGTGACCCCGGTCTACCATTCGGGAGGGCATAGCATCAATAGATGTGCTGCCC

      3450      3460      3470      3480      3490      3500      3510      3520
GAGTCAGGCAACTATGGATGAACGAAATAGACAGATCGCTGAGATAGGTGCCTCACTGATTAAGCATTGGTAACTGTCAG
CTCAGTCCGTTGATACCTACTTGCTTTATCTGTCTAGCGACTCTATCCACGGAGTGACTAATTCGTAACCATTGACAGTC

      3530      3540      3550      3560      3570      3580      3590      3600
ACCAAGTTTACTCATATATACTTTAGATTGATTTAAAACTTCATTTTTAATTTAAAAGGATCTAGGTGAAGATCCTTTTT
TGGTTCAAATGAGTATATATGAAATCTAACTAAATTTTGAAGTAAAAATTAAATTTTCCTAGATCCACTTCTAGGAAAAA

      3610      3620      3630      3640      3650      3660      3670      3680
GATAATCTCATGACCAAAATCCCTTAACGTGAGTTTTCGTTCCACTGAGCGTCAGACCCCGTAGAAAAGATCAAAGGATC
```

```
CTATTAGAGTACTGGTTTTAGGGAATTGCACTCAAAAGCAAGGTGACTCGCAGTCTGGGGCATCTTTTCTAGTTTCCTAG

      3690      3700      3710      3720      3730      3740      3750      3760
TTCTTGAGATCCTTTTTTTCTGCGCGTAATCTGCTGCTTGCAAACAAAAAAACCACCGCTACCAGCGGTGGTTTGTTTGC
AAGAACTCTAGGAAAAAAAGACGCGCATTAGACGACGAACGTTTGTTTTTTTGGTGGCGATGGTCGCCACCAAACAAACG

      3770      3780      3790      3800      3810      3820      3830      3840
CGGATCAAGAGCTACCAACTCTTTTTCCGAAGGTAACTGGCTTCAGCAGAGCGCAGATACCAAATACTGTCCTTCTAGTG
GCCTAGTTCTCGATGGTTGAGAAAAAGGCTTCCATTGACCGAAGTCGTCTCGCGTCTATGGTTTATGACAGGAAGATCAC

      3850      3860      3870      3880      3890      3900      3910      3920
TAGCCGTAGTTAGGCCACCACTTCAAGAACTCTGTAGCACCGCCTACATACCTCGCTCTGCTAATCCTGTTACCAGTGGC
ATCGGCATCAATCCGGTGGTGAAGTTCTTGAGACATCGTGGCGGATGTATGGAGCGAGACGATTAGGACAATGGTCACCG

      3930      3940      3950      3960      3970      3980      3990      4000
TGCTGCCAGTGGCGATAAGTCGTGTCTTACCGGGTTGGACTCAAGACGATAGTTACCGGATAAGGCGCAGCGGTCGGGCT
ACGACGGTCACCGCTATTCAGCACAGAATGGCCCAACCTGAGTTCTGCTATCAATGGCCTATTCCGCGTCGCCAGCCCGA

      4010      4020      4030      4040      4050      4060      4070      4080
GAACGGGGGGTTCGTGCACACAGCCCAGCTTGGAGCGAACGACCTACACCGAACTGAGATACCTACAGCGTGAGCATTGA
CTTGCCCCCCAAGCACGTGTGTCGGGTCGAACCTCGCTTGCTGGATGTGGCTTGACTCTATGGATGTCGCACTCGTAACT

      4090      4100      4110      4120      4130      4140      4150      4160
GAAAGCGCCACGCTTCCCGAAGGGAGAAAGGCGGACAGGTATCCGGTAAGCGGCAGGGTCGGAACAGGAGAGCGCACGAG
CTTTCGCGGTGCGAAGGGCTTCCCTCTTTCCGCCTGTCCATAGGCCATTCGCCGTCCCAGCCTTGTCCTCTCGCGTGCTC

      4170      4180      4190      4200      4210      4220      4230      4240
GGAGCTTCCAGGGGGAAACGCCTGGTATCTTTATAGTCCTGTCGGGTTTCGCCACCTCTGACTTGAGCGTCGATTTTTGT
CCTCGAAGGTCCCCCTTTGCGGACCATAGAAATATCAGGACAGCCCAAAGCGGTGGAGACTGAACTCGCAGCTAAAAACA

      4250      4260      4270      4280      4290      4300      4310      4320
GATGCTCGTCAGGGGGGCGGAGCCTATGGAAAAACGCCAGCAACGCGGCCTTTTTACGGTTCCTGGCCTTTTGCTGGCCT
CTACGAGCAGTCCCCCCGCCTCGGATACCTTTTTGCGGTCGTTGCGCCGGAAAAATGCCAAGGACCGGAAAACGACCGGA

      4330      4340      4350      4360      4370      4380      4390      4400
TTTGCTCACATGTTCTTTCCTGCGTTATCCCCTGATTCTGTGGATAACCGTATTACCGCCTTTGAGTGAGCTGATACCGC
AAACGAGTGTACAAGAAAGGACGCAATAGGGGACTAAGACACCTATTGGCATAATGGCGGAAACTCACTCGACTATGGCG

      4410      4420      4430      4440      4450      4460      4470      4480
TCGCCGCAGCCGAACGACCGAGCGCAGCGAGTCAGTGAGCGAGGAAGCGGAAGAGCGCCCAATACGCAAACCGCCTCTCC
AGCGGCGTCGGCTTGCTGGCTCGCGTCGCTCAGTCACTCGCTCCTTCGCCTTCTCGCGGGTTATGCGTTTGGCGGAGAGG

      4490      4500      4510      4520      4530      4540      4550      4560
CCGCGCGTTGGCCGATTCATTAATGCAGCTGGCACGACAGGTTTCCCGACTGGAAAGCGGGCAGTGAGCGCAACGCAATT
GGCGCGCAACCGGCTAAGTAATTACGTCGACCGTGCTGTCCAAAGGGCTGACCTTTCGCCCGTCACTCGCGTTGCGTTAA

      4570      4580      4590      4600      4610      4620      4630      4640
AATGTGAGTTAGCTCACTCATTAGGCACCCCAGGCTTTACACTTTATGCTTCCGGCTCGTATGTTGTGTGGAATTGTGAG
TTACACTCAATCGAGTGAGTAATCCGTGGGGTCCGAAATGTGAAATACGAAGGCCGAGCATACAACACACCTTAACACTC

      4650      4660
CGGATAACAATTTCACACAGGAAACAGCT
GCCTATTGTTAAAGTGTGTCCTTTGTCGA
```

pNR59 (*avr-14b* cDNA)

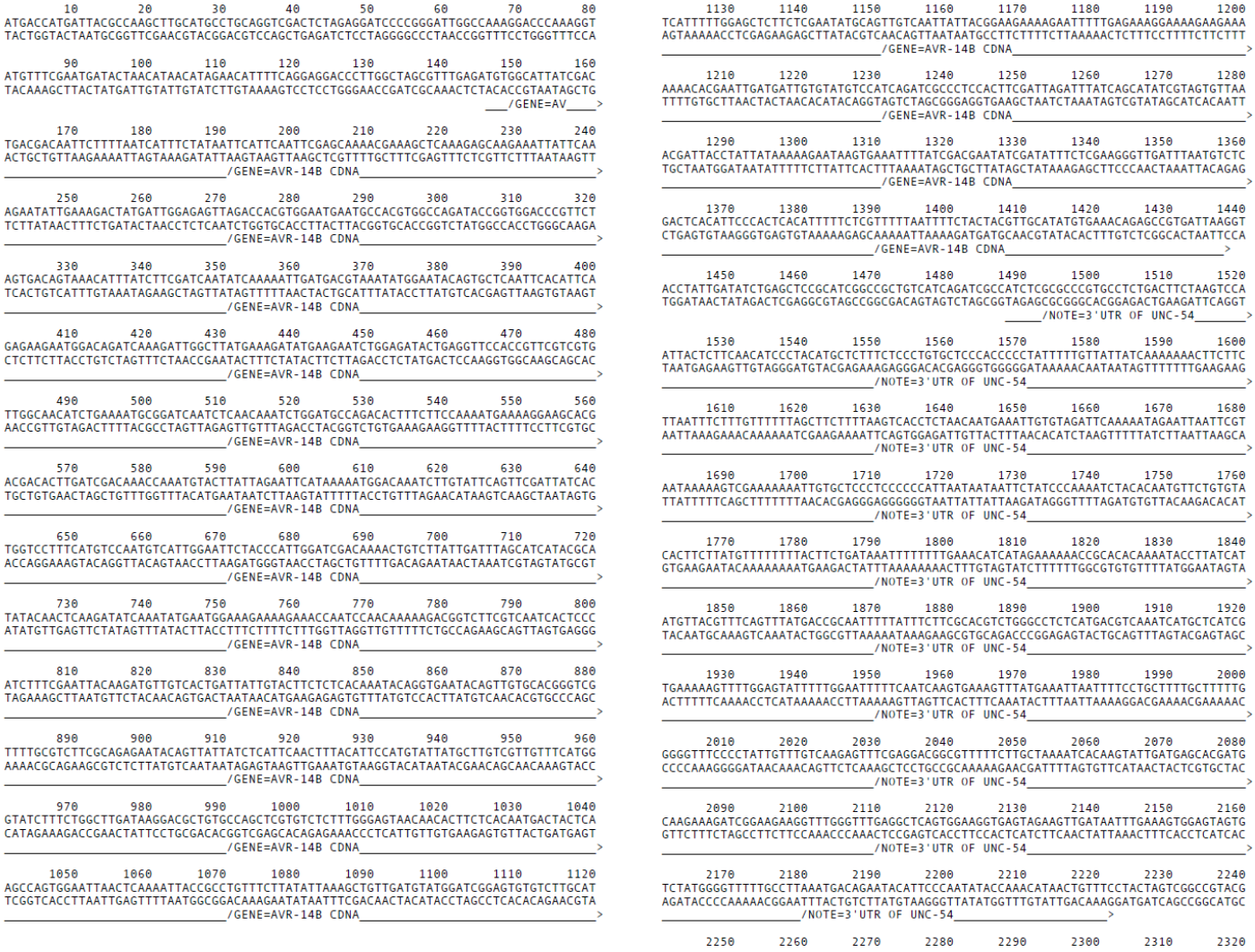

```
GGCCCTTTCGTCTCGCGCGTTTCGGTGATGACGGTGAAAACCTCTGACACATGCAGCTCCCGGAGACGGTCACAGCTTGT
CCGGGAAAGCAGAGCGCGCAAAGCCACTACTGCCACTTTTGGAGACTGTGTACGTCGAGGGCCTCTGCCAGTGTCGAACA

      2330      2340      2350      2360      2370      2380      2390      2400
CTGTAAGCGGATGCCGGGAGCAGACAAGCCCGTCAGGGCGCGTCAGCGGGTGTTGGCGGGTGTCGGGGCTGGCTTAACTA
GACATTCGCCTACGGCCCTCGTCTGTTCGGGCAGTCCCGCGCAGTCGCCCACAACCGCCCACAGCCCCGACCGAATTGAT

      2410      2420      2430      2440      2450      2460      2470      2480
TGCGGCATCAGAGCAGATTGTACTGAGAGTGCACCATATGCGGTGTGAAATACCGCACAGATGCGTAAGGAGAAAATACC
ACGCCGTAGTCTCGTCTAACATGACTCTCACGTGGTATACGCCACACTTTATGGCGTGTCTACGCATTCCTCTTTTATGG

      2490      2500      2510      2520      2530      2540      2550      2560
GCATCAGGCGGCCTTAAGGGCCTCGTGATACGCCTATTTTTATAGGTTAATGTCATGATAATAATGGTTTCTTAGACGTC
CGTAGTCCGCCGGAATTCCCGGAGCACTATGCGGATAAAAATATCCAATTACAGTACTATTATTACCAAAGAATCTGCAG

      2570      2580      2590      2600      2610      2620      2630      2640
AGGTGGCACTTTTCGGGGAAATGTGCGCGGAACCCCTATTTGTTTATTTTTCTAAATACATTCAAATATGTATCCGCTCA
TCCACCGTGAAAAGCCCCTTTACACGCGCCTTGGGGATAAACAAATAAAAAGATTTATGTAAGTTTATACATAGGCGAGT

      2650      2660      2670      2680      2690      2700      2710      2720
TGAGACAATAACCCTGATAAATGCTTCAATAATATTGAAAAAGGAAGAGTATGAGTATTCAACATTTCCGTGTCGCCCTT
ACTCTGTTATTGGGACTATTTACGAAGTTATTATAACTTTTTCCTTCTCATACTCATAAGTTGTAAAGGCACAGCGGGAA

      2730      2740      2750      2760      2770      2780      2790      2800
ATTCCCTTTTTTGCGGCATTTTGCCTTCCTGTTTTTGCTCACCCAGAAACGCTGGTGAAAGTAAAAGATGCTGAAGATCA
TAAGGGAAAAAACGCCGTAAAACGGAAGGACAAAAACGAGTGGGTCTTTGCGACCACTTTCATTTTCTACGACTTCTAGT

      2810      2820      2830      2840      2850      2860      2870      2880
GTTGGGTGCACGAGTGGGTTACATCGAACTGGATCTCAACAGCGGTAAGATCCTTGAGAGTTTTCGCCCCGAAGAACGTT
CAACCCACGTGCTCACCCAATGTAGCTTGACCTAGAGTTGTCGCCATTCTAGGAACTCTCAAAAGCGGGGCTTCTTGCAA

      2890      2900      2910      2920      2930      2940      2950      2960
TTCCAATGATGAGCACTTTTAAAGTTCTGCTATGTGGCGCGGTATTATCCCGTATTGACGCCGGGCAAGAGCAACTCGGT
AAGGTTACTACTCGTGAAAATTTCAAGACGATACACCGCGCCATAATAGGGCATAACTGCGGCCCGTTCTCGTTGAGCCA

      2970      2980      2990      3000      3010      3020      3030      3040
CGCCGCATACACTATTCTCAGAATGACTTGGTTGAGTACTCACCAGTCACAGAAAAGCATCTTACGGATGGCATGACAGT
GCGGCGTATGTGATAAGAGTCTTACTGAACCAACTCATGAGTGGTCAGTGTCTTTTCGTAGAATGCCTACCGTACTGTCA

      3050      3060      3070      3080      3090      3100      3110      3120
AAGAGAATTATGCAGTGCTGCCATAACCATGAGTGATAACACTGCGGCCAACTTACTTCTGACAACGATCGGAGGACCGA
TTCTCTTAATACGTCACGACGGTATTGGTACTCACTATTGTGACGCCGGTTGAATGAAGACTGTTGCTAGCCTCCTGGCT

      3130      3140      3150      3160      3170      3180      3190      3200
AGGAGCTAACCGCTTTTTTGCACAACATGGGGGATCATGTAACTCGCCTTGATCGTTGGGAACCGGAGCTGAATGAAGCC
TCCTCGATTGGCGAAAAAACGTGTTGTACCCCCTAGTACATTGAGCGGAACTAGCAACCCTTGGCCTCGACTTACTTCGG

      3210      3220      3230      3240      3250      3260      3270      3280
ATACCAAACGACGAGCGTGACACCACGATGCCTGTAGCAATGGCAACAACGTTGCGCAAACTATTAACTGGCGAACTACT
TATGGTTTGCTGCTCGCACTGTGGTGCTACGGACATCGTTACCGTTGTTGCAACGCGTTTGATAATTGACCGCTTGATGA

      3290      3300      3310      3320      3330      3340      3350      3360
TACTCTAGCTTCCCGGCAACAATTAATAGACTGGATGGAGGCGGATAAAGTTGCAGGACCACTTCTGCGCTCGGCCCTTC
ATGAGATCGAAGGGCCGTTGTTAATTATCTGACCTACCTCCGCCTATTTCAACGTCCTGGTGAAGACGCGAGCCGGGAAG

      3370      3380      3390      3400      3410      3420      3430      3440
CGGCTGGCTGGTTTATTGCTGATAAATCTGGAGCCGGTGAGCGTGGGTCTCGCGGTATCATTGCAGCACTGGGGCCAGAT
GCCGACCGACCAAATAACGACTATTTAGACCTCGGCCACTCGCACCCAGAGCGCCATAGTAACGTCGTGACCCCGGTCTA

      3450      3460      3470      3480      3490      3500      3510      3520
GGTAAGCCCTCCCGTATCGTAGTTATCTACACGACGGGGAGTCAGGCAACTATGGATGAACGAAATAGACAGATCGCTGA
CCATTCGGGAGGGCATAGCATCAATAGATGTGCTGCCCCTCAGTCCGTTGATACCTACTTGCTTTATCTGTCTAGCGACT

      3530      3540      3550      3560      3570      3580      3590      3600
GATAGGTGCCTCACTGATTAAGCATTGGTAACTGTCAGACCAAGTTTACTCATATATACTTTAGATTGATTTAAAACTTC
CTATCCACGGAGTGACTAATTCGTAACCATTGACAGTCTGGTTCAAATGAGTATATATGAAATCTAACTAAATTTTGAAG

      3610      3620      3630      3640      3650      3660      3670      3680
ATTTTTAATTTAAAAGGATCTAGGTGAAGATCCTTTTTGATAATCTCATGACCAAAATCCCTTAACGTGAGTTTTCGTTC
TAAAAATTAAATTTTCCTAGATCCACTTCTAGGAAAAACTATTAGAGTACTGGTTTTAGGGAATTGCACTCAAAAGCAAG

      3690      3700      3710      3720      3730      3740      3750      3760
CACTGAGCGTCAGACCCCGTAGAAAAGATCAAAGGATCTTCTTGAGATCCTTTTTTTCTGCGCGTAATCTGCTGCTTGCA
GTGACTCGCAGTCTGGGGCATCTTTTCTAGTTTCCTAGAAGAACTCTAGGAAAAAAAGACGCGCATTAGACGACGAACGT

      3770      3780      3790      3800      3810      3820      3830      3840
AACAAAAAAACCACCGCTACCAGCGGTGGTTTGTTTGCCGGATCAAGAGCTACCAACTCTTTTTCCGAAGGTAACTGGCT
TTGTTTTTTTGGTGGCGATGGTCGCCACCAAACAAACGGCCTAGTTCTCGATGGTTGAGAAAAAGGCTTCCATTGACCGA

      3850      3860      3870      3880      3890      3900      3910      3920
TCAGCAGAGCGCAGATACCAAATACTGTCCTTCTAGTGTAGCCGTAGTTAGGCCACCACTTCAAGAACTCTGTAGCACCG
AGTCGTCTCGCGTCTATGGTTTATGACAGGAAGATCACATCGGCATCAATCCGGTGGTGAAGTTCTTGAGACATCGTGGC

      3930      3940      3950      3960      3970      3980      3990      4000
CCTACATACCTCGCTCTGCTAATCCTGTTACCAGTGGCTGCTGCCAGTGGCGATAAGTCGTGTCTTACCGGGTTGGACTC
GGATGTATGGAGCGAGACGATTAGGACAATGGTCACCGACGACGGTCACCGCTATTCAGCACAGAATGGCCCAACCTGAG

      4010      4020      4030      4040      4050      4060      4070      4080
AAGACGATAGTTACCGGATAAGGCGCAGCGGTCGGGCTGAACGGGGGGTTCGTGCACACAGCCCAGCTTGGAGCGAACGA
TTCTGCTATCAATGGCCTATTCCGCGTCGCCAGCCCGACTTGCCCCCCAAGCACGTGTGTCGGGTCGAACCTCGCTTGCT

      4090      4100      4110      4120      4130      4140      4150      4160
CCTACACCGAACTGAGATACCTACAGCGTGAGCATTGAGAAAGCGCCACGCTTCCCGAAGGGAGAAAGGCGGACAGGTAT
GGATGTGGCTTGACTCTATGGATGTCGCACTCGTAACTCTTTCGCGGTGCGAAGGGCTTCCCTCTTTCCGCCTGTCCATA

      4170      4180      4190      4200      4210      4220      4230      4240
CCGGTAAGCGGCAGGGTCGGAACAGGAGAGCGCACGAGGGAGCTTCCAGGGGGAAACGCCTGGTATCTTTATAGTCCTGT
GGCCATTCGCCGTCCCAGCCTTGTCCTCTCGCGTGCTCCCTCGAAGGTCCCCCTTTGCGGACCATAGAAATATCAGGACA

      4250      4260      4270      4280      4290      4300      4310      4320
CGGGTTTCGCCACCTCTGACTTGAGCGTCGATTTTTGTGATGCTCGTCAGGGGGGCGGAGCCTATGGAAAAACGCCAGCA
GCCCAAAGCGGTGGAGACTGAACTCGCAGCTAAAAACACTACGAGCAGTCCCCCCGCCTCGGATACCTTTTTGCGGTCGT

      4330      4340      4350      4360      4370      4380      4390      4400
ACGCGGCCTTTTTACGGTTCCTGGCCTTTTGCTGGCCTTTTGCTCACATGTTCTTTCCTGCGTTATCCCCTGATTCTGTG
TGCGCCGGAAAAATGCCAAGGACCGGAAAACGACCGGAAAACGAGTGTACAAGAAAGGACGCAATAGGGGACTAAGACAC

      4410      4420      4430      4440      4450      4460      4470      4480
GATAACCGTATTACCGCCTTTGAGTGAGCTGATACCGCTCGCCGCAGCCGAACGACCGAGCGCAGCGAGTCAGTGAGCGA
CTATTGGCATAATGGCGGAAACTCACTCGACTATGGCGAGCGGCGTCGGCTTGCTGGCTCGCGTCGCTCAGTCACTCGCT

      4490      4500      4510      4520      4530      4540      4550      4560
GGAAGCGGAAGAGCGCCCAATACGCAAACCGCCTCTCCCCGCGCGTTGGCCGATTCATTAATGCAGCTGGCACGACAGGT
CCTTCGCCTTCTCGCGGGTTATGCGTTTGGCGGAGAGGGGCGCGCAACCGGCTAAGTAATTACGTCGACCGTGCTGTCCA

      4570      4580      4590      4600      4610      4620      4630      4640
TTCCCGACTGGAAAGCGGGCAGTGAGCGCAACGCAATTAATGTGAGTTAGCTCACTCATTAGGCACCCCAGGCTTTACAC
AAGGGCTGACCTTTCGCCCGTCACTCGCGTTGCGTTAATTACACTCAATCGAGTGAGTAATCCGTGGGGTCCGAAATGTG

      4650      4660      4670      4680      4690      4700
TTTATGCTTCCGGCTCGTATGTTGTGTGGAATTGTGAGCGGATAACAATTTCACACAGGAAACAGCT
AAATACGAAGGCCGAGCATACAACACACCTTAACACTCGCCTATTGTTAAAGTGTGTCCTTTGTCGA
```

pNR94 (*mgl-3* cDNA)

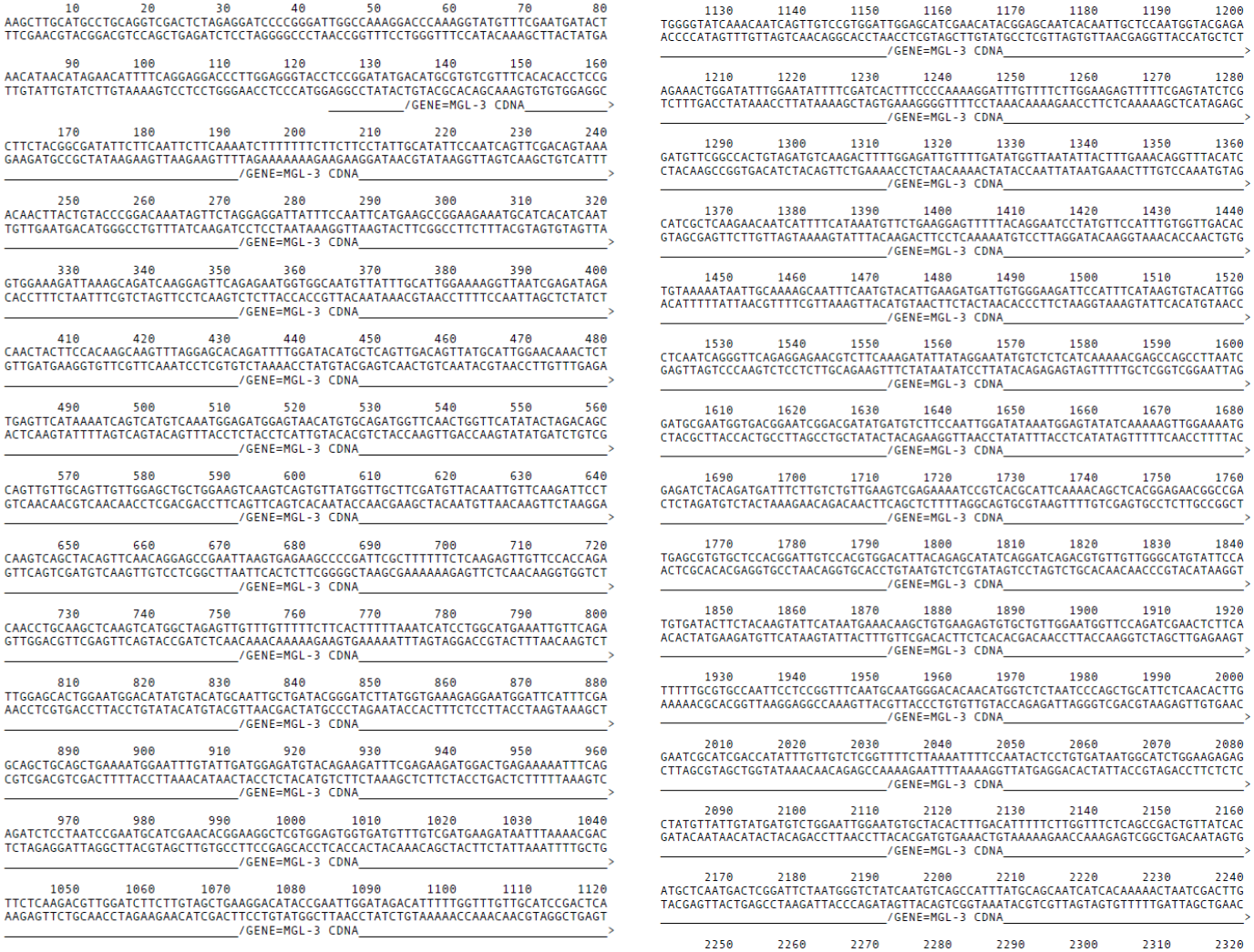

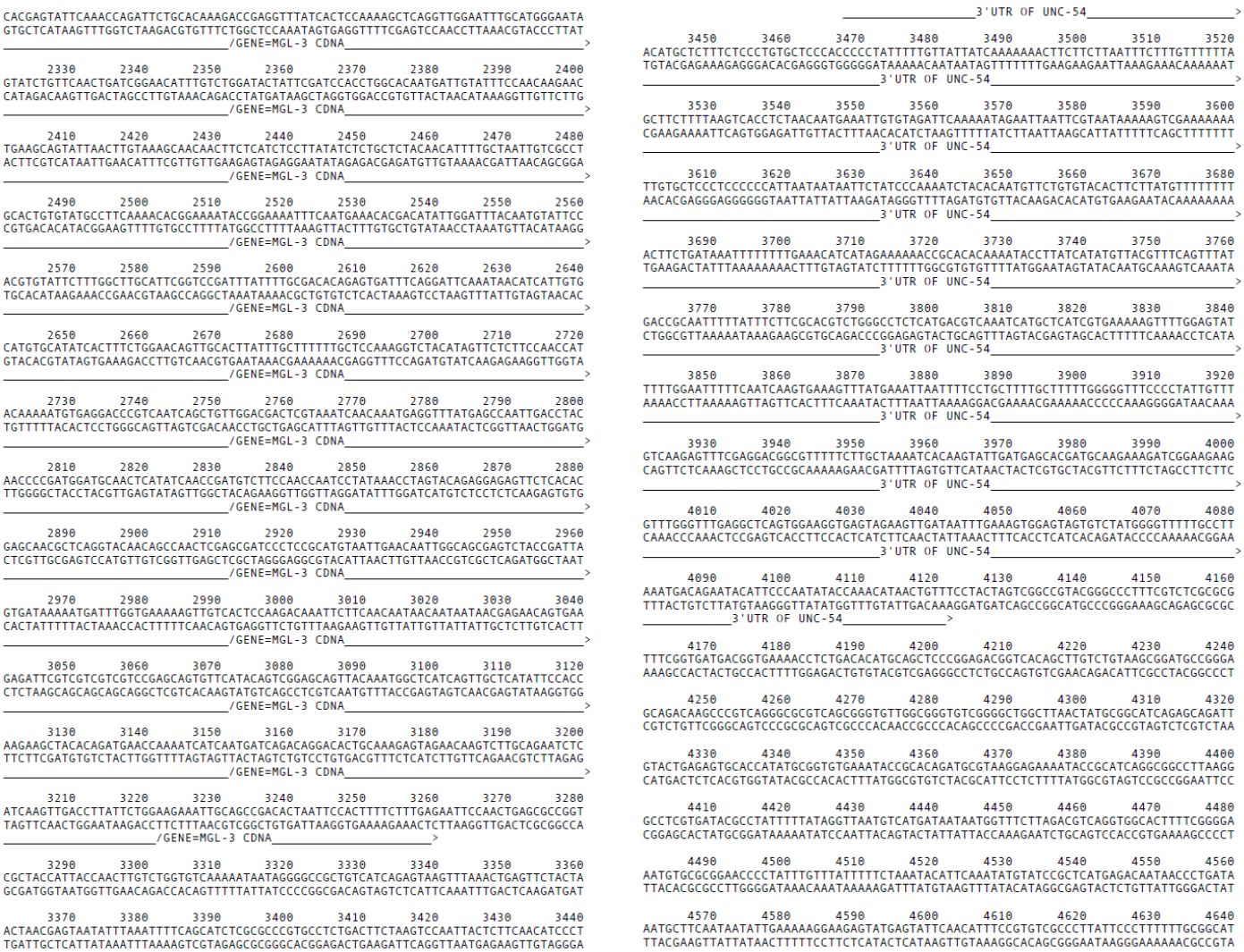
/GENE=MGL-3 CDNA
3'UTR OF UNC-54

```
      4650      4660      4670      4680      4690      4700      4710      4720
TTTGCCTTCCTGTTTTTGCTCACCCAGAAACGCTGGTGAAAGTAAAAGATGCTGAAGATCAGTTGGGTGCACGAGTGGGT
AAACGGAAGGACAAAAACGAGTGGGTCTTTGCGACCACTTTCATTTTCTACGACTTCTAGTCAACCCACGTGCTCACCCA

      4730      4740      4750      4760      4770      4780      4790      4800
TACATCGAACTGGATCTCAACAGCGGTAAGATCCTTGAGAGTTTTCGCCCCGAAGAACGTTTTCCAATGATGAGCACTTT
ATGTAGCTTGACCTAGAGTTGTCGCCATTCTAGGAACTCTCAAAAGCGGGGCTTCTTGCAAAAGGTTACTACTCGTGAAA

      4810      4820      4830      4840      4850      4860      4870      4880
TAAAGTTCTGCTATGTGGCGCGGTATTATCCCGTATTGACGCCGGGCAAGAGCAACTCGGTCGCCGCATACACTATTCTC
ATTTCAAGACGATACACCGCGCCATAATAGGGCATAACTGCGGCCCGTTCTCGTTGAGCCAGCGGCGTATGTGATAAGAG

      4890      4900      4910      4920      4930      4940      4950      4960
AGAATGACTTGGTTGAGTACTCACCAGTCACAGAAAAGCATCTTACGGATGGCATGACAGTAAGAGAATTATGCAGTGCT
TCTTACTGAACCAACTCATGAGTGGTCAGTGTCTTTTCGTAGAATGCCTACCGTACTGTCATTCTCTTAATACGTCACGA

      4970      4980      4990      5000      5010      5020      5030      5040
GCCATAACCATGAGTGATAACACTGCGGCCAACTTACTTCTGACAACGATCGGAGGACCGAAGGAGCTAACCGCTTTTTT
CGGTATTGGTACTCACTATTGTGACGCCGGTTGAATGAAGACTGTTGCTAGCCTCCTGGCTTCCTCGATTGGCGAAAAAA

      5050      5060      5070      5080      5090      5100      5110      5120
GCACAACATGGGGGATCATGTAACTCGCCTTGATCGTTGGGAACCGGAGCTGAATGAAGCCATACCAAACGACGAGCGTG
CGTGTTGTACCCCCTAGTACATTGAGCGGAACTAGCAACCCTTGGCCTCGACTTACTTCGGTATGGTTTGCTGCTCGCAC

      5130      5140      5150      5160      5170      5180      5190      5200
ACACCACGATGCCTGTAGCAATGGCAACAACGTTGCGCAAACTATTAACTGGCGAACTACTTACTCTAGCTTCCCGGCAA
TGTGGTGCTACGGACATCGTTACCGTTGTTGCAACGCGTTTGATAATTGACCGCTTGATGAATGAGATCGAAGGGCCGTT

      5210      5220      5230      5240      5250      5260      5270      5280
CAATTAATAGACTGGATGGAGGCGGATAAAGTTGCAGGACCACTTCTGCGCTCGGCCCTTCCGGCTGGCTGGTTTATTGC
GTTAATTATCTGACCTACCTCCGCCTATTTCAACGTCCTGGTGAAGACGCGAGCCGGGAAGGCCGACCGACCAAATAACG

      5290      5300      5310      5320      5330      5340      5350      5360
TGATAAATCTGGAGCCGGTGAGCGTGGGTCTCGCGGTATCATTGCAGCACTGGGGCCAGATGGTAAGCCCTCCCGTATCG
ACTATTTAGACCTCGGCCACTCGCACCCAGAGCGCCATAGTAACGTCGTGACCCCGGTCTACCATTCGGGAGGGCATAGC

      5370      5380      5390      5400      5410      5420      5430      5440
TAGTTATCTACACGACGGGGAGTCAGGCAACTATGGATGAACGAAATAGACAGATCGCTGAGATAGGTGCCTCACTGATT
ATCAATAGATGTGCTGCCCCTCAGTCCGTTGATACCTACTTGCTTTATCTGTCTAGCGACTCTATCCACGGAGTGACTAA

      5450      5460      5470      5480      5490      5500      5510      5520
AAGCATTGGTAACTGTCAGACCAAGTTTACTCATATATACTTTAGATTGATTTAAAACTTCATTTTTAATTTAAAAGGAT
TTCGTAACCATTGACAGTCTGGTTCAAATGAGTATATATGAAATCTAACTAAATTTTGAAGTAAAAATTAAATTTTCCTA

      5530      5540      5550      5560      5570      5580      5590      5600
CTAGGTGAAGATCCTTTTTGATAATCTCATGACCAAAATCCCTTAACGTGAGTTTTCGTTCCACTGAGCGTCAGACCCCG
GATCCACTTCTAGGAAAAACTATTAGAGTACTGGTTTTAGGGAATTGCACTCAAAAGCAAGGTGACTCGCAGTCTGGGGC

      5610      5620      5630      5640      5650      5660      5670      5680
TAGAAAAGATCAAAGGATCTTCTTGAGATCCTTTTTTTCTGCGCGTAATCTGCTGCTTGCAAACAAAAAAACCACCGCTA
ATCTTTTCTAGTTTCCTAGAAGAACTCTAGGAAAAAAAAGACGCGCATTAGACGACGAACGTTTGTTTTTTTGGTGGCGAT

      5690      5700      5710      5720      5730      5740      5750      5760
CCAGCGGTGGTTTGTTTGCCGGATCAAGAGCTACCAACTCTTTTTCCGAAGGTAACTGGCTTCAGCAGAGCGCAGATACC
GGTCGCCACCAAACAAACGGCCTAGTTCTCGATGGTTGAGAAAAAGGCTTCCATTGACCGAAGTCGTCTCGCGTCTATGG

      5770      5780      5790      5800      5810      5820      5830      5840
AAATACTGTCCTTCTAGTGTAGCCGTAGTTAGGCCACCACTTCAAGAACTCTGTAGCACCGCCTACATACCTCGCTCTGC
TTTATGACAGGAAGATCACATCGGCATCAATCCGGTGGTGAAGTTCTTGAGACATCGTGGCGGATGTATGGAGCGAGACG

      5850      5860      5870      5880      5890      5900      5910      5920
TAATCCTGTTACCAGTGGCTGCTGCCAGTGGCGATAAGTCGTGTCTTACCGGGTTGGACTCAAGACGATAGTTACCGGAT
ATTAGGACAATGGTCACCGACGACGGTCACCGCTATTCAGCACAGAATGGCCCAACCTGAGTTCTGCTATCAATGGCCTA

      5930      5940      5950      5960      5970      5980      5990      6000
AAGGCGCAGCGGTCGGGCTGAACGGGGGGTTCGTGCACACAGCCCAGCTTGGAGCGAACGACCTACACCGAACTGAGATA
TTCCGCGTCGCCAGCCCGACTTGCCCCCCAAGCACGTGTGTCGGGTCGAACCTCGCTTGCTGGATGTGGCTTGACTCTAT

      6010      6020      6030      6040      6050      6060      6070      6080
CCTACAGCGTGAGCATTGAGAAAGCGCCACGCTTCCCGAAGGGAGAAAGGCGGACAGGTATCCGGTAAGCGGCAGGGTCG
GGATGTCGCACTCGTAACTCTTTCGCGGTGCGAAGGGCTTCCCTCTTTCCGCCTGTCCATAGGCCATTCGCCGTCCCAGC

      6090      6100      6110      6120      6130      6140      6150      6160
GAACAGGAGAGCGCACGAGGGAGCTTCCAGGGGGAAACGCCTGGTATCTTTATAGTCCTGTCGGGTTTCGCCACCTCTGA
CTTGTCCTCTCGCGTGCTCCCTCGAAGGTCCCCCTTTGCGGACCATAGAAATATCAGGACAGCCCAAAGCGGTGGAGACT

      6170      6180      6190      6200      6210      6220      6230      6240
CTTGAGCGTCGATTTTTGTGATGCTCGTCAGGGGGGCGGAGCCTATGGAAAAACGCCAGCAACGCGGCCTTTTTACGGTT
GAACTCGCAGCTAAAAACACTACGAGCAGTCCCCCCGCCTCGGATACCTTTTTGCGGTCGTTGCGCCGGAAAAATGCCAA

      6250      6260      6270      6280      6290      6300      6310      6320
CCTGGCCTTTTGCTGGCCTTTTGCTCACATGTTCTTTCCTGCGTTATCCCCTGATTCTGTGGATAACCGTATTACCGCCT
GGACCGGAAAACGACCGGAAAACGAGTGTACAAGAAAGGACGCAATAGGGGACTAAGACACCTATTGGCATAATGGCGGA

      6330      6340      6350      6360      6370      6380      6390      6400
TTGAGTGAGCTGATACCGCTCGCCGCAGCCGAACGACCGAGCGCAGCGAGTCAGTGAGCGAGGAAGCGGAAGAGCGCCCA
AACTCACTCGACTATGGCGAGCGGCGTCGGCTTGCTGGCTCGCGTCGCTCAGTCACTCGCTCCTTCGCCTTCTCGCGGGT

      6410      6420      6430      6440      6450      6460      6470      6480
ATACGCAAACCGCCTCTCCCCGCGCGTTGGCCGATTCATTAATGCAGCTGGCACGACAGGTTTCCCGACTGGAAAGCGGG
TATGCGTTTGGCGGAGAGGGGCGCGCAACCGGCTAAGTAATTACGTCGACCGTGCTGTCCAAAGGGCTGACCTTTCGCCC

      6490      6500      6510      6520      6530      6540      6550      6560
CAGTGAGCGCAACGCAATTAATGTGAGTTAGCTCACTCATTAGGCACCCCAGGCTTTACACTTTATGCTTCCGGCTCGTA
GTCACTCGCGTTGCGTTAATTACACTCAATCGAGTGAGTAATCCGTGGGGTCCGAAATGTGAAATACGAAGGCCGAGCAT

      6570      6580      6590      6600      6610      6620      6630      6640
TGTTGTGTGGAATTGTGAGCGGATAACAATTTCACACAGGAAACAGCTATGACCATGATTACGCCAAGCTGTAAGTTTAA
ACAACACACCTTAACACTCGCCTATTGTTAAAGTGTGTCCTTTGTCGATACTGGTACTAATGCGGTTCGACATTCAAATT

      6650      6660      6670      6680      6690      6700      6710      6720
ACATGATCTTACTAACTAACTATTCTCATTTAAATTTTCAGAGCTTAAAAATGGCTGAAATCACTCACAACGATGGATAC
TGTACTAGAATGATTGATTGATAAGAGTAAATTTAAAAGTCTCGAATTTTTACCGACTTTAGTGAGTGTTGCTACCTATG

      6730      6740
GCTAACAACTTGGAAATGAAAT
CGATTGTTGAACCTTTACTTTA
```

pNR56 (*glc-3* cDNA)

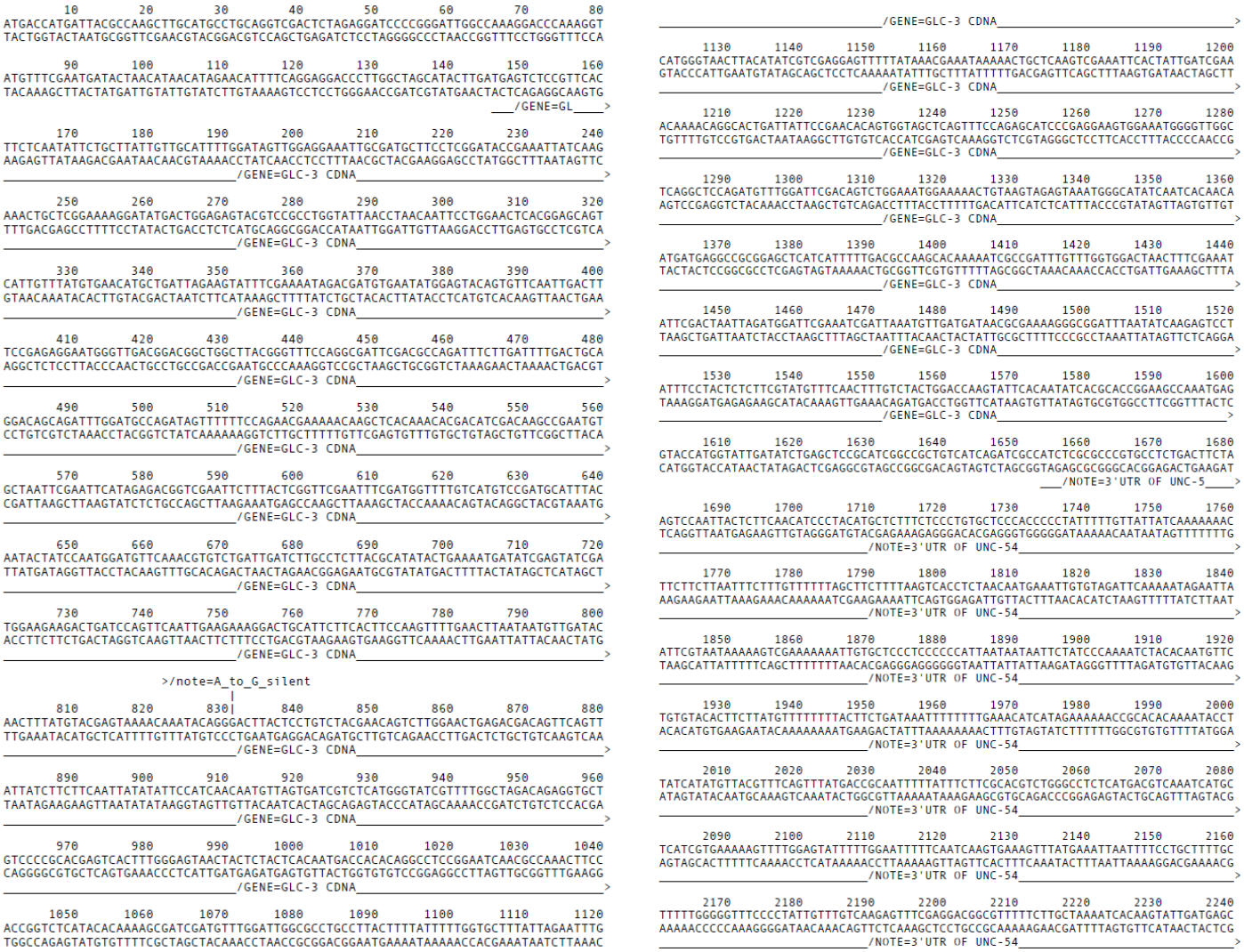

```
      2250       2260       2270       2280       2290       2300       2310       2320
ACGATGCAAGAAAGATCGGAAGAAGGTTTGGGTTTGAGGCTCAGTGGAAGGTGAGTAGAAGTTGATAATTTGAAAGTGGA
TGCTACGTTCTTTCTAGCCTTCTTCCAAACCCAAACTCCGAGTCACCTTCCACTCATCTTCAACTATTAAACTTTCACCT
_____________________________/NOTE=3'UTR OF UNC-54_____________________________>

      2330       2340       2350       2360       2370       2380       2390       2400
GTAGTGTCTATGGGGTTTTTGCCTTAAATGACAGAATACATTCCCAATATACCAAACATAACTGTTTCCTACTAGTCGGC
CATCACAGATACCCCAAAAACGGAATTTACTGTCTTATGTAAGGGTTATATGGTTTGTATTGACAAAGGATGATCAGCCG
_____________________/NOTE=3'UTR OF UNC-54_____________________>

      2410       2420       2430       2440       2450       2460       2470       2480
CGTACGGGCCCTTTCGTCTCGCGCGTTTCGGTGATGACGGTGAAAACCTCTGACACATGCAGCTCCCGGAGACGGTCACA
GCATGCCCGGGAAAGCAGAGCGCGCAAAGCCACTACTGCCACTTTTGGAGACTGTGTACGTCGAGGGCCTCTGCCAGTGT

      2490       2500       2510       2520       2530       2540       2550       2560
GCTTGTCTGTAAGCGGATGCCGGGAGCAGACAAGCCCGTCAGGGCGCGTCAGCGGGTGTTGGCGGGTGTCGGGGCTGGCT
CGAACAGACATTCGCCTACGGCCCTCGTCTGTTCGGGCAGTCCCGCGCAGTCGCCCACAACCGCCCACAGCCCCGACCGA

      2570       2580       2590       2600       2610       2620       2630       2640
TAACTATGCGGCATCAGAGCAGATTGTACTGAGAGTGCACCATATGCGGTGTGAAATACCGCACAGATGCGTAAGGAGAA
ATTGATACGCCGTAGTCTCGTCTAACATGACTCTCACGTGGTATACGCCACACTTTATGGCGTGTCTACGCATTCCTCTT

      2650       2660       2670       2680       2690       2700       2710       2720
AATACCGCATCAGGCGGCCTTAAGGGCCTCGTGATACGCCTATTTTTATAGGTTAATGTCATGATAATAATGGTTTCTTA
TTATGGCGTAGTCCGCCGGAATTCCCGGAGCACTATGCGGATAAAAATATCCAATTACAGTACTATTATTACCAAAGAAT

      2730       2740       2750       2760       2770       2780       2790       2800
GACGTCAGGTGGCACTTTTCGGGGAAATGTGCGCGGAACCCCTATTTGTTTATTTTTCTAAATACATTCAAATATGTATC
CTGCAGTCCACCGTGAAAAGCCCCTTTACACGCGCCTTGGGGATAAACAAATAAAAAGATTTATGTAAGTTTATACATAG

      2810       2820       2830       2840       2850       2860       2870       2880
CGCTCATGAGACAATAACCCTGATAAATGCTTCAATAATATTGAAAAAGGAAGAGTATGAGTATTCAACATTTCCGTGTC
GCGAGTACTCTGTTATTGGGACTATTTACGAAGTTATTATAACTTTTTCCTTCTCATACTCATAAGTTGTAAAGGCACAG

      2890       2900       2910       2920       2930       2940       2950       2960
GCCCTTATTCCCTTTTTTGCGGCATTTTGCCTTCCTGTTTTTGCTCACCCAGAAACGCTGGTGAAAGTAAAAGATGCTGA
CGGGAATAAGGGAAAAAACGCCGTAAAACGGAAGGACAAAAACGAGTGGGTCTTTGCGACCACTTTCATTTTCTACGACT

      2970       2980       2990       3000       3010       3020       3030       3040
AGATCAGTTGGGTGCACGAGTGGGTTACATCGAACTGGATCTCAACAGCGGTAAGATCCTTGAGAGTTTTCGCCCCGAAG
TCTAGTCAACCCACGTGCTCACCCAATGTAGCTTGACCTAGAGTTGTCGCCATTCTAGGAACTCTCAAAAGCGGGGCTTC

      3050       3060       3070       3080       3090       3100       3110       3120
AACGTTTTCCAATGATGAGCACTTTTAAAGTTCTGCTATGTGGCGCGGTATTATCCCGTATTGACGCCGGGCAAGAGCAA
TTGCAAAAGGTTACTACTCGTGAAAATTTCAAGACGATACACCGCGCCATAATAGGGCATAACTGCGGCCCGTTCTCGTT

      3130       3140       3150       3160       3170       3180       3190       3200
CTCGGTCGCCGCATACACTATTCTCAGAATGACTTGGTTGAGTACTCACCAGTCACAGAAAAGCATCTTACGGATGGCAT
GAGCCAGCGGCGTATGTGATAAGAGTCTTACTGAACCAACTCATGAGTGGTCAGTGTCTTTTCGTAGAATGCCTACCGTA

      3210       3220       3230       3240       3250       3260       3270       3280
GACAGTAAGAGAATTATGCAGTGCTGCCATAACCATGAGTGATAACACTGCGGCCAACTTACTTCTGACAACGATCGGAG
CTGTCATTCTCTTAATACGTCACGACGGTATTGGTACTCACTATTGTGACGCCGGTTGAATGAAGACTGTTGCTAGCCTC

      3290       3300       3310       3320       3330       3340       3350       3360
GACCGAAGGAGCTAACCGCTTTTTTGCACAACATGGGGGATCATGTAACTCGCCTTGATCGTTGGGAACCGGAGCTGAAT
CTGGCTTCCTCGATTGGCGAAAAAACGTGTTGTACCCCCTAGTACATTGAGCGGAACTAGCAACCCTTGGCCTCGACTTA

      3370       3380       3390       3400       3410       3420       3430       3440
GAAGCCATACCAAACGACGAGCGTGACACCACGATGCCTGTAGCAATGGCAACAACGTTGCGCAAACTATTAACTGGCGA
CTTCGGTATGGTTTGCTGCTCGCACTGTGGTGCTACGGACATCGTTACCGTTGTTGCAACGCGTTTGATAATTGACCGCT

      3450       3460       3470       3480       3490       3500       3510       3520
ACTACTTACTCTAGCTTCCCGGCAACAATTAATAGACTGGATGGAGGCGGATAAAGTTGCAGGACCACTTCTGCGCTCGG
TGATGAATGAGATCGAAGGGCCGTTGTTAATTATCTGACCTACCTCCGCCTATTTCAACGTCCTGGTGAAGACGCGAGCC

      3530       3540       3550       3560       3570       3580       3590       3600
CCCTTCCGGCTGGCTGGTTTATTGCTGATAAATCTGGAGCCGGTGAGCGTGGGTCTCGCGGTATCATTGCAGCACTGGGG
GGGAAGGCCGACCGACCAAATAACGACTATTTAGACCTCGGCCACTCGCACCCAGAGCGCCATAGTAACGTCGTGACCCC

      3610       3620       3630       3640       3650       3660       3670       3680
CCAGATGGTAAGCCCTCCCGTATCGTAGTTATCTACACGACGGGGAGTCAGGCAACTATGGATGAACGAAATAGACAGAT
GGTCTACCATTCGGGAGGGCATAGCATCAATAGATGTGCTGCCCCCTCAGTCCGTTGATACCTACTTGCTTTATCTGTCTA

      3690       3700       3710       3720       3730       3740       3750       3760
CGCTGAGATAGGTGCCTCACTGATTAAGCATTGGTAACTGTCAGACCAAGTTTACTCATATATACTTTAGATTGATTTAA
GCGACTCTATCCACGGAGTGACTAATTCGTAACCATTGACAGTCTGGTTCAAATGAGTATATATGAAATCTAACTAAATT

      3770       3780       3790       3800       3810       3820       3830       3840
AACTTCATTTTTAATTTAAAAGGATCTAGGTGAAGATCCTTTTTGATAATCTCATGACCAAAATCCCTTAACGTGAGTTT
TTGAAGTAAAAATTAAATTTTCCTAGATCCACTTCTAGGAAAAACTATTAGAGTACTGGTTTTAGGGAATTGCACTCAAA

      3850       3860       3870       3880       3890       3900       3910       3920
TCGTTCCACTGAGCGTCAGACCCCGTAGAAAAGATCAAAGGATCTTCTTGAGATCCTTTTTTTCTGCGCGTAATCTGCTG
AGCAAGGTGACTCGCAGTCTGGGGCATCTTTTCTAGTTTCCTAGAAGAACTCTAGGAAAAAAAGACGCGCATTAGACGAC

      3930       3940       3950       3960       3970       3980       3990       4000
CTTGCAAACAAAAAAACCACCGCTACCAGCGGTGGTTTGTTTGCCGGATCAAGAGCTACCAACTCTTTTTCCGAAGGTAA
GAACGTTTGTTTTTTTGGTGGCGATGGTCGCCACCAAACAAACGGCCTAGTTCTCGATGGTTGAGAAAAAGGCTTCCATT

      4010       4020       4030       4040       4050       4060       4070       4080
CTGGCTTCAGCAGAGCGCAGATACCAAATACTGTCCTTCTAGTGTAGCCGTAGTTAGGCCACCACTTCAAGAACTCTGTA
GACCGAAGTCGTCTCGCGTCTATGGTTTATGACAGGAAGATCACATCGGCATCAATCCGGTGGTGAAGTTCTTGAGACAT

      4090       4100       4110       4120       4130       4140       4150       4160
GCACCGCCTACATACCTCGCTCTGCTAATCCTGTTACCAGTGGCTGCTGCCAGTGGCGATAAGTCGTGTCTTACCGGGTT
CGTGGCGGATGTATGGAGCGAGACGATTAGGACAATGGTCACCGACGACGGTCACCGCTATTCAGCACAGAATGGCCCAA

      4170       4180       4190       4200       4210       4220       4230       4240
GGACTCAAGACGATAGTTACCGGATAAGGCGCAGCGGTCGGGCTGAACGGGGGGTTCGTGCACACAGCCCAGCTTGGAGC
CCTGAGTTCTGCTATCAATGGCCTATTCCGCGTCGCCAGCCCGACTTGCCCCCCCAAGCACGTGTGTCGGGTCGAACCTCG

      4250       4260       4270       4280       4290       4300       4310       4320
GAACGACCTACACCGAACTGAGATACCTACAGCGTGAGCATTGAGAAAGCGCCACGCTTCCCGAAGGGAGAAAGGCGGAC
CTTGCTGGATGTGGCTTGACTCTATGGATGTCGCACTCGTAACTCTTTCGCGGTGCGAAGGGCTTCCCTCTTTCCGCCTG

      4330       4340       4350       4360       4370       4380       4390       4400
AGGTATCCGGTAAGCGGCAGGGTCGGAACAGGAGAGCGCACGAGGGAGCTTCCAGGGGGAAACGCCTGGTATCTTTATAG
TCCATAGGCCATTCGCCGTCCCAGCCTTGTCCTCTCGCGTGCTCCCTCGAAGGTCCCCCTTTGCGGACCATAGAAATATC

      4410       4420       4430       4440       4450       4460       4470       4480
TCCTGTCGGGTTTCGCCACCTCTGACTTGAGCGTCGATTTTTGTGATGCTCGTCAGGGGGGCGGAGCCTATGGAAAAACG
AGGACAGCCCAAAGCGGTGGAGACTGAACTCGCAGCTAAAAACACTACGAGCAGTCCCCCCGCCTCGGATACCTTTTTGC

      4490       4500       4510       4520       4530       4540       4550       4560
CCAGCAACGCGGCCTTTTTACGGTTCCTGGCCTTTTGCTGGCCTTTTGCTCACATGTTCTTTCCTGCGTTATCCCCTGAT
GGTCGTTGCGCCGGAAAAATGCCAAGGACCGGAAAACGACCGGAAAACGAGTGTACAAGAAAGGACGCAATAGGGGACTA

      4570       4580       4590       4600       4610       4620       4630       4640
TCTGTGGATAACCGTATTACCGCCTTTGAGTGAGCTGATACCGCTCGCCGCAGCCGAACGACCGAGCGCAGCGAGTCAGT
AGACACCTATTGGCATAATGGCGGAAACTCACTCGACTATGGCGAGCGGCGTCGGCTTGCTGGCTCGCGTCGCTCAGTCA

      4650       4660       4670       4680       4690       4700       4710       4720
GAGCGAGGAAGCGGAAGAGCGCCCAATACGCAAACCGCCTCTCCCCGCGCGTTGGCCGATTCATTAATGCAGCTGGCACG
CTCGCTCCTTCGCCTTCTCGCGGGTTATGCGTTTGGCGGAGAGGGGCGCGCAACCGGCTAAGTAATTACGTCGACCGTGC

      4730       4740       4750       4760       4770       4780       4790       4800
ACAGGTTTCCCGACTGGAAAGCGGGCAGTGAGCGCAACGCAATTAATGTGAGTTAGCTCACTCATTAGGCACCCCAGGCT
TGTCCAAAGGGCTGACCTTTCGCCCGTCACTCGCGTTGCGTTAATTACACTCAATCGAGTGAGTAATCCGTGGGGTCCGA

      4810       4820       4830       4840       4850       4860       4870
TTACACTTTATGCTTCCGGCTCGTATGTTGTGTGGAATTGTGAGCGGATAACAATTTCACACAGGAAACAGCT
AATGTGAAATACGAAGGCCGAGCATACAACACACCTTAACACTCGCCTATTGTTAAAGTGTGTCCTTTGTCGA
```